How Push-off Influences Energetics and Mechanics of Human Walking

by

Tzu-wei Huang

A dissertation submitted in partial fulfillment
of the requirements for the degree of
Doctor of Philosophy
(Mechanical Engineering)
in the University of Michigan
2014

Doctoral Committee:

Professor Arthur D. Kuo, Chair
Professor Daniel P. Ferris
Associate Professor Brent Gillespie
Assistant Professor C. David Remy

Acknowledgements

I would like to thank…

Art Kuo for his mentorship, teaching me real science.

Mebers of my dissertation committee for the guidance and feedback.

Karl Zelik and Peter Adamczyk for teaching me how to do experiment.

HBCL members for all the advice and support.

My parents for supporting me to go for the PhD degree.

My sister for taking care of my Mom when I am in U.S.

My lovely wife Chiao-li, for her love, support and tolerating me.

All my other friends in Mustardseed fellowship, Taiwanese church and Michigan Taiwanese Student Association for all the good memeries.

Table of Contents

List of Figures

List of Tables

Abstract

The energetic cost of walking is important for mobility. The energetic cost of normal healthy people walking has been shown as a minimization objective for determining some gait parameters, but there lacks of understanding about the energetic cost for people walking with challenging conditions or various disabilities. It is well known that the energetic cost of walking with carried load increases substantively. Also, patients with ankle weakness due to pathologies have greater energetic cost of walking. Several prosthetic feet and ankle-foot orthoses (AFO) use elastic spring to restore ankle function by performing elastic push-off. However, there still lacks of mechanistic explanation how and why the energetic cost increases in these cases, and how the elastic push-off affect the energetic cost. In this thesis, I proposed mechanistic models for the energetic cost of human walking with carried load, with reduced push-off and with elastic push-off and then tested the model predictions with human subjects.

Three dynamic walking models were used to predict the energetic cost of these conditions. First, I used a rigid-leg walking model to predict the energetic cost of walking with carried load at different speed. The rigid-leg model can only predict the mechanical work of walking but cannot predict some gait parameters, such as double support duration, so I secondly used a compliant-leg walking model to offer complimentary explanations for walking with carried load. The same rigid-leg walking model was also used to predict the energetic cost of walking with reduced push-off. Finally, I used the springy ankle walking model to predict the energetic cost of walking with elastic push-off. I then measure the mechanical work performed by lower limb extremity and estimate the metabolic cost of healthy subjects walking with carried load, with restricted ankle and with compliant artificial feet to test the predictions.

The results of the experiments agreed with the predictions from the dynamic walking models. I found the energetic cost of these tasks can be explained by the mechanical work performed by lower extremity. The push-off greatly affects the energetic cost by modulating the heel-strike collision.

Chapter 1 Introduction

Walking is one of the most common activities in our daily life. Like all other activities, it requires energy to walk. The amount of energetic cost of walking depends on different conditions. It requires more energy to walk at faster speeds (Griffin et al., 2003). The gait parameters, such as step length (Grieve, 1968) and step width (Donelan et al., 2001b), can also affect the energetic cost of walking. Humans tend to choose their step frequency and step width to minimize the energetic cost in normal walking. The self-selected step frequency (Grieve, 1968) and step width (Donelan et al., 2001b) are always the optimum yielding minimal energetic cost. The mechanical work performed by lower extremity can explain the optimal value of step frequency and step width. Walking at slower step frequency or wider step width has more positive mechanical work performed by lower extremity and therefore has greater energetic cost. According to basic thermal dynamic law, it requires energy to perform active mechanical work. Margaria (1968) found the efficiency of 25 and -120% for positive and negative work respectively during human walking. The mechanical work has been showed to explain the energetic cost of normal human walking (Donelan et al., 2002a), but it is unclear if the energetic cost of walking with challenging conditions can also be explained by mechanical work.

The energetic cost of walking with challenging conditions, such as walking with carried load, is significant higher than normal walking. The energetic cost can double when walking with carried load about 40 % of the body weight (Griffin et al., 2003; Huang and Kuo, 2014). For patients with ankle weakness due to ankle arthroplasty (Doets et al., 2009) or pathologies such as multiple sclerosis, stroke or amputation (Bregman et al., 2011b; Waters and Mulroy, 1999) also have higher energetic cost for walking. Several prosthetic feet, ankle-foot orthoses and exoskeleton systems were designed to reduce the energetic cost of walking. However, why and

how the energetic cost increases with these conditions is still unclear. It is hard to design a device to improve the walking economy without understanding the mechanism behind the energetic cost.

In normal healthy human walking, the energetic cost can be explained by the amount of mechanical work performed by the lower extremity (Adamczyk and Kuo, 2009; Donelan et al., 2002b). Theoretically, no mechanical work is needed if an object is moving at a constant speed. However, the heel-strike collision at each step dissipates mechanical energy of walking and requires positive work to offset. One of the most effective way to perform positive work is ankle pus-off. Ankle performs a burst of positive work during late stance, termed as push-off. The ankle push-off during walking is considered to redirect the center of mass (COM) during step-to-step transition and reduce the heel-strike collision, according to a simplest dynamic walking model (Adamczyk and Kuo, 2009; Donelan et al., 2002b; Kuo et al., 2005a). This simplest dynamic walking model has successfully explained the relationship between preferred step length and walking velocity of normal walking (Donelan et al., 2001a; Kuo, 2001).

The mechanical work performed by lower extremity has been shown to be able to explain the energetic cost of normal walking, and the simplest dynamic walking model can explain the mechanical work based on push-off-collision relationship. In this thesis, I purposed the mechanical work and the simplest dynamic walking model can also explain the energetic cost of walking with challenging conditions.

The most common challenging condition is walking with carried load. It is well known that the cost of human walking increases substantively to carrying a load, but lacks of a mechanistic explanation (Goldman and Iampietro, 1962; Griffin et al., 2003; Soule et al., 1978). Therefore, in Chapter 2, I tested if the mechanical work performed by lower extremity can explain the energetic cost of healthy adults walking with carried load. I purposed an hypothesis based on the simplest dynamic walking model, in which the mechanical work performed by each leg on body center of mass (COM) and the energetic cost should be proportionate to the total mass of the body. An experiment of human walking with different carried loads is performed to test this hypothesis. We found linear relationship between all measurements of work and carried load. Also, we found linear relationship between the net metabolic rate and mechanical work performed on COM by each leg, yielding a delta efficiency of 16 % of mechanical work.

To explore the energetic cost of human walking with more challenging conditions, we tested human walking with carried load at different speeds. The energetic cost of walking with faster speed increases more severely than walking with carried load (Griffin et al., 2003), and the mechanical work performed by each leg on COM can explain the energetic cost for walking with no carried load at different speeds (Donelan et al., 2002d). An overall explanation for the energetic cost of walking with carried load and at different speeds is still missing. In Chapter 3, I predicted the mechanical work performed by each leg on COM as a function of total mass and walking speed based on the simplest rigid-leg dynamic walking model. The rigid-leg model predicts the mechanical work performed on COM should be proportionate to the body bass multiplies walking speed raised to the power of 3.42. I tested this prediction by testing healthy adults walking at different speeds with carried load. I found that the rigid leg model can explain the increases of the mechanical work performed on COM and the metabolic rate. The rigid-leg model can only predict the mechanical work performed on COM, so I used a compliant-leg model to predict other gait parameters such as double support duration as complement. The compliant-leg model predicts the double support duration should increase at faster speed. The compliant-leg model can explain the double support duration and COM fluctuations.

The energetic cost of walking with ankle weakness due to pathologies such as multiple sclerosis or stroke is higher than with normal intact ankle (Bregman et al., 2012; Waters and Mulroy, 1999). The less ankle push-off due to the ankle weakness could be a reason why the energetic cost is higher. However, in most patient groups it is impractical to isolate ankle weakness from other effects that accompany the diseased state. Therefore, I studied healthy subjects walking with restricted ankle motion, which reduced the ankle push-off, in Chapter 4. The simplest dynamic walking model predicts the energetic cost of human walking based on the push-off-collision relationship: the push-off preemptive to heel-strike can reduce heel-strike collision and energetic cost of walking. The model predicts that the less push-off would cause greater collision and requires more mechanical work to compensate causing higher energetic cost. I then estimate the metabolic rate and measure the collision work of healthy subjects walking with reduced push-off by ankle restriction. The results agreed with the prediction from simplest walking model and revealed the importance of restoring ankle push-off.

To restore ankle push-off, several prosthetic feet and AFOs use elasticity elements to store and return energy as push-off. The patients with ankle weakness or amputations usually prefer these devices, and the energetic cost of walking with these devices is significantly less than rigid ones. However, the elastic push-off has not been studied independently from other disabilities due to pathologies or amputations. Therefore, I studied how elastic push-off affects the energetic cost of healthy subjects walking with compliant artificial feet in Chapter 5. I used the springy ankle dynamic walking model (Zelik et al., 2014) to predict the energetic cost of walking with different level of elastic push-off by tuning the ankle stiffness and foot length. I estimate the metabolic rate and the mechanical work performed by lower extremity of healthy subjects walking with compliant artificial feet. The results show that the timing and the amount of elastic push-off, which depends on the ankle stiffness and foot length, affects the energetic cost of walking.

Chapter 2 Mechanics and Energetics of Load Carriage during Human Walking

Published in Journal of Experimental Biology (2014)

Abstract

Although humans clearly expend more energy to walk with an extra load, it is unclear what biomechanical mechanism explains contribute to that increase. One possible contribution is the mechanical work performed on the body center of mass (COM), which simple models predict should increase linearly with added mass. The work should be performed primarily by the lower extremity joints, although in unknown distribution, and cost a proportionate amount of metabolic energy. We therefore tested normal adults (N=8) walking at constant speed (1.25 m/s) with varying backpack loads up to about 40% of body weight. We measured mechanical work (both performed on the COM and joint work from inverse dynamics), as well as metabolic energy expenditure through respirometry. Both measures of work were found to increase approximately linearly with carried load, with COM work rate increasing by about 1.40 W for each 1 kg of additional load. The joints all contributed work, but the greatest increase in positive work was attributable to the ankle during push-off (about 45 – 60% of stride time), and the knee in the rebound after collision (12 – 30% stride). The hip performed increasing amounts of negative work, near the end of stance. Rate of metabolic energy expenditure also increased approximately linearly with load, by about 7.6 W for each 1 kg of additional load. The ratio of the increases in work and metabolic cost yielded a relatively constant efficiency of about 16%. The metabolic cost not explained by work appeared to be relatively constant with load and did not exhibit a particular trend. Most of the increasing cost for carrying a load appears to be explained by positive mechanical work, especially about ankle and knee, with both work and metabolic cost increasing nearly linearly with added mass.

Introduction

Humans expend considerably more effort to walk when carrying a backpack load. Metabolic energy expenditure increases sharply with the load carried, and can easily double for a moderate load (Goldman and Iampietro, 1962; Soule et al., 1978). Gait kinematics do not change nearly as much (Ghori and Luckwill, 1985; Tilbury-Davis and Hooper, 1999), suggesting that the energetic cost appears less due to an altered gait pattern than to the effort of transporting the load itself. Indeed, the forces and joint moments of walking do increase markedly with load, as does the electromyographic activity of muscles in the lower limbs and trunk (Ghori and Luckwill, 1985; Knapik et al., 1996). However, it remains difficult to predict how biomechanical variables should increase with load, and how they might mechanistically contribute to greater metabolic energy expenditure. This underscores the need for a mechanistic explanation for the metabolic cost of walking as a function of load.

A major contributor to metabolic cost is the active mechanical work performed by muscles. Physical principles dictate that active work must cost energy; muscles perform work with an empirically observed efficiency (defined as work divided by energetic cost) of 25% or less, as observed in a variety of human experiments and isolated muscle preparations (Margaria, 1976). Negative work also costs positive energy although at lower cost, with efficiency about -120%. During walking, work is performed on the body center of mass (COM) and to move body segments relative to the COM (Cavagna and Kaneko, 1977). The former appears dominated by work needed to redirect the COM between successive stance phases (Donelan et al., 2002a; Donelan et al., 2002b). This is because the COM moves atop a stance leg that behaves approximately like a pendulum (Fig. 2.1), and hence its velocity must be redirected from one pendulum-like arc to the next. A backpack load would be expected to add proportionately to the work needed to redirect the COM, and to add little to work performed for motions relative to the COM. Indeed, measurements of work performed on the COM do appear to increase with load (Grenier et al., 2012; Griffin et al., 2003). Much of that work is performed simultaneously as positive work by the trailing leg and negative work by the leading leg, and could account for much of the metabolic cost of walking (Donelan et al., 2002b).

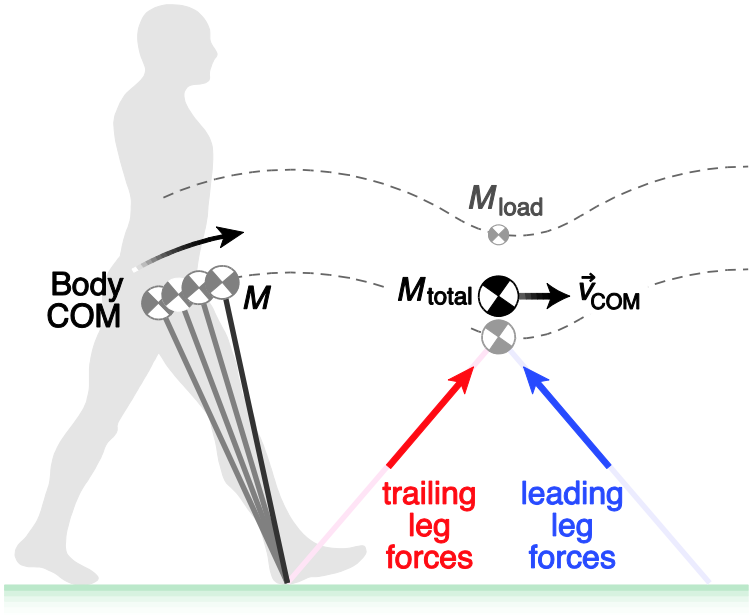

Figure 2.1: Mechanical work to redirect the center of mass during walking.
The body center of mass (COM) moves atop pendulum-like legs, so that motion during single support requires relatively little work. The COM moves in an arc, and its velocity v must be redirected from a downward-and-forward direction to an upward-and-forward direction when transitioning from one stance leg to the next. Each leg produces a ground reaction force (largely directed along the leg) to effect this transition, and consequently performs work on the COM. The addition of an extra load increases the total mass that must be redirected, with a proportional increase in work. That work is hypothesized to require additional metabolic energy expenditure.

There are also metabolic energetic costs other than for moving the COM. One example is a cost for moving the legs back and forth relative to the body. That cost may be associated more with activating muscle than with performing work (Doke and Kuo, 2007; Doke et al., 2005). It would be expected to contribute to walking energetics, but not to increase with a backpack load. Energy also appears to be expended to make small adjustments in foot placement from step to step, for balance control (O'Connor et al., 2012). Another possible cost is for supporting body weight, originally proposed by Taylor et al. (1980) for running gaits, but also applied to walking by Griffin et al. (2003). Such a cost should increase with carried load, presumably in amount separable from work. These and other energetic contributions are, unfortunately, far less straightforward to identify empirically. Perhaps an indication of their magnitude can be formed indirectly, from the metabolic cost changes that occur independently of work on the COM.

These metabolic energetic costs contributions may be estimated in comparison with mechanical work, which must therefore be quantified for walking. One empirical measure is the work performed on the COM by each limb (termed "COM work" here), defined as the integral of the vector dot product of the limb's ground reaction force against the COM velocity. Although it is a relatively simple measure, it can quantify the substantial work performed by the limbs against each other during double support (Donelan et al., 2002c), and as a function of load carriage (Grenier et al., 2012; Griffin et al., 2003). It does not, however, reveal which joints perform that work. That information is better revealed through the inverse dynamics technique, which estimates the resultant mechanical power from each joint ("joint work"). But neither inverse dynamics nor COM work can determine the actual work by muscles, nor can they isolate work performed by tendon (Alexander, 1991) and other soft tissues (Zelik and Kuo, 2010), which can contribute passively with little direct metabolic energy cost. Some such contributions can be quantified through imaging techniques such as ultrasound, particularly for the ankle (Fukunaga et al., 2001), but not as readily for the other joints. We consider COM work and joint work to be practically useful, if imperfect, measures for the work of walking. However, they have not previously been quantified together to help explain the metabolic cost of load carriage.

The complementary features of different work measures might reveal insight regarding load carriage during walking. An advantage of COM work is that it bears a straightforward link to a simple hypothesis, that COM work should increase linearly with carried load. Joint work can

then indicate where in the leg the work is performed, and its difference with COM work can indicate work for movements relative to the COM. If a carried load mainly affects COM work, then metabolic cost would be expected to increase proportionately, with an additional offset term that is constant relative to load. That offset term may indicate the metabolic cost for the work performed relative to the COM, as well as other metabolic costs not related to work. We therefore hypothesize that there would be a linear increase in COM work and metabolic cost as a function of carried load. Furthermore, those increases imply a linear dependence between work and metabolic energy expenditure. The present study is intended to test for such relationships between the mechanics and energetics of walking with a backpack load.

Method

We performed an experiment to measure healthy adults walking with a backpack load. We measured metabolic energy expenditure and gait kinematics and kinetics during treadmill walking. Kinetic measures consisted of COM work performed by the individual limbs as well as joint work for the ankle, knee, and hip. We tested for linear relationships between carried load and mechanical work, between load and metabolic energy expenditure, and between work and metabolic energy expenditure. The details of the experiment are presented below, followed by a brief explanation of the mechanism by which carried load should translate into work.

Experiment

Eight subjects (N = 8, 6 male and 2 female) were tested while walking with a backpack load at a constant speed of 1.25 m·s^{-1}. Four loads ranging 6.8 – 20.4 kg (steel weights of 15, 25, 35, 45 lbs) were tested, carried by an external-frame backpack (3.8 kg) with standard shoulder straps and hip belt. The loads were placed behind the back, about 0.23 m higher than sacrum. Normal walking without a backpack was also tested for reference. Subjects ranged 19-26 years of age and had average body mass M of 71.1±12.0 kg (mean ± s.d.), and leg length L, 0.99±0.03 m. All subjects provided informed consent prior to the study, according to Institutional Review Board procedures.

We measured the rate of oxygen consumption and carbon dioxide production (in mL per min) to estimate the metabolic energy expenditure rate, expressed in units of power (W) using standard conversion factors (Brockway, 1987a). Each walking trial lasted at least 8 minutes, with the first 3 minutes discarded to ensure steady state, and average power computed from the remaining duration. Net metabolic rate $\dot{E}$ was calculated by subtracting metabolic power for quiet standing (109.54±20.32 W, 0.0507±0.0065 dimensionless) from the gross metabolic power.

We calculated instantaneous COM work rate P_{COM} as the inner product of ground reaction force $\vec{F}$ of each leg and COM velocity $\vec{v}_{\mathrm{COM}}$ (Donelan et al., 2002c),

$$P_{\mathrm{COM}} = \vec{F} \cdot \vec{v}_{\mathrm{COM}} . \qquad (2\text{-}1)$$

The ground reaction force under each leg was measured with a custom instrumented, split-belt treadmill (Collins et al., 2009). The COM velocity was computed from the integration of total ground reaction force, subject to constraints on periodicity. The positive work per stride W^{+}_{COM}

was calculated from the integration of positive intervals of instantaneous COM work rate P_{COM} over each stride, and the average rate of positive COM work $\dot{W}^{+}_{\mathrm{COM}}$ was defined as the positive COM work per stride divided by stride time and multiplied by 2 for two legs (and similarly for negative work, $\dot{W}^{-}_{\mathrm{COM}}$). Thus, while work per stride is a single-leg quantity, mechanical work rate is for both legs, to facilitate comparison with net metabolic rate to yield apparent efficiency. We also qualitatively examined four phases of COM work rate defined from positive and negative intervals: Collision, Rebound, Preload and Push-off (Donelan et al., 2002b). We also measured other gait parameters such as step length, step time and double support time.

Joint work was computed from joint powers using inverse dynamics methods. An optical motion capture system (VICON, LA) was used to capture lower extremity kinematics, and inverse dynamics analysis was performed using standard software (Visual3D, Germantown) for calculating joint angles, moments and powers for ankle, knee, and hip, in three dimensions. A six degree-of-freedom model was used for each segment (Hanavan Jr., 1964), although only sagittal plane angles and moments are plotted for simplicity. Positive joint work per stride was calculated from the integration of positive intervals of joint power over each step. As a simple summary for an entire leg, we defined summed joint power as net power from ankle, knee, and hip of one leg. Positive summed joint work per stride W^{+}_{joint} was defined as the integration of positive intervals of summed joint power. Similar integrations were performed for negative work quantities (e.g., W^{-}_{joint}). Average work rates were defined as work per stride multiplied by 2 and divided by stride time.

To serve as the primary independent variable in the study, we defined total mass M_{total} as the combined mass of the body M plus the added mass M_{load} of the load including backpack and load. Measurements were reported in dimensionless form, using base units of body mass M, standing leg length L (ground to greater trochanter), and gravitational acceleration g. For example, masses were normalized by M (average 71.1 kg), moment and work by MgL (average 692.66 N-m), power by $Mg^{1.5}L^{0.5}$ (average 2176.12 W) and step length by L (0.99 m).

Model and Data analysis

We analyzed the data with respect to three relationships between carried mass, mechanical work, and metabolic energy expenditure. The first such relationship was for the dependency between rate of mechanical work performed on the COM and added mass. Simple models of dynamic

walking (Fig. 2.1) predict that work must be performed to redirect the COM velocity between pendulum-like steps (Kuo, 2002a). Push-off from the trailing leg performs positive work at the end of one stance phase. This is followed by a Collision of the leading leg, which performs negative work at the beginning of the next stance phase. Experiments show that COM redirection also occurs during stance, in a burst of positive work termed Rebound, followed by negative work termed Pre-Load (Donelan et al., 2002b), that appear to interact with Collision and Push-off. Just as kinetic energy is proportional to mass, so is the work performed on the COM each, proportional to $M_{\text{total}} v^2 s^2$, where v is walking speed and s is step length (Adamczyk and Kuo, 2009; Donelan et al., 2002b). Previous studies have shown carried mass to have little effect on step length at a fixed speed . We therefore expect that for a fixed speed, the positive COM work per step will increase in proportion to added mass (load + backpack weight),

$$W^{+}_{\text{COM}} = c \cdot M_{\text{load}} + d, \tag{2-2}$$

where c is an empirical coefficient of proportionality, and d is a constant representing work independent of load.

The second relationship tested was between rate of metabolic energy expenditure and added mass. We expect that COM work should account for a substantial fraction of metabolic cost, and therefore the metabolic rate $\dot{E}$ should also increase according to

$$\dot{E} = c' \cdot M_{\text{load}} + d', \tag{2-3}$$

where c' is an empirical coefficient and d' is a constant representing energy cost independent of load (and the prime symbol $'$ refers to metabolic energy as opposed to work). An example of the latter is basal metabolism, which proceeds regardless of task. The combination of work and energy expenditure are also made more explicit by the third relationship,

$$\dot{E} = \frac{1}{\eta} \cdot \dot{W}^{+}_{\text{COM}} + \dot{E}_0 \,, \tag{2-4}$$

where the empirical efficiency η is expected not to exceed 25% (Margaria, 1976), and constant $\dot{E}_0$ represents metabolic energy cost independent of work. The η defined here represents the change in metabolic cost per change in work, sometimes termed a delta efficiency (Gaesser and Brooks, 1975). It is also possible that there are other contributions to energy expenditure that

also change with total mass, but are unrelated to COM work, which would be expected to appear as a residual error in Eqn. 4.

We used linear regression to test these hypothesized relationships. We performed standard least squares regression, with M_{load} as the independent variable, for Eqns. 2 and 3. We used total least squares to test for Eqn. 4, treating both $\dot{W}^{+}_{\mathrm{COM}}$ and $\dot{E}$ as subject to measurement error. To focus on linear trends that apply across different individuals, each regression was performed with a single slope across all subjects (reported with a corresponding 95% confidence interval, c.i.) and a separate offset for each individual. The offsets account for the fact that individuals can differ in many respects not related to the independent variable, such as body mass distribution, muscle fiber composition, and basal metabolic rate. These can result in different amounts of work and energy expenditure for normal walking, and therefore to considerable variation in the offsets. To summarize these effects, graphical results are presented with the mean offset across individuals, and tabular results include the standard deviation (s.d.) of offsets across individuals. We also examined residual errors in the linear fits to test for metabolic costs not hypothesized here, such as energy expended with increasing mass but not explained by work.

We also tested for other trends that were less hypothesis-based. We tested how the positive joint work per stride (W^{+}_{ank}, W^{+}_{kne}, and W^{+}_{hip} for ankle, knee, and hip, respectively) changed as a function of total mass, and similarly for negative work per stride (W^{-}_{ank}, W^{-}_{kne}, W^{-}_{hip}). There is no fundamental principle governing how work should be apportioned between the joints, and so we applied linear regression to determine and quantify the dependence, rather than to test a specific hypothesis. We did, however, expect the positive summed joint work per stride W^{+}_{joint} to increase linearly with mass, because the joints are ultimately responsible for the positive work performed on the COM (Eqn. 2). Similarly, we expected negative summed joint work per stride W^{-}_{joint} to increase in magnitude with mass. Its magnitude should also be less than the positive summed joint work, because some negative work is performed passively through deformation of soft tissues (Zelik and Kuo, 2010).

Results

Walking with a backpack load caused a number of energetic and biomechanical effects. As expected, subjects expended more metabolic energy when carrying heavier loads, with an approximately linear increase in net metabolic rate with load. Biomechanical effects most notably included increased mechanical work, both in terms of COM work and joint work. Work rate increased approximately linearly with load, similar to net metabolic rate. As a result, net metabolic rate and work rate also increased in approximately linear proportion to each other. The specifics of these results, as well as other associated findings, are presented below and are also quantified in Table 2.1.

To serve as a baseline for comparisons, normal walking condition values were as follows. At the fixed walking speed of 1.25 m/s, subjects walked with average step length 0.662 m, step width 0.142 m, step time 0.532 s, and double support time 0.179 s. Average positive COM work per stride was 23.6 J, and positive summed joint work per stride 48.8 J. Gross metabolic rate was about 344 W, and net metabolic rate 232 W. The net metabolic cost of transport, defined as metabolic rate divided by walking speed (all in dimensionless units), was 2.57.

Load had little effect on most step parameters (Fig. 2.2). There were no significant changes in step length, width (Fig. 2.2A), and duration (Fig. 2.2B) with carried load. However, step width variability did increase significantly ($P = 0.01$, Fig. 2.2 C) and approximately linearly with total mass, by about 50% over the range of loads studied. Step length variability did not change significantly ($P = 0.06$, Fig. 2.2D). Although there was no significant change in step duration, the duration of double support did increase slightly, by about 30%. As a fraction of step period, double support times increased from about 29% to 38%.

Table 2-1: Quantitative results for walking with a backpack load.
Data shown include normal, unloaded walking in both dimensional SI units (first column) and dimensionless (second column, "d'less") form (mean ± s.d.). Linear fit parameters for slope and offset are also shown, in dimensionless form (mean ± c.i., 95% confidence interval). Degree of fit is indicated by R^2 values, and statistical significance of the linear trends by P-values for significance of overall fit. Statistically significant (S, final column) trends ($P < 0.05$) are indicated by an asterisk *.

	Normal (SI)	Normal (d'less)	Slope ± c.i.	Offset ± s.d.	R^2	P	S
Step length, mean	0.662 ± 0.024 m	0.666 ± 0.022	-0.0029 ± 0.0440	0.6738 ± 0.0161	0.00	0.89	
Step width, mean	0.142 ± 0.038 m	0.143 ± 0.040	0.0308 ± 0.0312	0.1345 ± 0.0333	0.19	0.05	
Step period, mean	0.53 ± 0.02 s	1.67 ± 0.05	0.0536 ± 0.1060	1.6763 ± 0.0507	0.05	0.30	
Step length, RMS	0.024 ± 0.009 m	0.025 ± 0.008	0.0302 ± 0.0316	0.0172 ± 0.0056	0.18	0.06	
Step width, RMS	0.023 ± 0.004 m	0.023 ± 0.004	0.0268 ± 0.0183	0.0231 ± 0.0082	0.34	0.01	*
DS duration	0.18 ± 0.05 s	0.56 ± 0.16	0.4059 ± 0.2720	0.4611 ± 0.0785	0.35	0.01	*
COM work rate, $\dot{W}^{+}_{\mathrm{COM}}$	55.98 ± 16.24 W	0.0203 ± 0.0037	0.0458 ± 0.0075	0.0197 ± 0.0048	0.90	7E-12	*
COM work rate, $\dot{W}^{-}_{\mathrm{COM}}$	-46.67 ± 8.08 W	-0.0215 ± 0.0032	-0.0355 ± 0.0091	-0.0195 ± 0.0033	0.79	3E-8	*
COM work, W^{+}_{COM}	23.63 ± 5.73 J	0.0333 ± 0.0062	0.0785 ± 0.0128	0.0331 ± 0.0079	0.90	7E-12	*
COM work, W^{-}_{COM}	-24.75 ± 4.03 J	-0.0352 ± 0.0062	-0.0612 ± 0.0153	-0.0327 ± 0.0051	0.80	2E-8	*
Joint work, W^{+}_{joint}	48.80 ± 9.20 J	0.0426 ± 0.0086	0.0982 ± 0.0491	0.0530 ± 0.0171	0.49	4E-4	*
Joint work, W^{-}_{joint}	-16.37 ± 4.46 J	-0.0141 ± 0.0033	-0.0496 ± 0.0238	-0.0326 ± 0.0114	0.51	2E-4	*
Ankle work, W^{+}_{ank}	25.39 ± 4.88 J	0.0363 ± 0.0071	0.0659 ± 0.0145	0.0351 ± 0.0083	0.83	2E-9	*
Ankle work, W^{-}_{ank}	-14.36 ± 4.55 J	-0.0206 ± 0.0066	-0.0322 ± 0.0129	-0.0220 ± 0.0094	0.60	2E-5	*
Knee work, W^{+}_{kne}	9.34 ± 2.22 J	0.0132 ± 0.0024	0.0421 ± 0.0113	0.0128 ± 0.0034	0.77	8E-8	*
Knee work, W^{-}_{kne}	20.44 ± 4.56 J	-0.0290 ± 0.0051	-0.0080 ± 0.0112	-0.0342 ± 0.0085	0.11	0.15	
Hip work, W^{+}_{hip}	33.34 ± 10.72 J	0.0483 ± 0.0195	0.0298 ± 0.0302	0.0277 ± 0.0127	0.19	0.05	
Hip work, W^{-}_{hip}	-0.84 ± 0.74 J	-0.0012 ± 0.0010	-0.0490 ± 0.0421	0.0011 ± 0.0097	0.24	0.03	*
Metabolic rate, $\dot{E}$	231.6 ± 57.1 W	0.105 ± 0.015	0.249 ± 0.055	0.0858 ± 0.0188	0.83	3E-9	*
Gross rate, $\dot{E}_{\mathrm{gross}}$	343.8 ± 67.8 W	0.156 ± 0.013	0.249 ± 0.055	0.1364 ± 0.0188	0.83	4E-9	*

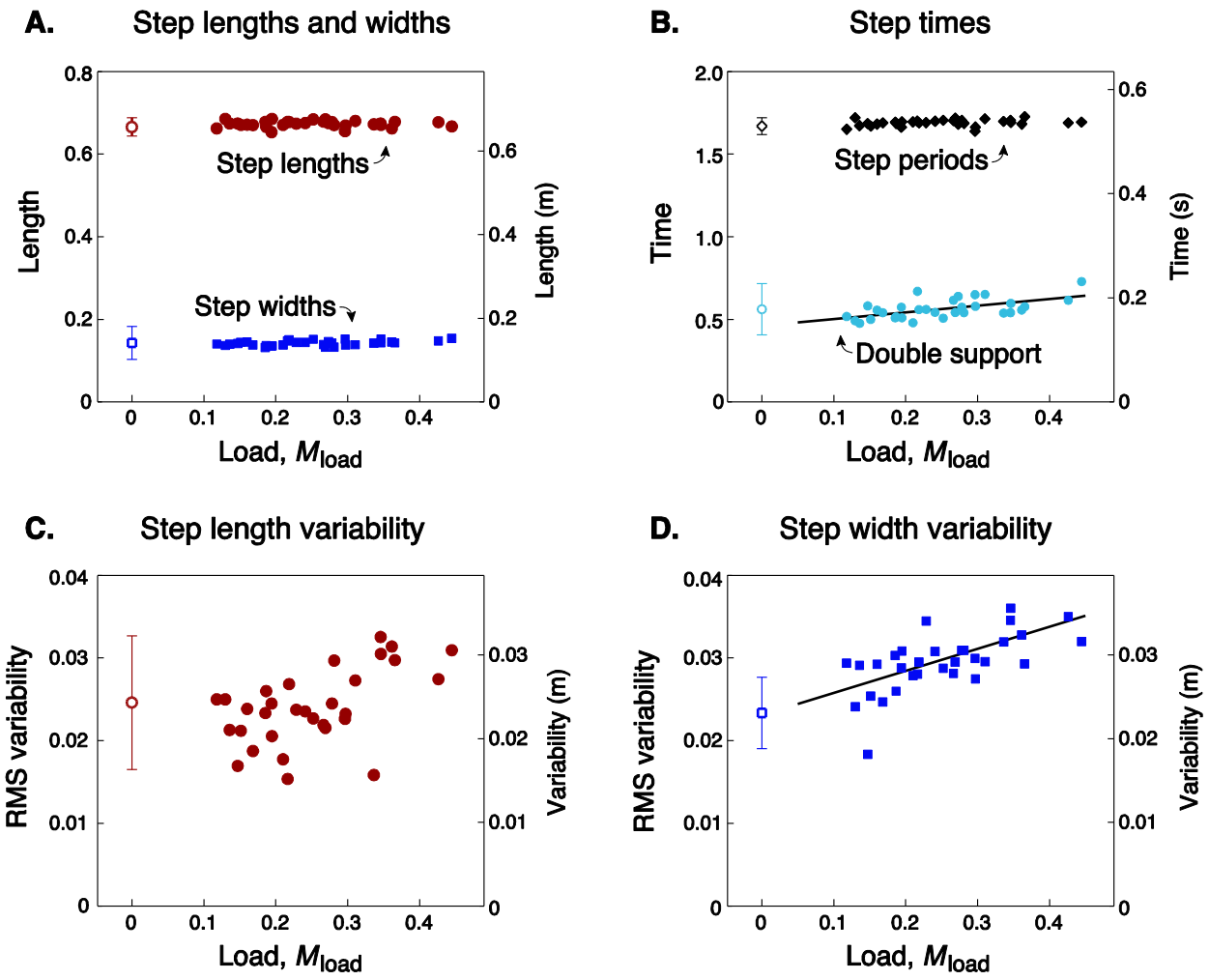

Figure 2.2: Step parameters for walking with a backpack load.
(A) Average step length and width as a function of load, as a fraction of unloaded body weight (N = 8). (B) Average step period and double support duration as a function of load. (C) Step length and (D) step width variability as a function of load, where variability is defined as root-mean-square (RMS) deviations from average steps. Solid lines represent significant linear trends with added mass ($P < 0.05$). Of the step parameters shown, only double support and step width variability exhibited significant trends, both increasing with load. Open symbols represent normal unloaded walking (with error bars for s.d.). Left-hand vertical axes show dimensionless quantities, using body mass M, leg length L, and gravitational acceleration g as base units. Right-hand vertical axes show dimensional SI units.

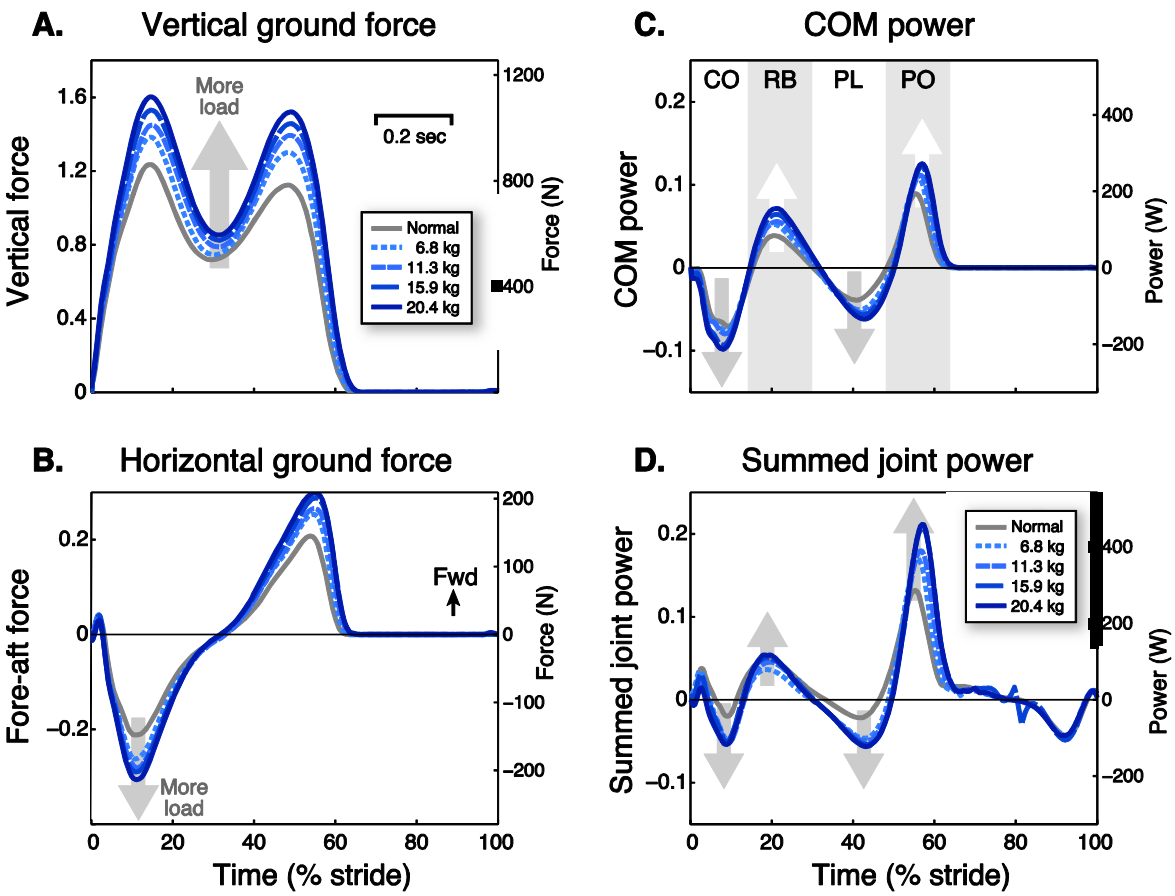

Figure 2.3: Force and power measures as a function of stride time, for different loads.
(A) Vertical ground reaction force and (B) horizontal (fore-aft) ground reaction force vs. percent stride time. (C) Instantaneous COM (center-of-mass) power P_{COM} vs. time, defined as dot product of COM velocity with ground reaction force from one leg. (D) Summed joint power vs. time, defined as sum of powers from ankle, knee, and hip from one leg. Left-hand vertical axes show dimensionless quantities, right-hand vertical axes show dimensional SI units. Data shown are trajectories averaged across subjects ($N = 8$).

In terms of mechanics, there are several qualitative observations to be made regarding the force and power trajectories (Fig. 2.3). The amplitudes of vertical and horizontal ground reaction forces increased with load (Fig. 2.3A & B), most notably in the two peaks of the vertical force. A similar trend may be observed from the COM work rate trajectories (Fig. 2.3C). Amplitudes appeared to increase with load for each of the four phases of positive or negative COM work, Collision, Rebound, Preload, and Push-off. That effect is mirrored by the summed joint power trajectories (Fig. 2.3D), which behaved roughly similarly with increasing load. Examining the joints individually (Fig. 2.4), there appeared to be little change in joint angle trajectories with load. The amplitudes of joint moments and powers did increase with load.

We next examine how work and metabolic energy expenditure rates increase with load (Fig. 2.5). The rate of positive work performed on the COM ($\dot{W}^{+}_{\mathrm{COM}}$) increased approximately linearly with total mass, and nearly doubled across the range of loads studied. Subjects performed about 1.40 W of additional positive mechanical work rate for each additional 1 kg carried by backpack (Fig. 2.5A). They also expended about 7.62 W of additional metabolic power for each additional 1 kg carried by backpack, at the designated speed of 1.25 m/s (Fig. 2.5B). Net metabolic power nearly doubled across the loads tested. To illustrate the effect of the normalization procedure, which was intended to reduce scatter due to differences in subject body mass and leg length, results are presented in terms of absolute physical units of power (W) vs. mass (kg), as well as using dimensionless variables (Figs. 2.5C and 2.5D, respectively). The linear fits for both work and metabolic cost also yield residuals (Figs. 2.5C and 2.5D), which did not obviously reveal any additional trends.

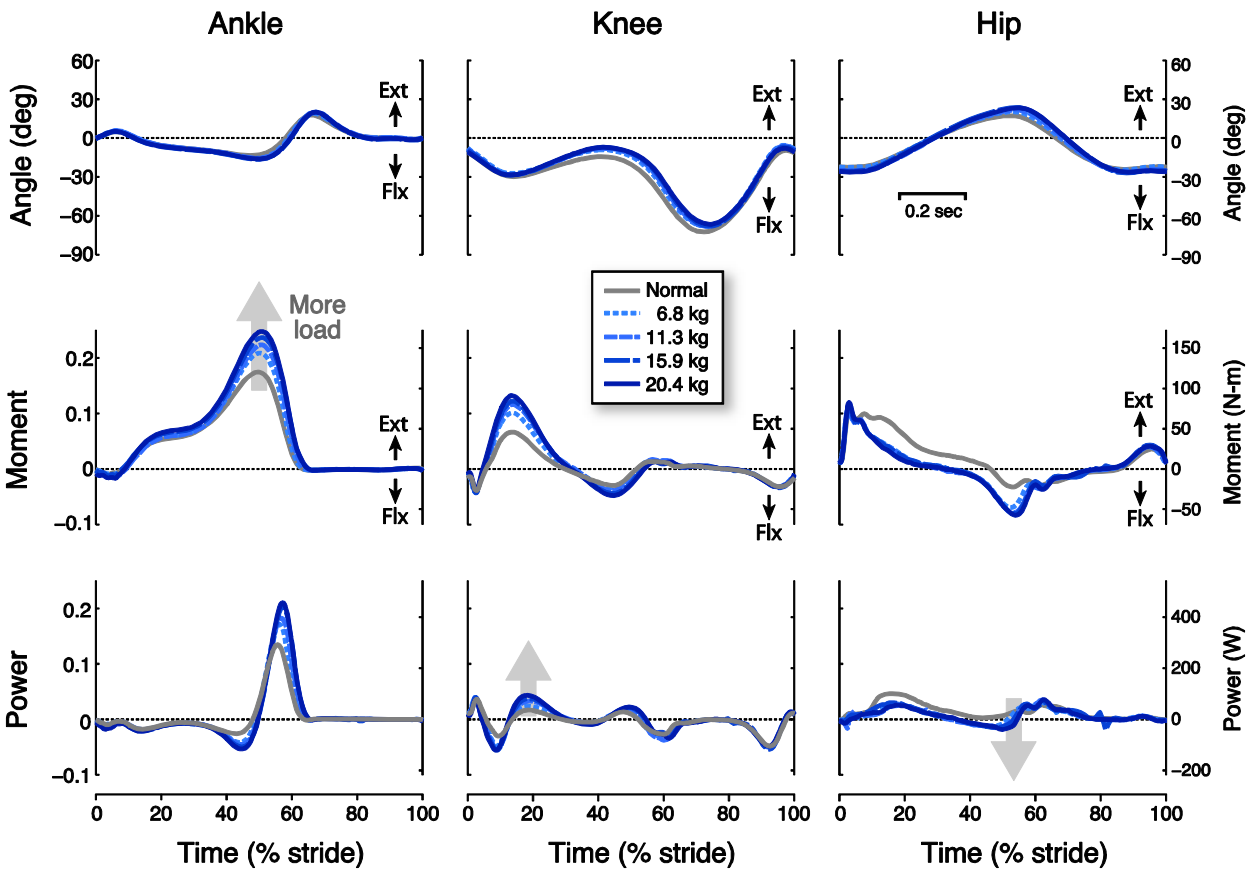

Figure 2.4: Joint kinematics and kinetics vs. stride time for walking with different loads. Angle, moment, and power trajectories are shown for ankle, knee, and hip joints. Left-hand vertical axes show dimensionless quantities, right-hand vertical axes show dimensional SI units. Data shown are trajectories averaged across subjects (N = 8). Positive angles and moments are defined in extension (Ext) as opposed to flexion (Flx).

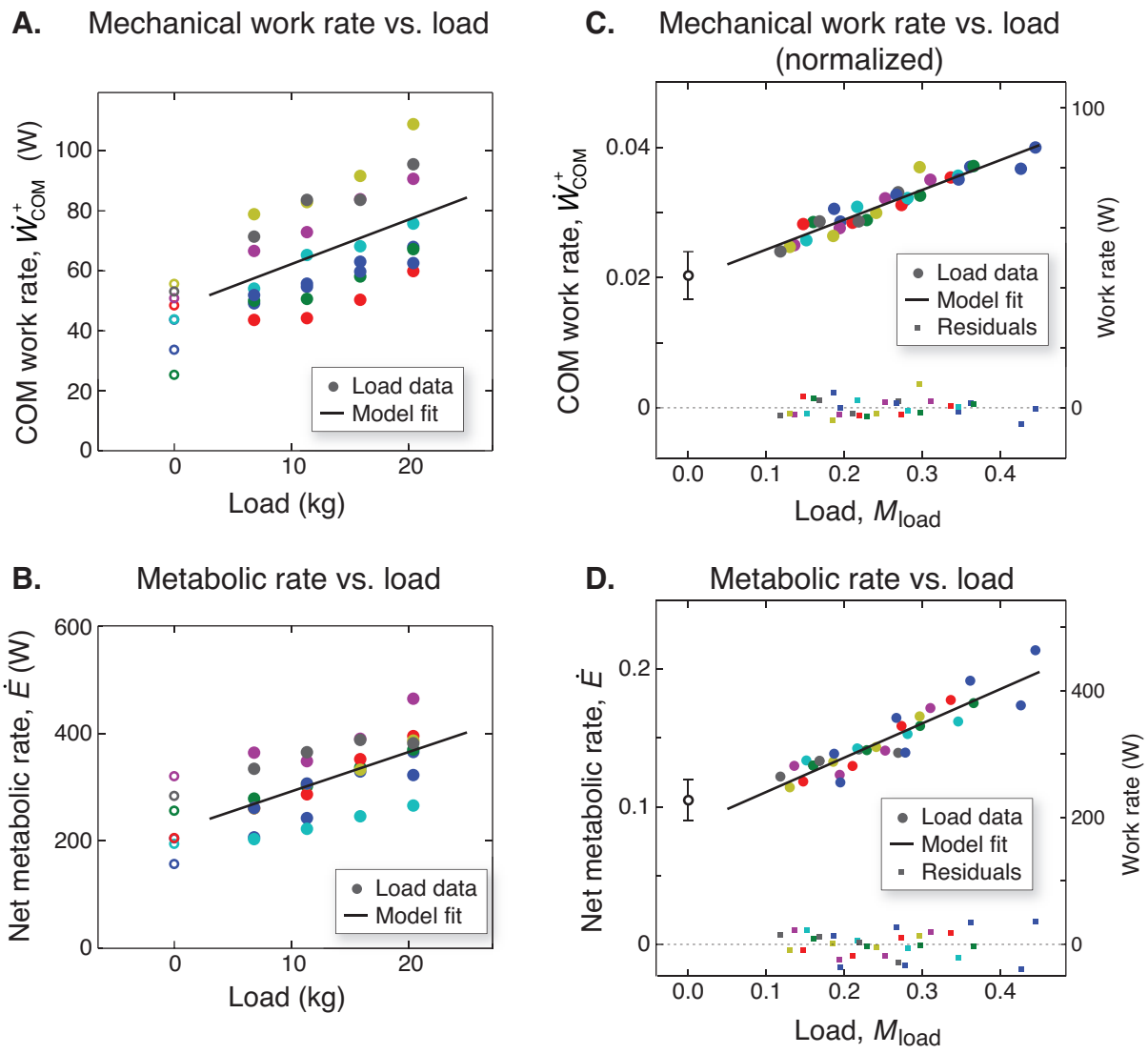

Figure 2.5: Mechanical work and metabolic energy cost as a function of load, with and without normalization.

(A) Rate of positive work $\dot{W}^{+}_{COM}$ performed on the COM and (B) Net metabolic rate $\dot{E}$ vs. added load, both in un-normalized form. Each subject's data are denoted by a separate color; open symbols denote normal, unloaded walking. (C) Normalized mechanical work rate and (D) net metabolic rate vs. load, along with residuals after subtracting the linear trend from data. Statistically significant linear trends were observed for both work and metabolic data (P = 7E-12 and 3E-9, respectively). Normalization procedure includes non-dimensionalization, using body mass M, leg length L, and gravitational acceleration g as base units. In addition, a separate y-intercept was determined for each subject's linear trend, reducing variability due to differing constant offsets. Net metabolic rate is defined as gross rate minus the rate for quiet standing. Data points for individual subjects are distinguished by color.

The work trends may be examined more closely on a per-stride basis. The work performed on the COM, and from the summed joints, both increased approximately linearly with load (Fig. 2.6A). The slopes of these increases were not significantly different (COM work per stride increased 0.76 ± 0.12 J per 1 kg of load, and joint work by 0.96 ± 0.48 J; $P = 0.77$, analysis of covariance). The amount of positive COM work was close to the negative COM work, indicating zero net mechanical work for steady state walking, but the sum of negative joint work was much less than sum of positive work, implying the soft tissue work also increased with load (Zelik and Kuo, 2012a). Examining the individual joints (Fig. 2.6B), they generally performed positive work increasing approximately linearly with load. Work is normally performed by the ankle, hip, and knee, in decreasing order of contributions. With carried loads, however, the greatest increases were at the ankle, knee, and (with marginal significance) hip, in decreasing order. The joints also normally perform negative work at the knee, ankle, and hip (in decreasing order of magnitude). With load these magnitudes increased at the hip and ankle, with no significant effect at the knee.

Work and metabolic energy expenditure may also be compared against each other (Fig. 2.7). A total least squares fit between COM work rate and metabolic rate yields slope 6.394 ± 0.246 (c.i.) and offset -0.051 ± 0.008 (Eqn. 4). The inverse of the slope yields an efficiency $\eta = 0.156 \pm 0.006$ for COM work. A similar calculation with summed joint power yields an efficiency 0.163 ± 0.059 for summed joint work.

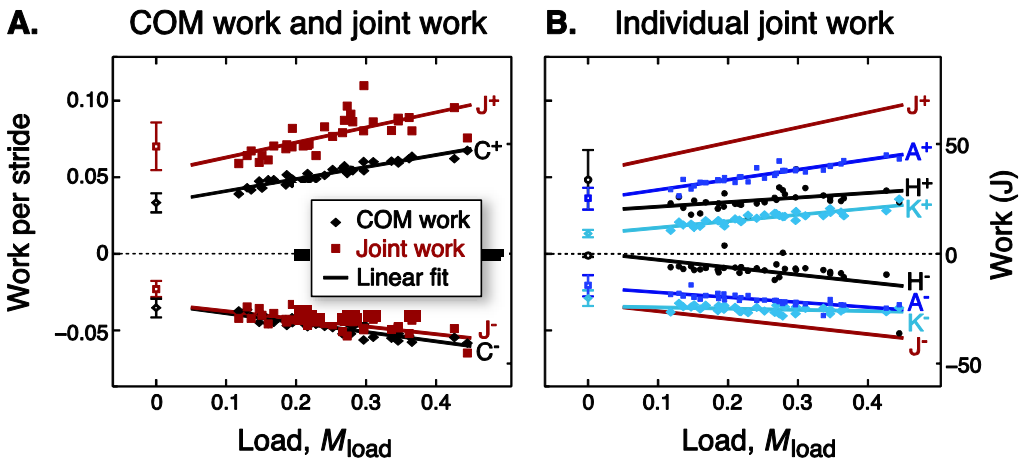

Figure 2.6: Mechanical work as a function of load mass.

(A) Average positive COM work W^{+}_{COM} and summed joint work per stride W^{+}_{joint} (labeled C^{+} and J^{+}, respectively), along with negative work (C^{-} and J^{-}). (B) Positive work by ankle, knee, and hip joints (A^{+}, K^{+}, H^{+}, respectively; negative work also shown), compared to summed joint work per stride. Linear trends (denoted by lines, $N = 8$) were fit to each measure, and were statistically significant ($P < 0.05$) in all cases except for negative knee work and positive hip work. Open symbols represent normal unloaded walking (with error bars for s.d.). Left-hand vertical axes show dimensionless quantities, right-hand vertical axes show dimensional SI units.

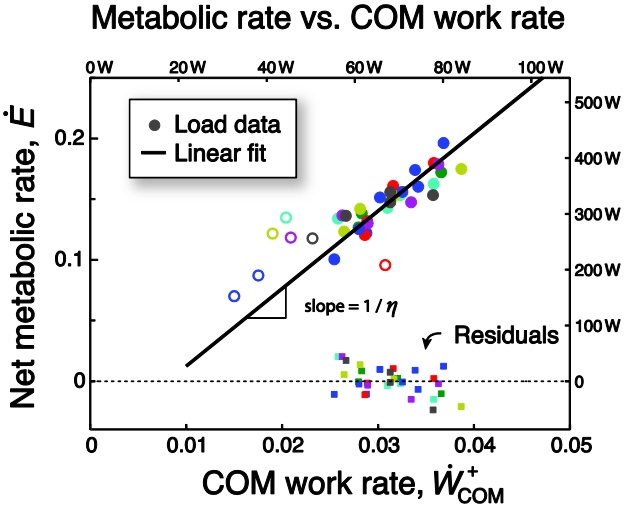

Figure 2.7: Net metabolic rate vs. positive COM work rate for walking with varying amounts of backpack load.
Also shown are residuals after subtracting a linear trend fit (solid line; total least squares fit applied to load data only). A significant trend was found with slope 6.394 (± 0.246 c.i., 95% confidence interval) and offset -0.051 ± 0.008 (s.d.). Reciprocal of slope yields $\eta = 0.156 \pm 0.006$, meaning a delta efficiency of positive work of about 16%. No obvious trend was observed in the residuals. Left-hand vertical axes show dimensionless quantities, right-hand vertical axes show dimensional SI units, and similarly for bottom and top axes. Data points for individual subjects are distinguished by color.

Discussion

This experiment was intended to test whether a carried load proportionally increases the work performed on the COM, and whether that work leads to a proportional increase in metabolic energy expenditure. We had hypothesized that a backpack load mainly affects the inertia of the COM, which must be redirected in the transition between pendulum-like steps. The load should also have little effect on the work performed for motions relative to the COM, and on other metabolic energetic costs not related to work. Our results yielded three main linear proportionalities between load, mechanical work, and metabolic energy expenditure. We next consider how well the results agreed with these expectations, and examine the complementary measures of joint work, which may indicate how the body performs the greater workload.

Backpack loading resulted in approximately proportionate increases in mechanical work (Fig. 2.6). A linear fit suggests that the increased COM work is largely explained by the added mass. This is because redirection of the COM is determined mainly by mass, walking speed, and step length (Adamczyk and Kuo, 2009). Here, only mass was varied (as the independently controlled variable) and speed was kept fixed. Subjects tended to maintain nearly the same step parameters (Fig. 2.2) and joint kinematics (Fig. 2.4), leaving little opportunity to change how the COM was redirected. This means that COM work is mainly determined by how much mass is redirected, as predicted by Eqn. 2. An approximately linear increase was also observed in the positive summed joint work (W^{+}_{joint}). This is largely as expected, because COM work must largely result from actions at the joints. In addition, the joints also perform work to move the limbs relative to the COM, as indicated by the difference between summed joint work and COM work (Fig. 6; about 38% of summed joint work). While most of the joint work may be attributable to moving the COM, a smaller amount of work is also performed to move body segments relative to the COM.

The individual joint powers reveal more detail about the distribution of work (Fig. 2.4). We had no prediction for the apportionment between joints, but much of the increase with load appeared to occur at the ankle during Push-off, which produces the largest proportion of the positive work in both unloaded and loaded walking. The knee also performed increasing positive work, mostly during Rebound (Fig. 2.4 knee power). In contrast, the hip only performed marginally more work with mass. As for negative work, its magnitude also increased, primarily at the hip, and mostly near the end of swing phase. This might aid the faster swing that occurred with increasing double

support time and relatively constant stride time (Birrell and Haslam, 2009; Martin and Nelson, 1986). These various changes in joint work accounted for the largely parallel changes in summed joint work and COM work with load.

Closer examination of joint work also reveals possible roles of tendon and other soft tissues. Tendons are highly elastic, as exhibited by considerable passive energy return at the ankle during walking (Fukunaga et al., 2001). Here, increasing mass led to greater amplitude in the sequence of ankle Pre-load and Push-off, where negative and then positive work is performed. Similarly, the amplitude of negative Collision work of the knee was apparently accompanied by greater positive Rebound work (Fig. 2.4 knee power). Both sequences may benefit from elastic energy return, as is implied by our terminology (Donelan et al., 2002b; Kuo et al., 2005b). Indeed, the increase in double support duration (Fig. 2.2D) is consistent with a spring-mass system, whose natural frequency decreases with greater mass. The amplitude of both COM and joint powers also increase with mass (Figs. 2.3B and D), also consistent with a driven mass-spring oscillation, as previously proposed by Holt et al. (2003). Aside from tendon elasticity, other soft tissues such as the viscera and heel pad can act as passive, damped elastic elements. They can thus perform work not captured by inverse dynamics (Zelik and Kuo, 2010; Zelik and Kuo, 2012a). Here, the negative summed joint work was considerably lesser in magnitude than the corresponding positive work, ranging about 57 – 61% of positive work for the loads examined. This suggests some negative work was performed by soft tissue deformation (DeVita et al., 2007; Zelik and Kuo, 2010) and not captured by joint work, because the body must perform equal amounts of positive and negative work to walk at steady speed. These results suggest the possibility of elastic and damped elastic energy return during walking with load carriage.

We also observed an approximately linear increase in net metabolic rate with load (Fig. 2.5D), expected from Eqn. 3. The cost may be described by the increase in net metabolic rate per extra load as a fraction of body weight (c' in Eqn. 3), with a value of about 0.25, which exceeds the corresponding value of 0.11 for net metabolic rate of normal unloaded walking (or 0.16 for gross rate, Table 1). These measures suggest that humans expend relatively more energy to carry a backpack load than to carry an equivalent amount of their own body mass. The metabolic cost is also consistent with the approximately linear increase observed for mechanical work (Fig. 2.5B), assuming a constant efficiency. The observed delta efficiency (Eqn. 4) was about $\eta = 15.6\%$ for

positive COM work, and about 16.3% for positive summed joint work. These are somewhat lower than the typical 25% efficiency for positive work by muscle (or 21% if the cost of negative work is also included; Donelan et al., 2002b). Both work measures may tend to underestimate actual muscle work, due to positive work at one muscle that inadvertently cancels negative work by another, even though both may exact a metabolic cost. This may occur in the form of co-contraction about a single joint, or as cancellation across multiple joints. Motion capture-based measures of mechanical work cannot generally resolve such effects, nor can they easily quantify passive work by elastic tendon. We nevertheless prefer simple measures such as COM work, because its trends can be predicted from simple models, whereas those for the individual joint powers are far more challenging to predict from first principles. As a complementary measure, summed joint power is also relatively simple and helps to indicate work performed for body motions relative to the COM (Zelik and Kuo, 2010).

A number of other factors aside from work are expected to contribute to metabolic energy expenditure. Walking also requires maintenance of balance and motion of the arms and legs relative to the body, among other features. It is possible that load carriage places increasing demands on balance, as perhaps indicated by increasing step width variability (Fig. 2.3). Such variability is thought to contribute to energy expenditure (O'Connor et al., 2012), but in quite small amount relative to the large increases observed here. These and other costs appear to contribute quite substantially to the overall cost of walking, but relatively little to the change in energy expended with increasing backpack load.

Our results may be compared with other published studies. Others have reported relatively subtle changes in step parameters and kinematics with moderate loads (Harman et al., 2000; Martin and Nelson, 1986), which appeared to occur here as well. There are few other studies quantifying joint work as a function of load (e.g. peak power quantified by Chow et al., 2005), but the results for unloaded walking appear consistent with the literature (Winter, 2005; Zelik and Kuo, 2010). As for COM work, our measure (W^{+}_{COM}) is equivalent to the "individual limb external work" of Griffin et al. (2003), and to the "total work" of Grenier et al. (2012) which sums the "external work" for combined limbs with the "internal work during double contact". (There are inconsistent definitions implied for "external" and "internal" within the literature, and so we

prefer the term "COM work.") Accounting for the different walking speeds applied, our work results are largely consistent with those studies.

Our metabolic energy results are also comparable to the literature. A number of previous studies have reported approximately linear increases with mass (Griffin et al., 2003; Pierrynowski et al., 1981; Soule et al., 1978). For an extra load of 30% body mass, we observed the equivalent of about 40% increased gross metabolic cost, similar previous reports (Pierrynowsi et al., 1981; Quesada et al., 2000). It must be noted that some studies have reported somewhat lower metabolic costs, for example 20 – 35% by Griffin et al. (2003) depending on speed, and about 25% by Grenier et al. (2012). Studies often differ in the means of load attachment, which included a waist belt (Griffin et al., 2003) and military load attachment (Grenier et al., 2012), which could affect metabolic costs. Our subjects were also relatively unpracticed with the backpack, whereas others (e.g., Grenier et al., 2012; Polcyn et al., 2002) have examined practiced infantrymen, who may be better adapted to carrying a backpack. Despite these and other differences, most studies appear to agree on an approximately proportionate metabolic cost increase with added mass, if not the actual value of that proportionality.

Our results also lead to slightly different conclusions from some other studies. Griffin et al. (2003) found that locomotor efficiency, defined as COM work rate divided by net metabolic rate, varied with load and speed between about 16 and 28%. That non-constancy led them to conclude that work cannot explain the metabolic cost of load carriage, in favor of a metabolic cost of generating force to support body weight. We suspect the variation in efficiency results from non-zero offsets present in work and energy data. Non-zero offsets arise for a variety of reasons, including the somewhat arbitrary designation of quiet standing as the baseline for net metabolic rate. Our preference is to ignore the offsets and concentrate on the changes in energy and work (Fig. 7) in delta efficiency, which does appear to be quite consistent, and can explain metabolic energy expenditure in terms of work. Although we cannot eliminate other costs for load carriage, they must either be independent of load, or contribute to the constant offset or the (rather small) residual (Fig. 7), or be correlates of work that are therefore difficult to separate from work. Regarding the residual, we have observed substantial residuals for other tasks such as bouncing about the ankles that we believe to be costly and unrelated to work (Dean and Kuo, 2011). Yet there was no obvious trend in the residuals found here. Furthermore, re-examination of Griffin et

al.'s (2003) data yields a fairly constant delta efficiency (of about 27% with $R^2 = 0.96$ for a fit through means across subjects for 16 combinations of speed and load), and a similar offset to what we observed ($\dot{E}_0$ of 0.010 vs. 0.008). For our data, we can also form a conservative estimate of the minimum cost of work, by assuming that the positive work measured here was not an underestimate, and that negative work has no energetic cost. Applying an efficiency of 25% efficiency, positive mechanical work alone would still account for a minimum of about two-thirds of the metabolic cost we observed. This leads us to favor mechanical work as the primary cause of increased metabolic cost for load carriage, similar to the conclusions of Grenier et al. (2012).

Our experiment entailed a number of simplifications. Subjects walked on a smooth treadmill surface at fixed speed, whereas typical load carriage is often performed at self-selected, non-constant speed and on uneven ground, where there may be additional metabolic costs and challenges to balance. We also examined only moderate loads, whereas heavier loads may entail a more nonlinear and greater relative metabolic cost (Soule et al., 1978) and different kinematics (Attwells et al., 2006; Birrell and Haslam, 2009). We also did not study the effect of the load's position on the back, which can potentially affect the COM location and energy expenditure (Stuempfle et al., 2004). We instead placed the loads at one consistent location on the back, as might be typical of many applications. As discussed above, the measures of COM work and joint work are both imperfect indicators of actual muscle work. Muscle work, even if the accurately measured, also does not necessarily indicate actual metabolic cost, as when activation and deactivation costs are high (Dean and Kuo, 2011). These limitations may cause differences between the results reported here and actual walking with load carriage.

There are nevertheless some findings that may apply to load carriage in general. A backpack load increases the mass that must be redirected through COM work, appears to have relatively little effect on gait kinematics and the amount of redirection. The result is a proportionate increase in COM work, accomplished mostly by the ankle and knee for positive work, and the hip for negative work. The increases in COM work (and summed joint work) appear to translate into a proportional increase in metabolic energy expenditure. While other metabolic costs might also contribute to walking, their contributions appeared to be either relatively fixed despite added mass, or correlated with (and therefore not separable from) the work we observed. The largest

effect of a carried backpack load appears to be a proportional increase in mechanical work, with a proportional increase in metabolic cost.

Chapter 3 Dynamic walking model predicts the energetic cost of human walking with carried loads and different speed

Abstract

The energetic cost of human walking increases with both walking speed and carried load. The mechanical work performed by the legs on the center of mass by each leg seems to explain the energetic cost as a function of each variable alone. However, there lacks a biomechanical mechanism explaining how and why mechanical work should increase with both walking speed and carried load. In this study, we used two dynamic walking models with rigid legs and compliant legs to provide an explanation of how the energetics and mechanics of human walking are changed at different walking speeds and carried load, and compared to the empirical results.

A dynamic walking model with rigid legs predicts that the mechanical work performed on the body center of mass during walking is a function of walking speed, total mass and step frequency. We therefore tested normal adults (N = 9) walking at different speeds (1.0-1.75 m/s) and carried loads (6.8 – 20.4 kg). We measured the mechanical work performed on the body center of mass and metabolic energy expenditure through respirometry. The metabolic energy expenditure is proportionate to the mechanical work with a constant delta efficiency of 16.9%. The mechanical work performed on the body center of mass was found as a function of total mass, walking speed and step frequency, as predicted by the rigid leg model. However, the rigid leg model cannot explain the ground reaction force and the double support duration of walking at different speed and with different carried loads. We therefore use a compliant leg walking model to explain how ground reaction force and double support duration change with walking speeds and carried loads. We found a good match between the empirical data and the SLIP model simulation if we choose leg stiffness and step length as a certain function of total mass and walking speed.

Introduction

Humans expend considerably more effort to walk at faster speed and with carried loads. Metabolic energy expenditure increases sharply with walking speed and the carried load, as does the mechanical work performed by the lower extremity muscles(Grenier et al., 2012; Griffin et al., 2003). According to basic physical principles, it requires energy to perform active mechanical work. The metabolic energy expenditure of human walking at faster speed and with carried load can be the result of performing extra active mechanical work, but there lacks of mechanistic explanation how the mechanical work increases with the walking speed and carried load. The purpose of this study is to provide mechanistic explanation how the walking speed and carried load affect the energetics and mechanics of human walking, using two simplified dynamic walking models.

Two types of pendulum-like dynamic walking models are sometimes used to explain energetics and mechanics of human walking. The first one is the simplest inverted pendulum model, termed as rigid-leg model in this study. The body center of mass (COM) is located near the pelvis and moves in an arc determined by the pendulum-like stance leg (Fig. 3.1). The COM velocity must be redirected upward between the end of one step and the beginning of the next (Adamczyk and Kuo, 2009; Kuo, 2002b). This entails negative, dissipative work by the leading leg's collision with ground, which is compensated by positive push-off work from the trailing leg (Donelan et al., 2002b). The energetic cost depends on the amount of positive push-off work, which is a function of walking speed, carried load and step frequency. This model has been tested to for speed alone and load alone, but has not been tested for both speed and load together. The limitation of rigid-leg model is that there is no double support period and the shape of vertical ground reaction force is pretty different from the empirical human walking data. The vertical ground reaction force of human walking has an M-shape profile, but the rigid-leg model has a single hump profile with two instantaneous impulses.

The second type of model is the spring-loaded inverted pendulum (SLIP) model, here termed as compliant-leg model, which assumes each leg acts like a linear spring. The periodic dynamics of leg springs determines the mechanics of walking. The compliant-leg model can generate human-like ground reaction force (Geyer et al., 2006; Whittington and Thelen, 2008) and has double support phase. Kim and Park (2011) used the compliant-leg model to characterize the leg

stiffness of human walking and found leg stiffness increase for faster walking speed. Holt et al.(2003) also used a compliant-knee model to characterize the knee stiffness increases with walking speed and carried load. Nevertheless, the compliant-leg model cannot predict the mechanical work because of the passive-spring assumption and the spring constant is arbitrary.

In this study, we test whether the rigid and complaint legs can provide complementary prediction, and whether there is a degree of compatibility between the two models. We first used a rigid-leg dynamic walking model to predict how the mechanical work perform on the center of mass (COM work) by each leg increases as a function of walking speed, total mass and step frequency. We then used the compliant-leg model to predict how double support period changes with carried loads and walking speeds.

Method

We first used the rigid-leg model to predict how mechanical work changes with different total mass (carried load) and walking speed, then we used the compliant-leg model to predict how double support duration changes with total mass and walking speed. We then tested healthy adults walking with carried loads and different walking speeds. We measured the metabolic energy expenditure and the mechanical work performed on the COM by each leg. We compared the experimental results to the rigid-leg model and compliant-leg model.

Model

Both rigid and compliant leg models have concentrated mass at pelvis and infinitesimal mass at each foot. The legs rotate freely about pelvis during swing with no cost. We modulated the step length and walking speed using a hip spring. The relationship between step length and walking speed is based on empirical result from previous study (Grieve, 1968) . All the units are dimensionless.

$$s \propto v^{0.42} \tag{3-1}$$

Rigid-leg model

The rigid-leg model has two degree of freedom during single support phase, comprising the rotations for each leg (Fig. 3.1 A). During stance phase, the COM moves atop the stance leg along the inverted pendulum arc. At the step-to-step transition, the COM velocity is redirected from the trailing leg inverted pendulum arc to the leading leg inverted pendulum arc in part by the impulsive collision. The kinetic energy is dissipated by the collision and equal amount of positive work is required to offset the energy loss. The energy dissipated by collision can be reduced by applying positive work, termed push-off, immediately preemptive to the collision. The total positive work, including the work performed by push-off and during stance phase, can be minimized with an equal amount of push-off and collision and no extra work during stance phase. The amount of positive work per step W_{PO} for optimized case depends on the total mass M, COM velocity before heel-strike v^{-} and the ankle between legs α.

$$W_{\mathrm{PO}} = \frac{M}{2}(v^{-}\tan(\alpha))^2 \tag{3-2}$$

Simplify Eqn 3-1 by substituting v^- by average walking speed v and using a small angle approximation.

$$\tan(\alpha) \approx \alpha \approx \frac{s}{2} \tag{3-3}$$

$$W_{\mathrm{PO}} \propto Mv^2s^2 \tag{3-4}$$

In steady state walking, the step length s, walking speed v and step frequency f yield the following relationship.

$$s = v/f \tag{3-5}$$

Substitute Eqn. 3-4 into Eqn. 3-3

$$W_{\mathrm{PO}} \propto Mv^4f^{-2} \tag{3-6}$$

The positive work per step W_{PO} indicates how much mechanical work is required for each step. The average positive work rate, defined as work per step W_{PO} times step frequency f, yields

$$\dot{W}_{\mathrm{PO}} \propto Mv^4f^{-1} \tag{3-7}$$

We test for Eqn 3-7 from the empirical data to verify this model. Also, the relationship between step length and walking speed ($s \propto v^{0.42}$) can be applied here (Grieve, 1968). Therefore, Eqn. 3-7 becomes

$$\dot{W}_{\mathrm{PO}} \propto Mv^{3.42} \tag{3-8}$$

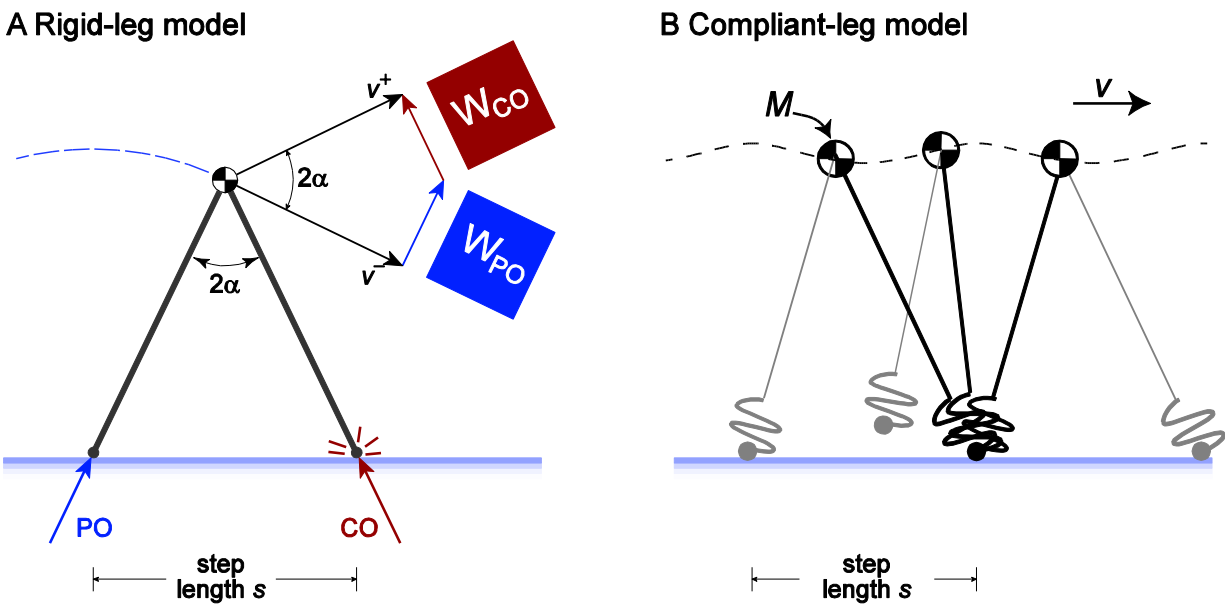

Figure 3.1: Rigid-legged (A) and compliant-leg model (B).

Compliant-leg model

The compliant-leg model has a linear spring for each leg (Fig. 3.1B). We searched for the limit cycle for different walking speeds and total mass by changing the initial condition at the beginning of a gait and the stiffness hip spring. We modulated the step length according to Eqn. 3-1(Grieve, 1968).

We therefore choose the natural frequency of the mass-spring system for stance leg to match the step frequency

$$2\pi f \propto \omega_n = \sqrt{k_{\text{leg}}/M} \tag{3-9}$$

Substitute Eqn 3-9 into Eqn 3-10, the leg stiffness becomes a function of total mass and walking speed.

$$k_{\text{leg}} \propto 4\pi^2 M v^{1.16} \tag{3-10}$$

We added a constant term to Eqn. 3-10 and tuned the constant slightly for a reasonable result. We ended up using Eqn. 3-12 for leg stiffness.

$$k_{\text{leg}} = 4\pi^2 M v^{1.16} + 5 \tag{3-11}$$

In summary, we constrained the step length s, total mass M, walking speed v and leg stiffness k_{leg}, and then searched for a limit cycle. We calculated the mechanical power performed by each leg (COM power), ground reaction forces, COM velocity, and double support duration of model walking with different walking speeds (0.32-0.50 dimensionless unit) and total mass (1-1.4 dimensionless unit).

Simulations show that the amplitude of COM power increases with faster walking speeds (Fig. 3.2 A) and total mass (Fig. 3.2 B). The peaks of ground reaction forces in vertical and horizontal direction also increas with faster walking speed (Fig. 3.2 C) and total mass (Fig. 3.2 D). However, the trough of the vertical ground reaction force around between the peaks decreases with faster speeds (Fig. 3.2 C), in contrast to the increasing of trough with heavier loads (Fig. 3.2 D). The COM velocity trajectories in forward direction shift up for faster speeds and the trajectories in vertical direction fluctuates with larger amplitude for faster speeds (Fig. 3.2 E). The COM velocity trajectories have no significant change with increased loads. The effects on COM velocity trajectories can be better visualized by the hodograph (Fig. 3.2 G & H), which is plotted with forward velocity as horizontal axis and vertical velocity as vertical axis. As walking speed increases, the hodograph shifts to the right, and expanded in vertical direction, indicating more vertical displacement of COM.

The average positive COM work rate, defined as the positive COM work per step times step frequency, increases with faster walking speeds (Fig. 3.3 A) and heavier carried loads (Fig. 3.3 B). The double support duration decreases with faster walking speed (Fig. 3.3 C) but increases with carried loads (Fig. 3.3 D).

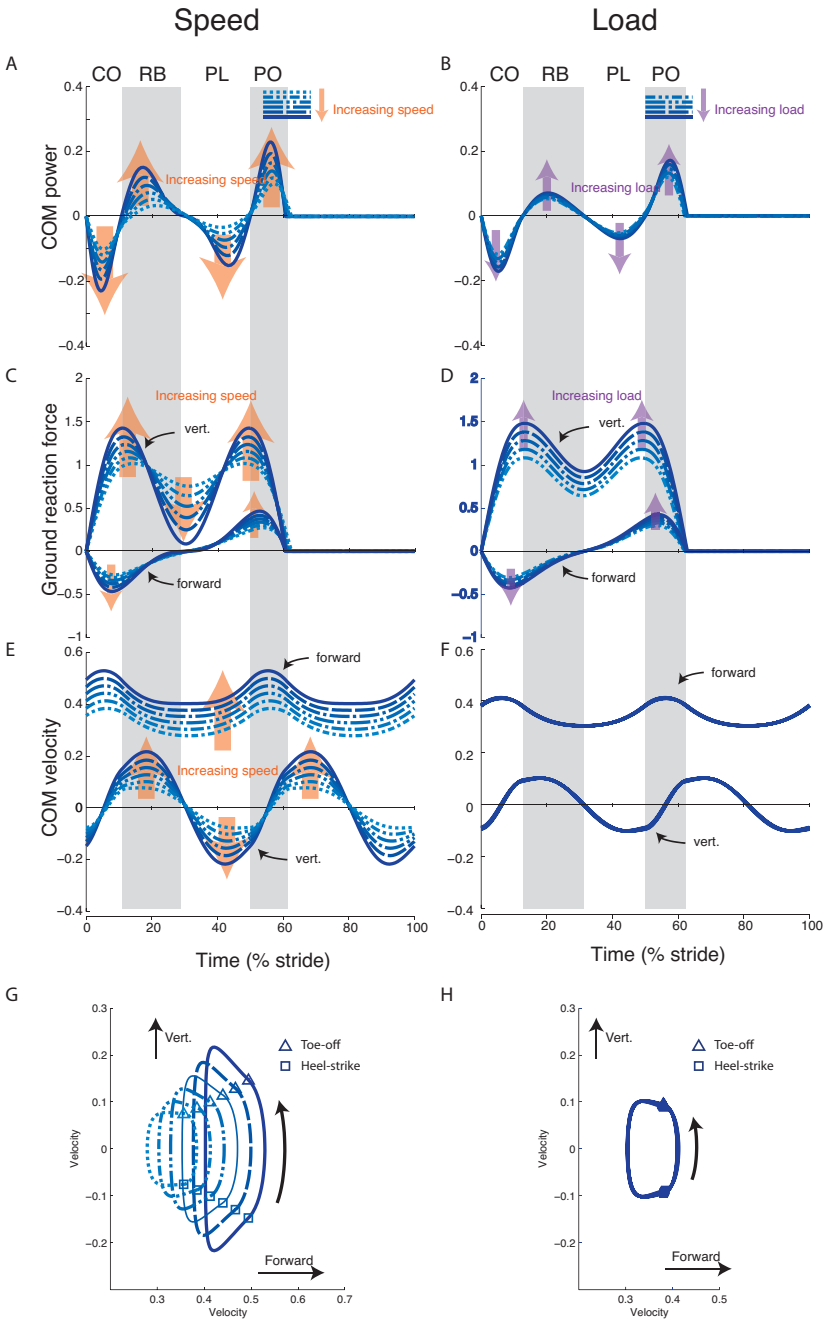

Figure 3.2: Compliant-leg simulation results: COM power, ground reaction force and velocity. (Left column) Walking with increasing speed and constant load ($M = 1, v = 0.32 - 0.5$). (Right column) Walking with increasing load and constant speed ($M = 1 - 1.4, v = 0.4$). The instantaneous COM power (A & B), ground reaction force (C & D) and COM velocity (E & F) measures as a function of stride time for different walking speed (left column) and loads (right column). Hodograph of COM velocity (G & H). Stance phase is divided into Collision (CO), Rebound (RB), Preload (PL) and Push-off (PO) regarding to the sign of COM power.

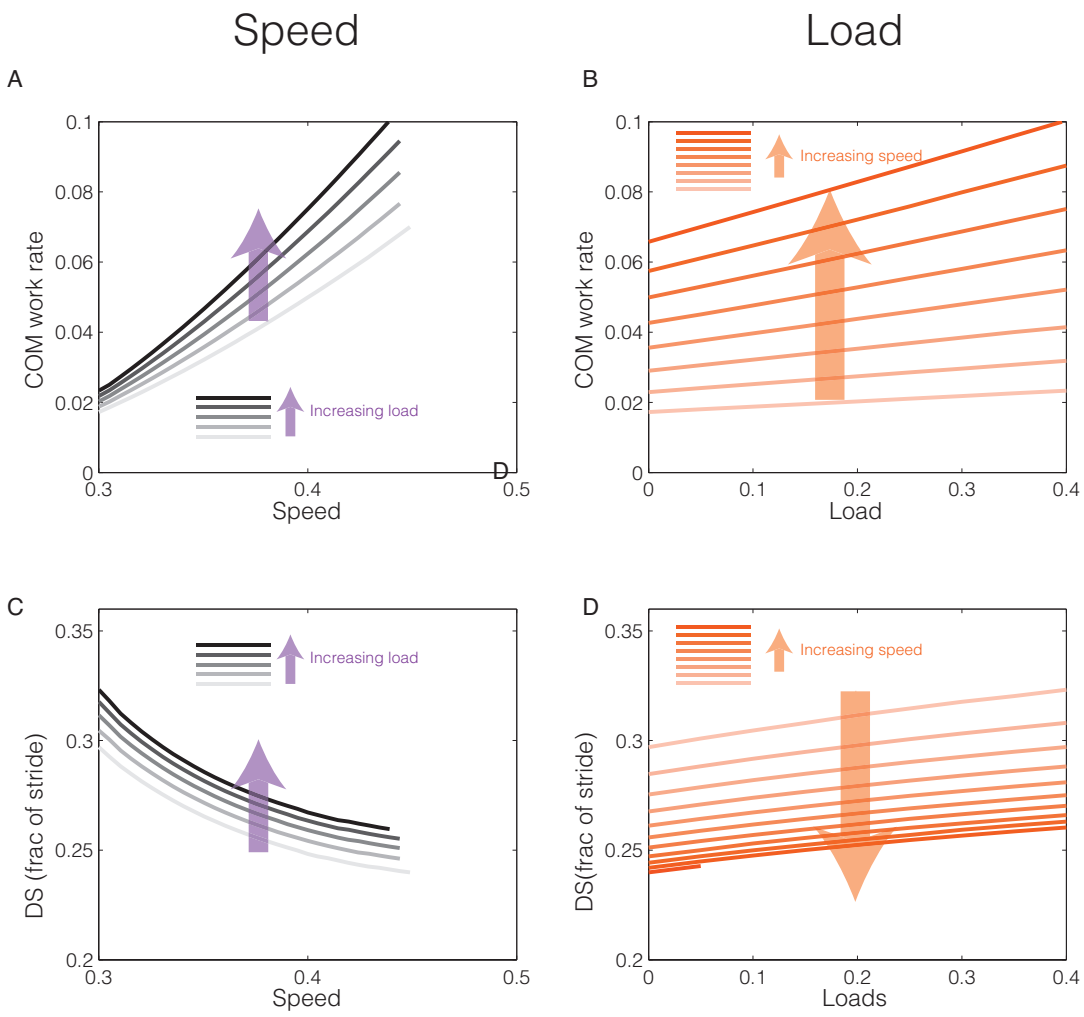

Figure 3.3: Compliant-leg simulation results: COM work rate and double support duration. Average positive COM work rate (A & B) and double support (DS) duration (C & D) as functions of speeds and loads. (Left column) Walking with increasing speed and constant load ($M = 1, v = 0.32 - 0.5$). (Right column) Walking with increasing load and constant speed ($M = 1 - 1.4, v = 0.4$).

Experiment

To test rigid-leg model predictions, we measured the mechanical work perform by each leg on body COM and the net metabolic rate as function of speed and load. We also measured the double support duration, COM power and velocity trajectories to compare to the simulation results of compliant-leg model.

Nine healthy adults (N = 9, 7 male and 2 female) were tested walking with different carried loads (6.8 – 20.4 kg) and speeds (1.0-1.75 $m \cdot s^{-1}$). Subjects ranged 18-29 years of age and had average body mass M of 78.6±12.8 kg (mean±s.d.) and leg length L, 0.97±0.06 m. We tested subject walking at their preferred step frequency and step length for each trial. We estimated the metabolic rate of steady state walking with indirect respirometry. A custom instrumented force treadmill was used to measure the ground reaction force during walking (Collins et al., 2009). All subjects provided informed consent prior to the study, according to Institutional Review Board procedures.

The metabolic rate was expressed in units of power using standard conversion factors (Brockway, 1987a). Each walking trial lasted at least 8 minutes, with the first 3 minutes discarded to ensure steady state, and average power computed from the remaining duration. Net metabolic rate $\dot{E}$ was calculated by subtracting metabolic power for quiet standing (105.13±21.28 W,0.042±0.006 dimensionless) from the gross metabolic power.

The instantaneous COM work rate P_{COM} is defined as the inner product of ground reaction force $\vec{F}$ of each leg and COM velocity $\vec{v}_{\mathrm{COM}}$ (Donelan et al., 2002c),

$$P_{\mathrm{COM}} = \vec{F} \cdot \vec{v}_{\mathrm{COM}} . \tag{3-13}$$

The COM velocity was computed from the integration of total ground reaction force, subject to constraints on periodicity. The positive work per stride W^{+}_{COM} was calculated from the integration of positive intervals of instantaneous COM work rate P_{COM} over each stride, and the average rate of positive COM work $\dot{W}^{+}_{\mathrm{COM}}$ was defined as the positive COM work per stride divided by stride time and multiplied by 2 for two legs (and similarly for negative work, $\dot{W}^{-}_{\mathrm{COM}}$). Thus, while work per stride is a single-leg quantity, average mechanical work rate is for both legs, to facilitate comparison with net metabolic rate to yield apparent efficiency. We also qualitatively examined four phases of COM work rate defined from positive and negative intervals: Collision, Rebound, Preload and Push-off (Donelan et al., 2002b).

We analyzed data with respect to the predictions from the rigid legged dynamic walking model using least squares regression method. We expect the positive COM work rate will increase depending on the added mass, walking speed and step frequency according to Eqn. 3-7.

Contracting the rigid-leg model (Eqn. 3-7) with the preferred step frequency and speed relationship, we expect the positive COM work will increase proportionately to $Mv^{3.42}$(Eqn 3-8). We also expect a linear relationship between the positive COM work rate and the net metabolic rate with a constant delta efficiency.

Results

Walking with a carried load and at faster speeds caused increases in ground reaction force, COM work rate and net metabolic rate. The positive COM work rate increased as a function of carried load and speed, agreeing with the rigid legged dynamic walking model prediction (Eqn 3-7 and 3-8). The net metabolic rate can be explained by the positive COM work rate, with a constant delta efficiency of 16%.

Several qualitative observations can be made regarding the power, force and velocity trajectories (Fig. 3.4). The amplitude of COM work rate in each phase increases with walking speed and carried load (Fig. 3.4 A & B). Carried load seems to have a uniform effect on COM work rate in each phase, but increasing walking speed seems to result greater increase of amplitude of COM work rate during collision than other phases. Similarly, the ground reaction force (Fig. 3.4 C & D) increased with walking speed and carried load. Walking speed seems to have greater effect on the first peak of vertical ground reaction force than the second one, contracting to the uniform increase due to carried load. The forward COM velocity trajectories shift upward as walking speed increase, and the amplitude of vertical COM velocity increases with walking speed (Fig 3.4 E). The COM velocity trajectories appear unchanged with carried load (Fig. 3.4 F). The effects on COM velocity trajectories can be better visualized by the hodograph (Fig. 3.4 G & H), which is a plot of the vertical vs. forward components of COM velocity. As walking speed increases, the hodograph shifts to the right, and expanded in vertical direction, indicating more vertical displacement of COM.

The positive and negative COM work rate ($\dot{W}^{+}_{\mathrm{COM}}$ & $\dot{W}^{-}_{\mathrm{COM}}$) increase with carried walking speed and carried load (Fig. 3.5 A&B). Both positive and negative COM work rates increased approximately with the walking speed raised to the power of 3.42 (Fig. 3.5 A), and linearly to the carried load (Fig. 3.5 B) as predicted in Eqn. 3-8. Similarly, the net metabolic rate increased approximately with the walking speed raised to the power of 3.42 (Fig. 3.5 C), and linearly to the carried load (Fig. 3.6D). We then tested the Eqn. 3-7 that positive COM work rate depends on

carried load M, walking speed v and step frequency f. We found a significant linear relationship between COM work rate and Mv^4f^{-1} with a slope of 0.48 ± 0.07 (95% confident interval, c.i. Fig 3.6A). We also tested the same relationship including the preferred step frequency and walking speed relationship (Eqn. 3-8), and found a significant linear relationship between COM work rate and $Mv^{3.42}$ with a slope of 0.83 ± 0.19 (95% confident interval, c.i. Fig 3.6 B). Finally we tested the linear relationship between net metabolic rate and positive COM work rate, and found a significant slope of 5.93 ± 0.10 (Fig 3.8), which corresponded to a delta efficiency η of 16.9 %.

Walking speeds and carried load also affected gait parameters. The step length s increased substantially with walking speed (Fig. 3.8 A), but has no significant change to carried loads (Fig. 3.8 A). We tested for the linear relationship between step length and walking speed to the power of 0.42, according to Grieve (1968). We found a significant slope of 1.26 ± 0.05. Similarly, the step frequency f increased with walking speed (Fig. 3.9 C), and maintain relatively unchanged to carried loads (Fig. 3.9 D). We tested the linear relationship between step frequency and walking speed to the power of 0.58 and found a significant slope of 2.51 ± 0.13. The double support duration decreased with walking speed (Fig. 3.9 E) and increased with carried load (Fig. 3.9E).

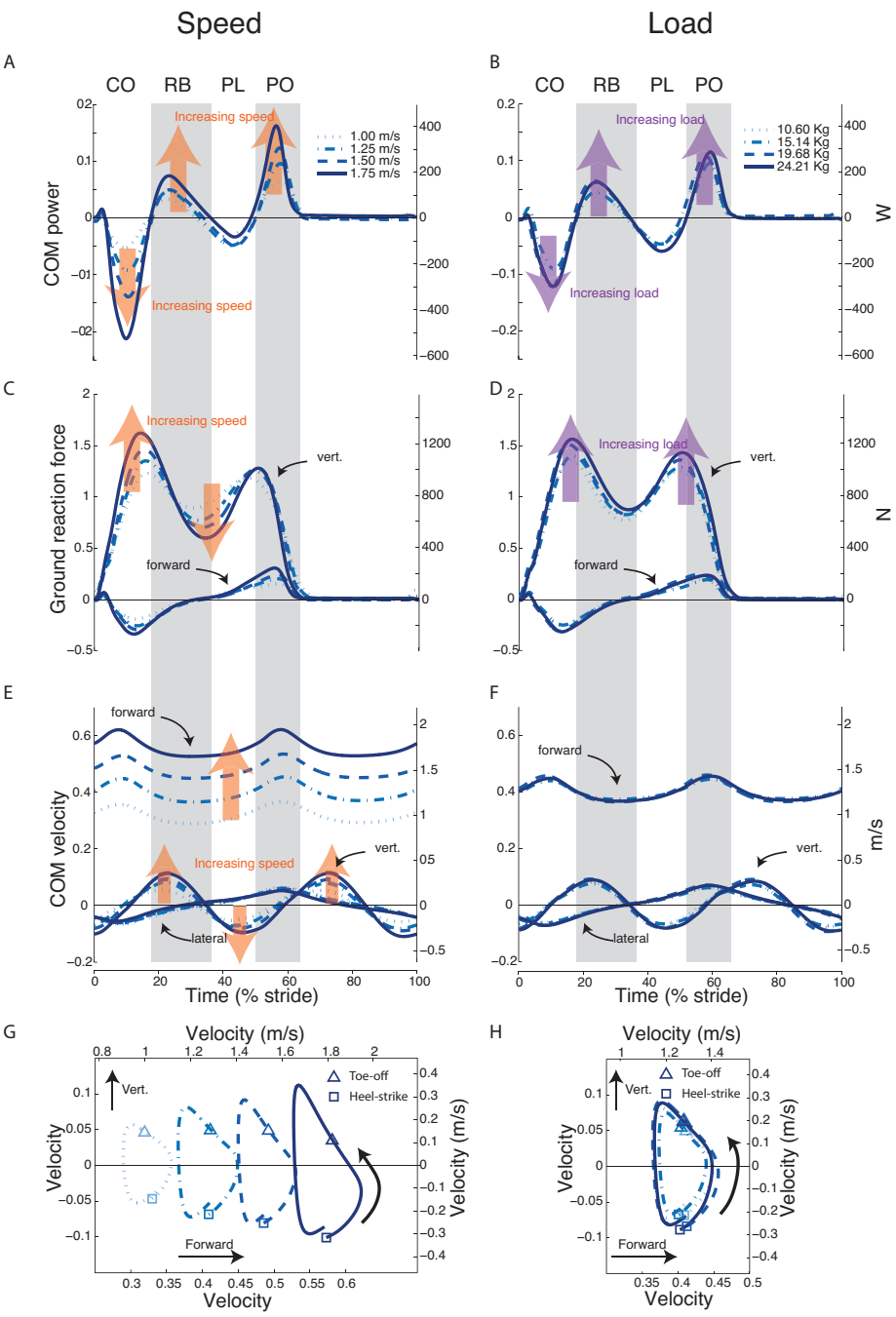

Figure 3.4: Experimental results: COM power, ground reaction forces and COM velocity trajectories for different loads and walking speeds.
Instantaneous COM work rate. (A & B), ground reaction force (C & D) and COM velocity (E & F) measures as a function of stride time for different walking speed (first column) and loads (second column). Hodograph of COM velocity (G & H). Left-hand vertical and bottom horizontal axes show dimensionless quantities, right-hand vertical and top horizontal axes show dimensional SI units. Data shown are trajectories of one representative subject (N = 1).

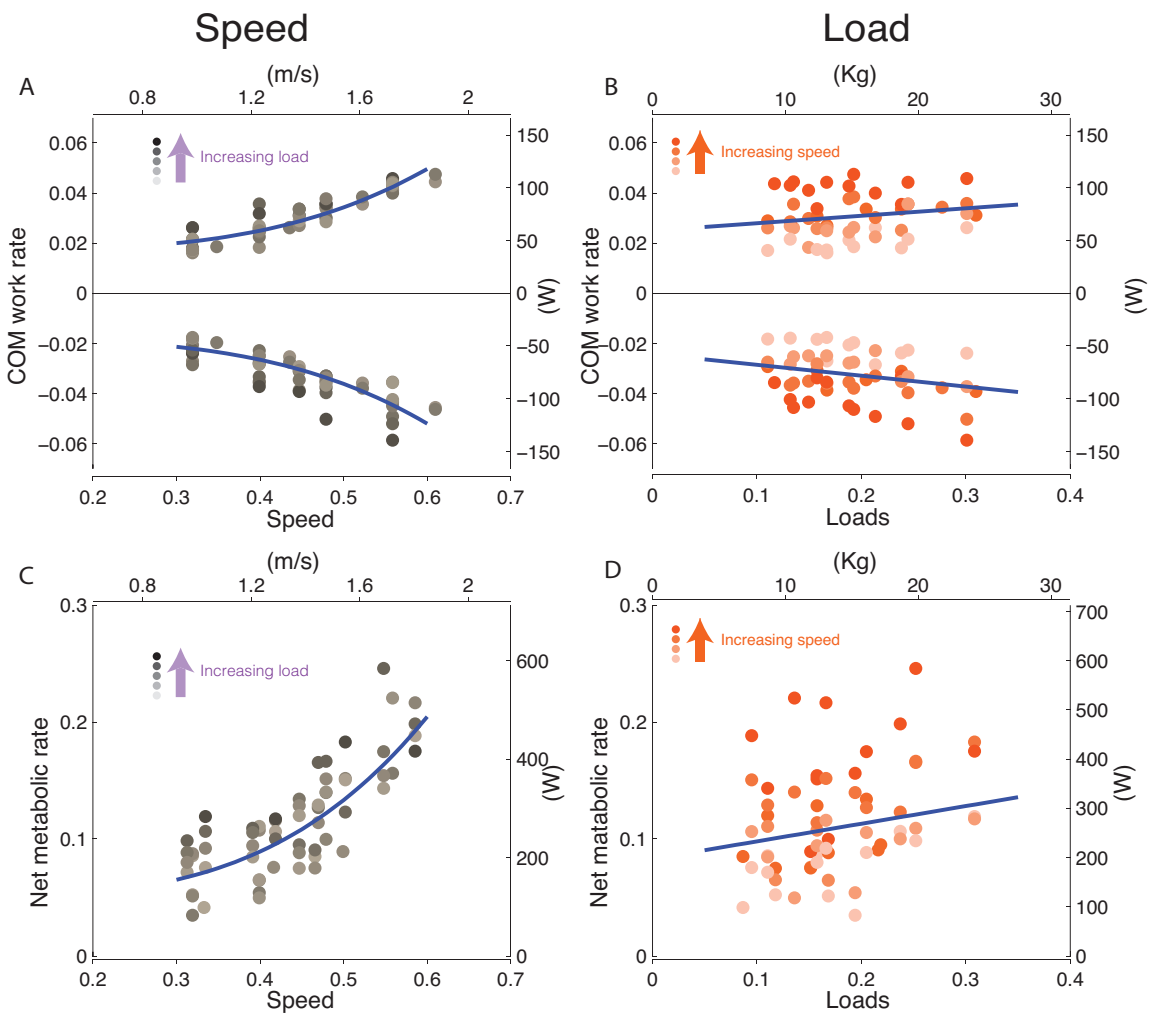

Figure 3.5: AverageCOM work rate and net metabolic rate as function of walking speed and carried load.
The positive and negative COM work rate increased with walking speed to the power of 3.42 (A), and proportionately to carried load (B). The net metabolic rate has similar trend as COM work rate (C & D). Left-hand vertical and bottom horizontal axes show dimensionless quantities, right-hand vertical and top horizontal axes show dimensional SI units. Each data point represent one trial of one subject (N = 9). The darkness indicates different carried loads (A & C) and walking speeds (B & D). The darker is for heavier loads and faster speeds respectively.

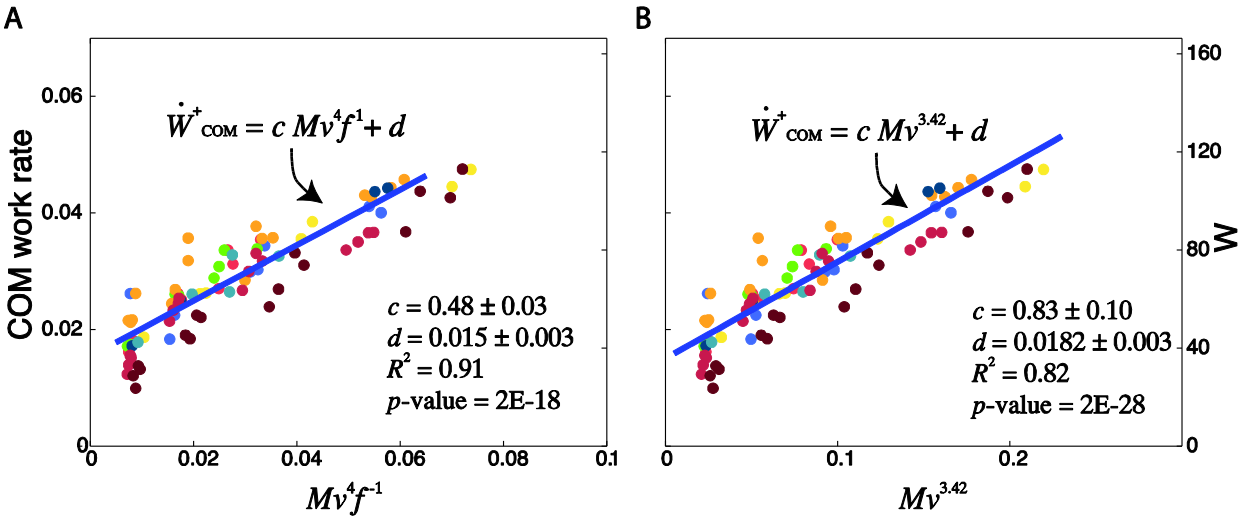

Figure 3.6: Positive COM work rate as functions of total mass, walking speed and step frequency. (A) Positive COM work rate is proportionate to Mv^4f^{-1} as predicted in Eqn 3-7. (B) Positive COM work rate is proportionate to $Mv^{3.42}$ as predicted in Eqn 3-8. Left-hand vertical and bottom horizontal axes show dimensionless quantities, right-hand vertical and top horizontal axes show dimensional SI units. Each color represent one subject (N = 6).

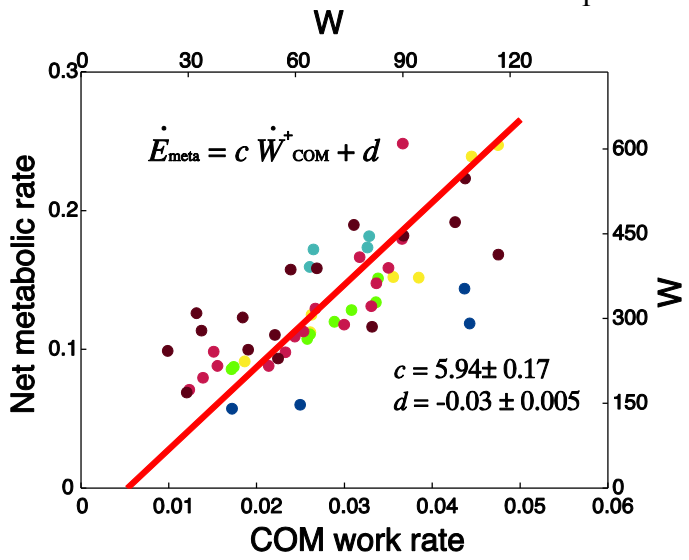

Figure 3.7: The net metabolic rate as function of positive COM work rate for walking at varying speeds and loads.
Left-hand vertical and bottom horizontal axes show dimensionless quantities, right-hand vertical and top horizontal axes show dimensional SI units. Each color represent one subject (N = 6).

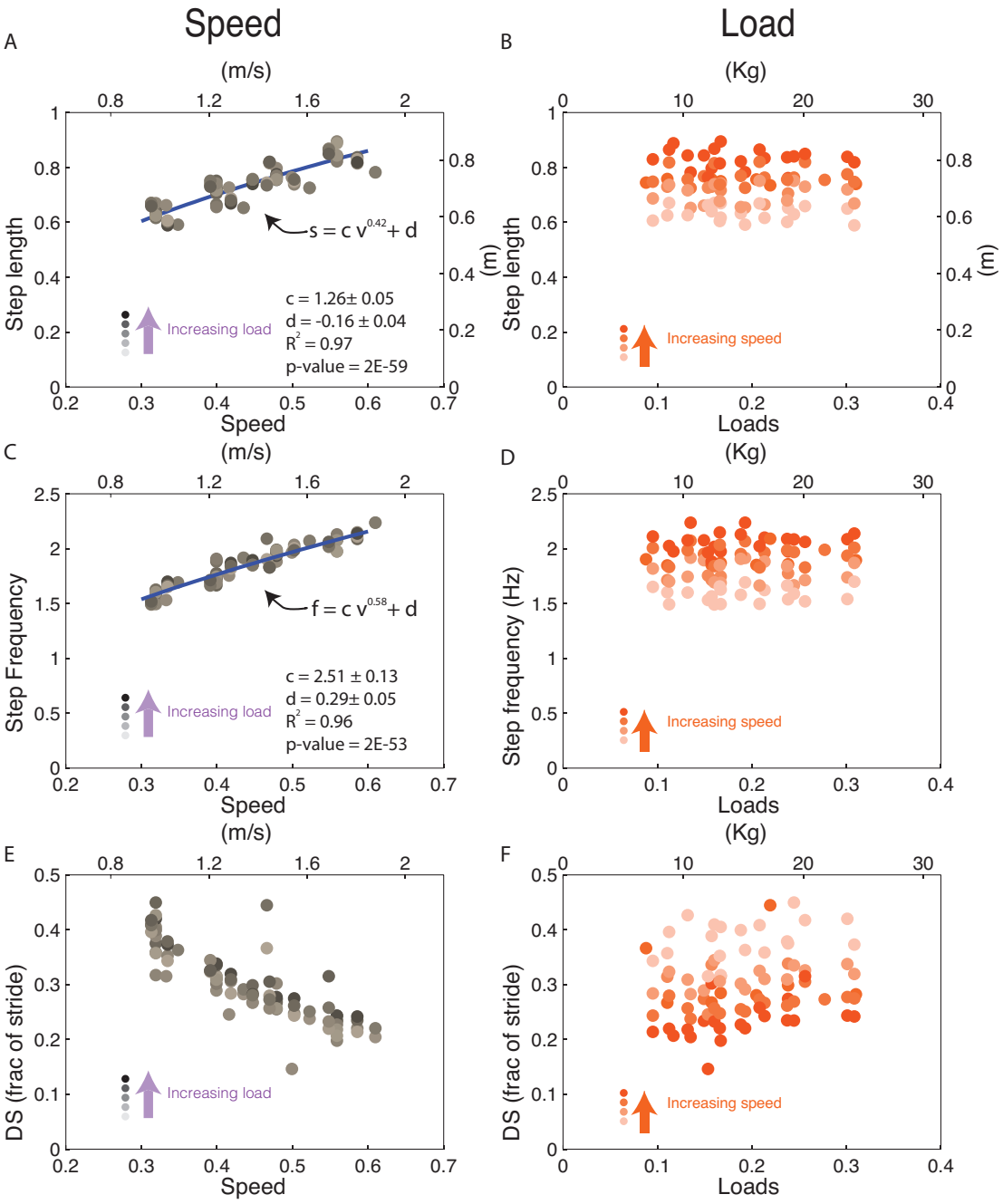

Figure 3.8: Step parameters.
Step length as a function of walking speeds. (A) and carried loads (B). Step frequency as a function of walking speeds (C) and carried loads (D). Double support duration as a function of walking speeds (E) and carried loads (F). Left-hand vertical and bottom horizontal axes show dimensionless quantities, right-hand vertical and top horizontal axes show dimensional SI units. Each data point represent one trial of one subject (N = 9). Shading of symbols denotes different

carried loads (A , C & E) and walking speeds (B, D& F). The darker is for heavier loads and faster speeds respectively.

Discussion

This study was intended to provide a mechanistic explanation for how energetic cost and the mechanics of human walking change with walking speed and carried load. We used rigid-leg and compliant-leg models to predict how human gait changes with different walking speeds and carried load. The net metabolic rate was found to be approximately proportionate to the COM work rate (with a constant delta efficiency η of 16.9 %), which implies that the mechanical work performed on the COM by each leg is a main determinant of energetic cost. The COM work rate were found to follow the prediction from the rigid-leg model, which predicts the COM work rate is a function of total mass M, walking speed v and step frequency f (Eqn. 3-7, Fig 3.6 A). The rigid-leg model predicts that energetic cost is highly depending on the positive work performed on the COM, which is to offset energy dissipated by the heel-strike collision. The results of net metabolic rate and COM work rate imply the energetic cost of walking is highly depends on the heel-strike collision, as hypothesized by the rigid-leg model (Kuo, 2002a). The rigid-leg model predicts the amount of positive work perform on the COM based on the assumption of equal amount of push-off and collision relationship. There is an underlying assumption behind this relationship that humans prefer to their gait with the minimum energetic cost. This assumption allows us to derive the analytical solution of the positive COM work as the function of walking speed v, carried load M_{load} and step frequency f. Furthermore, we used the empirical step length and speed relationship (Donelan et al., 2001a; Grieve, 1968) to simplify our analytical solution.

In the compliant-leg simulation, we found a good match at the double support duration (Fig. 3.8 E & F), which decreased with faster walking speed and increased with carried load. There were two main assumptions in the compliant-leg model simulation. The first one was that step length is a function of walking speed (Grieve, 1968). This relationship can be explained by minimizing the energetic cost of rigid-leg model with a cost of swing leg (Kuo, 2001). Another assumption was that the leg stiffness is to modulate the natural frequency to match with the step frequency, so we have the leg stiffness k_{leg} is proportionate to the total mass M times walking speed v. Previous studies also found similar trends of leg stiffness for walking (Holt et al., 2003; 2011). It

is possible that the leg stiffness is just closely coupled with the step frequency of walking, which we choose for minimal energetic cost.

The compliant-leg model also had reasonable agreement with the COM power, ground reaction force and COM velocity (Fig. 3.3 vs. Fig. 3.5), COM work rate (Fig. 3.4 vs. Fig. 3.6 and Fig. 3.7), in terms of the trend of the change with respect to the walking speeds and carried loads. However, there are several small discrepancies. The ground reaction force and COM work rate are higher in the compliant leg model results than the empirical results. The double support duration is smaller in compliant leg model results than the empirical results. Another discrepancy in the shape of vertical ground reaction force and COM power trajectories. As walking speed increases, the first peak of vertical ground reaction force increases much faster than the second peak, and the M-shape becomes more asymmetric (Fig. 3.5 B). This causes greater increase of negative COM collision work than the increase of positive COM push-off work (Fig. 3.5 A). The discrepancies may be due to the over simplification of the model. There is not foot in our compliant-leg model. A curved foot could lead to a smoother ground reaction force of walking and less COM work. Also, we constrained the step length as a function of walking speed and the leg stiffness as a function of total mass and walking speed (Eqn. 3-12). These constraints may also lead to the discrepancies.

Obviously, the energetic cost of human walking does not only depend on the mechanical work. Other factors, such as muscle force (Griffin et al., 2003) and muscle co-contraction (Unnithan et al., 1996), could also affect the energetic cost of walking. In this study, we found the COM work rate is one of the main factors which can explain the how the energetic cost of human walking increase with walking speeds and carried load. The other factors either remained unchanged for different walking speeds and carried loads, or were coupled with the mechanical work. For example, the muscle force, which could be highly correlated to the ground reaction force, may affect the energetic cost of human walking, but is couple with the mechanical work since the work is defined as force dot displacement.

The rigid-leg model has two limitations to explain human gait. The first is the instantaneous double support phase, which assumes the impulsive push-off and collision. The second is the non-human-like vertical ground reaction force. The vertical ground reaction force of human walking has an M-shape profile which rigid-leg model cannot regenerate. The double support

duration and the shape of ground reaction force are also changed with walking speed and carried load. Therefore we used the compliant-leg model to explain these left over phenomena.

Despite the discrepancies, several conclusions appear to be supported. The rigid-leg model predicts the increases of COM work rate for different walking speeds and carried loads. The compliant-leg model, with the natural frequency corresponding to the step frequency, predicts the double support duration and COM fluctuations. Simple models have more predictive value than complex models. Even a minor increase in complexity requires parameter choices, which either requires more assumptions or has to be systematically tuned. Finally, the net metabolic rate is proportionate to the COM work rate.

Chapter 4 Mechanical and energetic consequences of reduced ankle plantarflexion in human walking

Submitted in Journal of Experimental Biology

Abstract

The human ankle produces a large burst of "push-off" mechanical power late in the stance phase of walking, impairment of which leads to considerably greater energy expenditure. It has not been shown experimentally whether the energetic penalty results from poorer efficiency when the other leg joints substitute for the ankle's push-off work, or from a higher overall demand for work due to some special feature of push-off. Here we show that greater metabolic energy expenditure is indeed explained by a greater demand for work. This is predicted by a simple model of walking on pendulum-like legs, because proper push-off reduces collision losses from the leading leg. We tested this by experimentally restricting ankle push-off bilaterally in healthy adults ($N = 8$) walking on a treadmill, using ankle-foot orthoses with steel cables limiting motion. These produced up to about 50% reduction in ankle push-off power and work, resulting in up to about 50% greater net metabolic power expenditure to walk at the same speed. For each 1 J reduction in ankle work, we observed about 0.6 J more dissipative work by the other leg, 1.3 J more positive work from the leg joints overall, and 3.94 J more metabolic energy expended. Loss of ankle push-off required more positive work elsewhere, principally at the knee. Subjects appeared to perform that additional work at relatively high efficiency. Normal ankle push-off appears to be important for the economy of walking.

Introduction

During human walking, the ankle produces the highest mechanical power among the joints, in a burst late in the stance phase termed *push-off*. Its importance is illustrated by cases of impaired or reduced push-off, which generally result in considerably more metabolic energy expenditure to walk (Doets et al., 2009; van Engelen et al., 2010; Waters and Mulroy, 1999). If walking were only a matter of supplying a requisite amount of forward propulsion, then other joints might be expected to supply a greater proportion of the mechanical work to offset the reduced push-off work, and not necessarily at higher metabolic cost. The actual energetic penalty suggests that the

normal push-off conveys some unique advantage, perhaps in its timing or spatial location, that is not presently understood. To gain insight on this matter, we propose and test a mechanistic explanation for the disadvantages of reduced ankle push-off.

Ankle push-off appears to be important to walking economy. The ankles normally produce a burst of positive push-off power peaking at more than 2.5 W/kg (e.g., Zelik and Kuo, 2010). That peak is more than three times the maximum power produced by the other joints, and is reduced considerably with gait pathologies. For example, the peak can be reduced by more than half in patients with multiple sclerosis, individuals recovering from stroke (Bregman et al., 2011a), and those with ankle arthrodesis or arthroplasty (Singer et al., 2013). The energetic penalty varies considerably with severity and condition, but typically entails an increase of 30% or more in net metabolic power (subtracting the cost of upright standing from gross power) expended to walk at the same speed (Doets et al., 2009; Torburn et al., 1995; Waters and Mulroy, 1999).

The energy expenditure of walking is explained in part by the mechanical work performed in the transition between pendulum-like steps (Kuo et al., 2005a). The body center of mass (COM) is located near the pelvis and moves in an arc determined by the pendulum-like stance leg (Fig. 1). The COM velocity must be redirected upward between the end of one step and the beginning of the next (Adamczyk and Kuo, 2009; Kuo, 2002b). This entails negative, dissipative work by the leading leg's collision with ground, which is compensated by positive push-off work from the trailing leg (Donelan et al., 2002b). If push-off is timed to begin just before the collision, it also theoretically reduces the loss during this step-to-step transition (Kuo, 2002b). Indeed, in cases of total ankle arthroplasty, reduced push-off results in greater collision losses and greater metabolic energy expenditure (Doets et al., 2009). But one discrepancy is that the overall positive work performed on the COM is not observed to increase (Doets et al., 2009), as would be expected from the imbalance between push-off and collision. The theory of step-to-step transitions would therefore appear to only partially explain the effects of reduced push-off.

There are two potential explanations for this discrepancy. The first is that the muscles might perform additional mechanical work not observed in previous studies. Work performed on the COM is a summary of work from an entire limb, convenient for indicating when the two limbs simultaneously perform positive and negative work (Donelan et al., 2002c). But it is also an incomplete measure, because it does not indicate when one joint performs work that cancels that

out another within the single limb (Donelan et al., 2002b). It is possible that reduced push-off does indeed increase the overall positive work performed during a step, if measured at the joints instead of the limbs. The alternative possibility is that there is nothing special about push-off so long as propulsion and a requisite amount of work is performed elsewhere in the body. The energetic penalty of reduced push-off might instead be explained by poor efficiency of muscular propulsion, as might be the case with co-morbidities accompanying limb loss or joint fusion, rather than the mechanics of COM motion as we have theorized.

In the present study, we propose to address these questions in two ways. First, we present a simple dynamic walking model to demonstrate the theoretical effects of bilaterally reduced push-off. Although the model does not predict how the joints will compensate for reduced push-off, it does suggest that overall work will increase, even if not captured by work performed on the COM. Second, we experimentally test human subjects walking with artificial constraints on ankle push-off. We test healthy subjects and focus on the effects of reduced push-off alone, rather than the co-morbidities of pathological gait. The experiment allows for continuous adjustment of the degree of constraint, which facilitates identification of trends associated with reduced push-off. We test whether the overall amount of mechanical work by the joints increases with artificially reduced push-off as predicted by the step-to-step transition hypothesis, or whether the energetic penalty is explained better by poor efficiency of the joints that perform compensatory work according to the propulsion hypothesis.

Method

Model

We used a dynamic walking model (Fig. 4.1) to predict the effects of reduced push-off on locomotion dynamics and energetics. In the "simplest walking model" (Kuo, 2002b), the legs behave like ideal pendulums, with the body center of mass (COM) moving in an inverted pendulum arc atop the stance leg. With each footfall, an impulsive collision redirects the COM velocity to a new arc determined by the leading leg. This collision performs negative work on the COM, and requires positive work to offset the loss. The most economical solution is an impulsive push-off just prior to, and equal in magnitude to, the leading leg collision (Fig. 4.1A).

This reduces the collision loss and allows walking speed to be maintained with the least positive work. These principles have been found to predict the mechanical and energetic effects of walking with, for example, greater step lengths (Donelan et al., 2002b) and step widths (Donelan et al., 2001a).

There are several consequences if the optimal push-off is reduced (Fig. 4.1B). First, reduced push-off increases the leading leg's ensuing collision. Second, the imbalance in push-off and collision work requires more positive work to be performed elsewhere in the stride, in the interval after collision and before the next push-off, referred to here as the *middle-stance* phase. Third, the imbalance also requires more positive work overall from the push-off and middle-stance phases. All of these effects are predicted quantitatively by models described previously (Adamczyk and Kuo, 2009; Kuo, 2002b; Kuo et al., 2005a), as summarized in the Appendix. The overall result is that collision work W_{CO} is predicted to change with push-off work W_{PO} according to

$$W_{\mathrm{CO}} \approx -\frac{Ms^2v^2}{2L^2} + \sqrt{W_{PO}}\left(\frac{2sv}{L}\right) \quad (1) \qquad (1)$$

where s denotes step length, L leg length, M body mass, and v^- the COM velocity just prior to push-off. To ensure zero net work over a gait cycle, the stance phase work between collision and push-off, termed middle-stance work W_{MS}, is

$$W_{\mathrm{MS}} = -W_{\mathrm{CO}} - W_{\mathrm{PO}} \quad (2)$$

When push-off work is reduced, the magnitudes of collision and middle-stance work both increase for a given walking speed and step length (Fig. 4.1B). These effects are approximately linear for push-off reductions up to about 50% (Fig. 4.1C), for conditions similar to the experiment conducted here (equivalent to dimensionless speed of 0.44 and step length 0.78, using M, L, and gravitational acceleration g as base units). Although this model is quite crude compared to the complexity of actual human walking, it is sufficient to demonstrate the general trends in work that should result from reduced push-off, so long as the legs behave like pendulums.

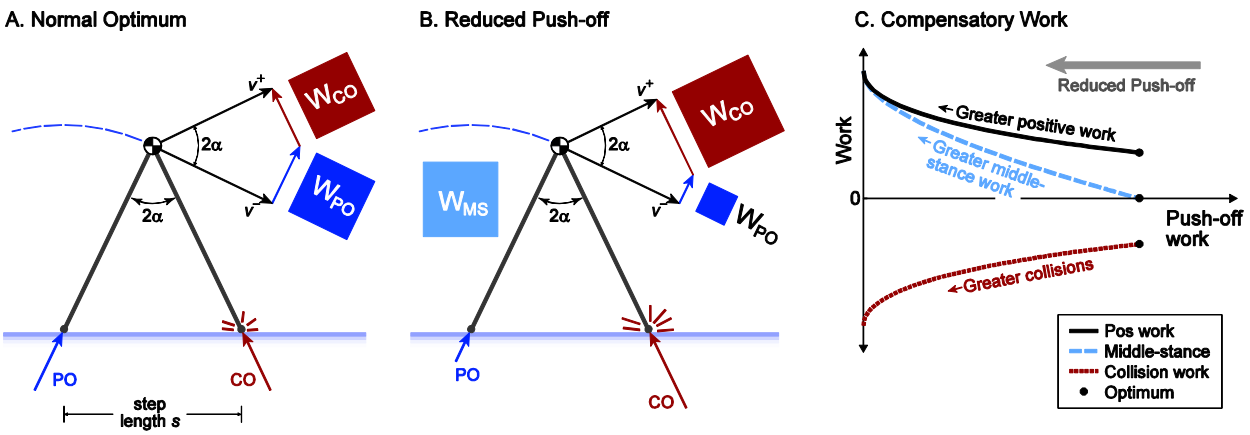

Figure 4.1 Dynamic walking model predicts effects of reduced push-off work.
(A) Model has pendulum-like legs supporting body center of mass (COM), whose velocity must be redirected from v^- at end of one stance phase to v^+ at beginning of the next stance phase. This is most economical when positive push-off work is performed just before and in equal magnitude to the leading leg's negative collision work (impulses PO and CO, respectively, perform work W_{PO} and W_{CO} proportional to square of impulses; Kuo, 2002). (B) With reduced push-off capacity, the collision is greater and dissipates more energy. The COM velocity must be increased during the rest of the step, requiring net positive "middle-stance" work, W_{MS}, and greater positive work overall. (C) Model prediction of collision and middle-stance work as a function of push-off work, for walking at fixed speed and step length. Starting from most economical case (right-most point on plot), reduced push-off work leads to greater magnitudes of negative collision work and positive middle-stance work. Symbols: step length s, leg angle α.

Experiment

We tested the model by measuring the work performed by healthy adults while they walked with restricted ankle plantarflexion. Rather than control push-off explicitly, we found it more practical to control kinematic displacement of the ankle. We therefore tested whether this restriction was indeed able to affect ankle work as intended, and in turn cause the predicted increases in overall positive mechanical work and overall metabolic cost.

We tested eight healthy adults walking at 1.40 m · s^{-1} while wearing bilateral ankle-foot orthoses (AFO, Bledsoe Brace System, Grand Prairie, Texas, USA) modified to restrict ankle plantarflexion range of motion (Fig. 4.2). This was achieved through the addition of steel cables between the shank and fore-foot. We applied five controlled conditions with different cable lengths (including one with no restriction). For comparison, we also applied a separate normal shod condition, in which subjects wore their normal street shoes. Subjects were young adults (aged 21-27, 6 males and 2 females) with body mass M of 76.6 ± 8.8 Kg (mean ± s.d.), leg length

L of 0.95 ± 0.06 m. All subjects provided written informed consent prior to the study, according to Institutional Review Board procedures.

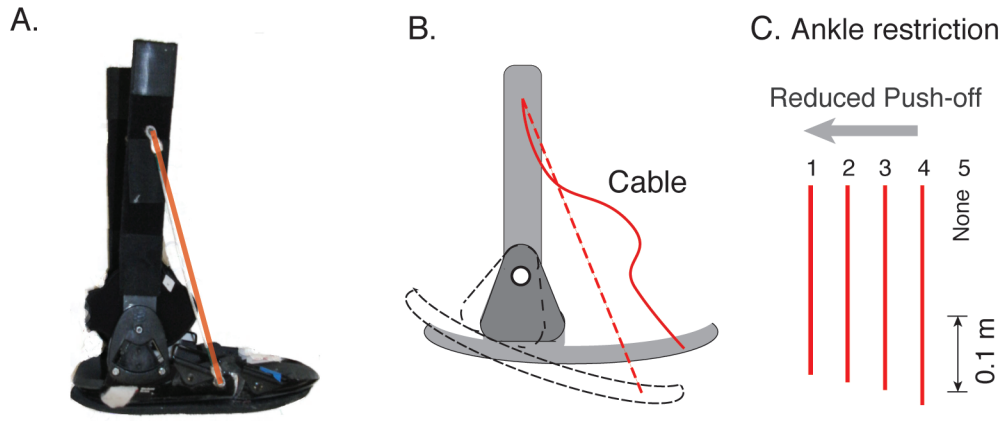

Figure 4.2 Method for experimentally reducing push-off.
(A) An ankle-foot orthosis (AFO) was modified with steel cables restricting plantarflexion motion on both sides. (B) Diagram shows relative lengths of cables (25 – 29 cm) for five constraint conditions experienced by human subjects walking at constant speed (1.40 m · s^{-1}).

The data collected included joint kinematics and kinetics, mechanical work performed on the COM, and metabolic energy expenditure. Subjects walked on a split-belt instrumented treadmill (Bertec, Columbus, OH, USA) that yielded ground reaction forces from the individual legs. Lower extremity kinematic data were recorded using a marker-based motion capture system (Phasespace, San Leandro, CA, USA). We measured oxygen consumption and carbon dioxide production using a wireless portable respirometry system (CareFusion, Vernon Hills, IL, USA).

We quantified mechanical work performed on the COM and by the lower extremity joints. The instantaneous COM work rate P_{COM} was calculated as the inner product of ground reaction force $\vec{F}$ of each leg and COM velocity $\vec{v}_{\mathrm{COM}}$ (Donelan et al., 2002c), where the velocity was computed by integrating the total ground reaction force, subject to constraints on periodicity. The stride was defined as starting and ending at consecutive same-side heelstrikes and was examined in terms of three phases defined by zero-crossings of COM work rate: collision (about 0 – 18%), middle-Stance (about 18 – 49%), and push-off (about 49 – 66%). The work rate was integrated over each of these intervals (W_{CO}, W_{MS}, and ,W_{PO}, respectively), and separately over the positive intervals to yield positive work per stride, W^{+}. The middle-stance work includes two phases we

have previously referred to as rebound and pre-load (Donelan et al., 2002b); these were lumped together here because the model only predicts trends in overall work between collision and push-off. We also measured other gait parameters such as step length, step time and double support time.

Joint kinematics and kinetics were computed from ground reaction force and motion capture data using standard methods. We used commercial software (Visual3D, Germantown, MD, USA) to calculate joint angles, moments and powers for ankle, knee, and hip, in three dimensions. As a simple summary of power from an entire leg, we calculated summed joint power P_{joint} by adding together the powers from ankle, knee, and hip of one leg. Positive (negative) joint work per stride was defined as the integral of positive (negative) intervals of each joint power. We also calculated the positive (negative) summed joint work per stride W^{+}_{joint} (W^{-}_{joint}) by adding together the positive (negative) ankle, knee and hip work of one leg. For simplicity, only sagittal plane angles and moments are plotted here, although power and work quantities were calculated in three dimensions.

We estimated the net metabolic rate of energy expenditure from oxygen consumption and carbon dioxide production data. These data were collected over walking trials of at least 6 minutes, with only the final 3 minutes of each trial retained for analysis to ensure steady state. Gross metabolic energy expenditure (in W) was calculated using standard conversion factors (Brockway, 1987a). Net metabolic rate $\dot{E}$ was defined as the gross metabolic rate for walking minus that for quiet standing (110 ± 22 W).

To account for differences in subject body size and facilitate comparison with the model, measurements were normalized to dimensionless form, using base units of body mass *M*, standing leg length *L* (ground to greater trochanter), and gravitational acceleration *g*. The mean normalization constant for force was therefore Mg (average 751.87 N), for work MgL (717.10 J), and for power $Mg^{1.5}L^{0.5}$ (2299.82 W). We performed statistical tests to test three main predictions. The first was to determine whether kinematic ankle restriction could reduce push-off work, examined through repeated measures analysis of variance (ANOVA) across conditions. We then tested whether the following work quantities increased with reduced push-off work: collision work W_{CO}, middle-stance work W_{MS}, and total positive work W^{+}. Finally, an increase

in total positive work should lead to an increase in net metabolic rate $\dot{E}$ as a function of push-off work. These were all tested with linear regression against push-off work W_{PO}, with a significant slope indicated by its 95% confidence interval. The threshold of significance for all tests was set at $\alpha = 0.05$. We also examined several other quantities such as joint work measures, but there were no specific predictions other than that total joint work should increase with reduced push-off.

Results

Restricted ankle plantarflexion had a substantial effect on the mechanics and energetics of walking. We found that the ankle constraints did reduce push-off work as intended, which in turn led to increases in positive work performed elsewhere, as well as greater metabolic cost. These effects occurred despite no statistically significant differences in step length, step frequency, and double support time (see Table 4-1). Below we first describe some qualitative observations of the effects on time-varying variables, followed by quantitative summaries of the mechanical and energetic effects over an entire stride.

We qualitatively observed a number of effects from the ankle restriction conditions. Examining the ankle (Fig. 4.3), angular displacement was reduced by as much as about 40 deg, and peak power was substantially reduced during push-off (particularly near 60% stride), although the ankle moment trajectory was relatively unaffected. While the constraints were generally effective in reducing plantar-flexor motion in a controlled manner, depending on their normal range of ankle motion and alignment of the AFO some subjects were relatively unaffected by the two least restrictive conditions,. There were also effects on the force and power trajectories (Fig. 4.4). The first peak of the vertical ground reaction force tended to increase with greater restriction, whereas the second peak tended to decrease (Fig. 4.4A). The anterior-posterior force exhibited decreasing amplitude with greater ankle restriction (Fig. 4.4B). These caused corresponding changes in instantaneous COM work rate: amplitude of push-off work rate decreased while collision amplitude increased with degree of restriction (Fig. 4.4C). During middle-stance, subjects performed positive and then negative work, yielding slightly negative work overall, in the normal shod condition. With increasing ankle restriction, the middle-stance trajectory shifted toward positive. This was true for both the positive and negative intervals of this phase, which

are termed rebound and preload, respectively (Donelan et al., 2002b; Kuo et al., 2005a). The summed joint power, defined as sum of ankle, knee and hip power, had a similar trend during that interval, also shifting to the positive, indicating more positive work overall (Fig. 4.4D).

There are related observations regarding joint mechanics (Fig. 4.5). In addition to the effects at the ankle mentioned above, we observed stance phase knee flexion to increase with greater restriction, along with knee extension moment (Fig. 4.5A). This occurred in the interval beginning slightly before and ending after middle-stance, about 5 – 40% of stride. This was accompanied by more negative knee power during collision, and greater positive ankle power during the earlier (rebound) portion of middle-stance. We observed much smaller changes in kinematics and kinetics of the hip angle, moment and power. Examining the positive and negative joint work per stride, these had relatively linear trends as a function of COM push-off (Fig. 4.5B). Swing phase appeared to be relatively unaffected by the ankle restrictions.

The observations above are supported by quantitative examination of the mechanical work performed on the COM (Fig 4.6). Significant differences were observed in COM push-off work, mid-stance work and collision work across ankle restriction conditions (repeated measures ANOVA, P = 1E-12, 7E-3 and 1E-9, respectively). With increasing restriction, push-off decreased from about 19.1 J to 11.8 J, middle-stance work increased from about -2.7 J to 6.8 J, and collision work increased from about -19.38 J to 6.82 J.

We next examine the main changes in work as a function of COM push-off work as a continuous variable (rather than the discrete experimental conditions). As push-off was reduced, ankle positive work and negative work per stride decreased significantly in magnitude (Fig. 4.5B; quantitative summary in Table 1). Ankle restriction also had slightly less effect on ankle work itself than on COM Push-off, with a slope of 0.75 (change in ankle positive work per change in COM push-off). At the knee, both positive and negative work increased significantly in magnitude with the degree of push-off restriction, with slopes -1.41 and 0.89, respectively (where negative slope means knee power decreased with increasingly push-off). At the hip, only positive work increased significantly with degree of restriction, with slope -0.67. In terms of COM work per stride, collision work magnitude increased with reduced push-off (Fig. 4.7A), as evidenced by a significant linear trend between the two, with slope 0.64 (change in collision work divided by change in push-off work). Correspondingly, middle-stance work also increased

(i.e., became more positive, Fig. 4.7A) with reduced push-off work, with slope -1.32. Total positive COM work did not change significantly with reduced push-off work (Fig. 4.7A). The positive sum of joint work per stride decreased with a slope of -1.33 (Fig. 4.7B). Negative summed joint work increased in magnitude, with slope 0.60.

Net metabolic rate also increased with reduced push-off (Fig. 4.7C). The slope of the change, expressed dimensionlessly, was -2.34 ± 0.59 (change in metabolic rate divided by change in push-off work). Comparing rates directly (change in metabolic rate divided by change in push-off work rate for both legs), the equivalent slope was -3.94 ± 0.96.

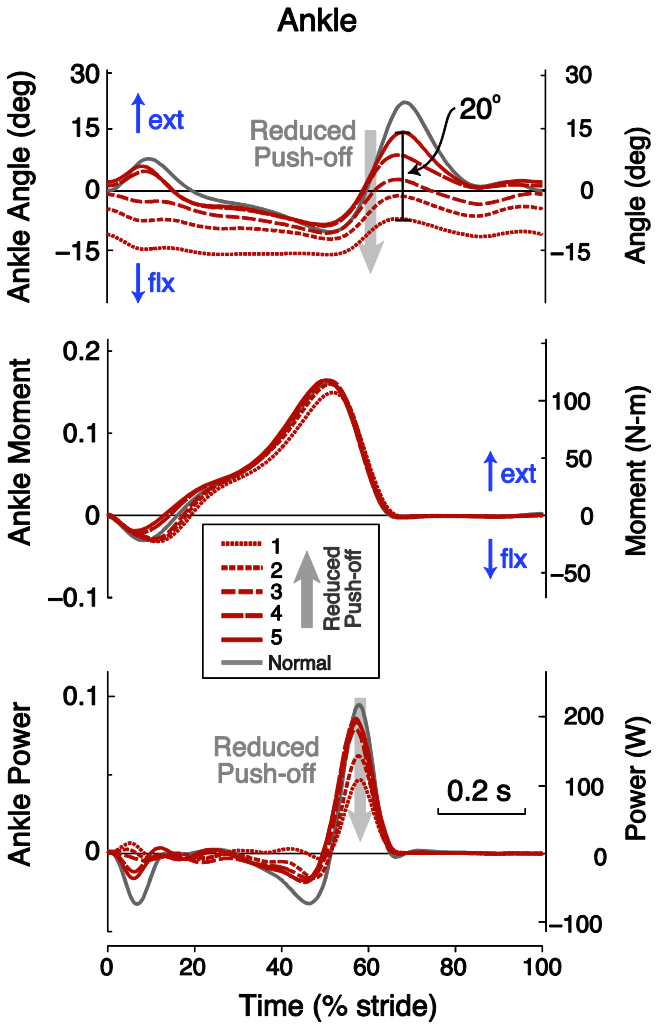

Figure 4.3 Ankle angle, moment, and power vs. stride time for all experimental conditions. Shown are averaged trajectories across subjects ($N = 8$) over one full stride (defined by same-side heelstrikes), with increasing push-off restriction (solid line to dotted lines), as well as normal shod walking (solid gray line). Quantities are shown in terms of dimensionless units (left-

hand vertical axes), using body mass, leg length, and gravitational acceleration as base units. Equivalent SI units are shown on right-hand axes.

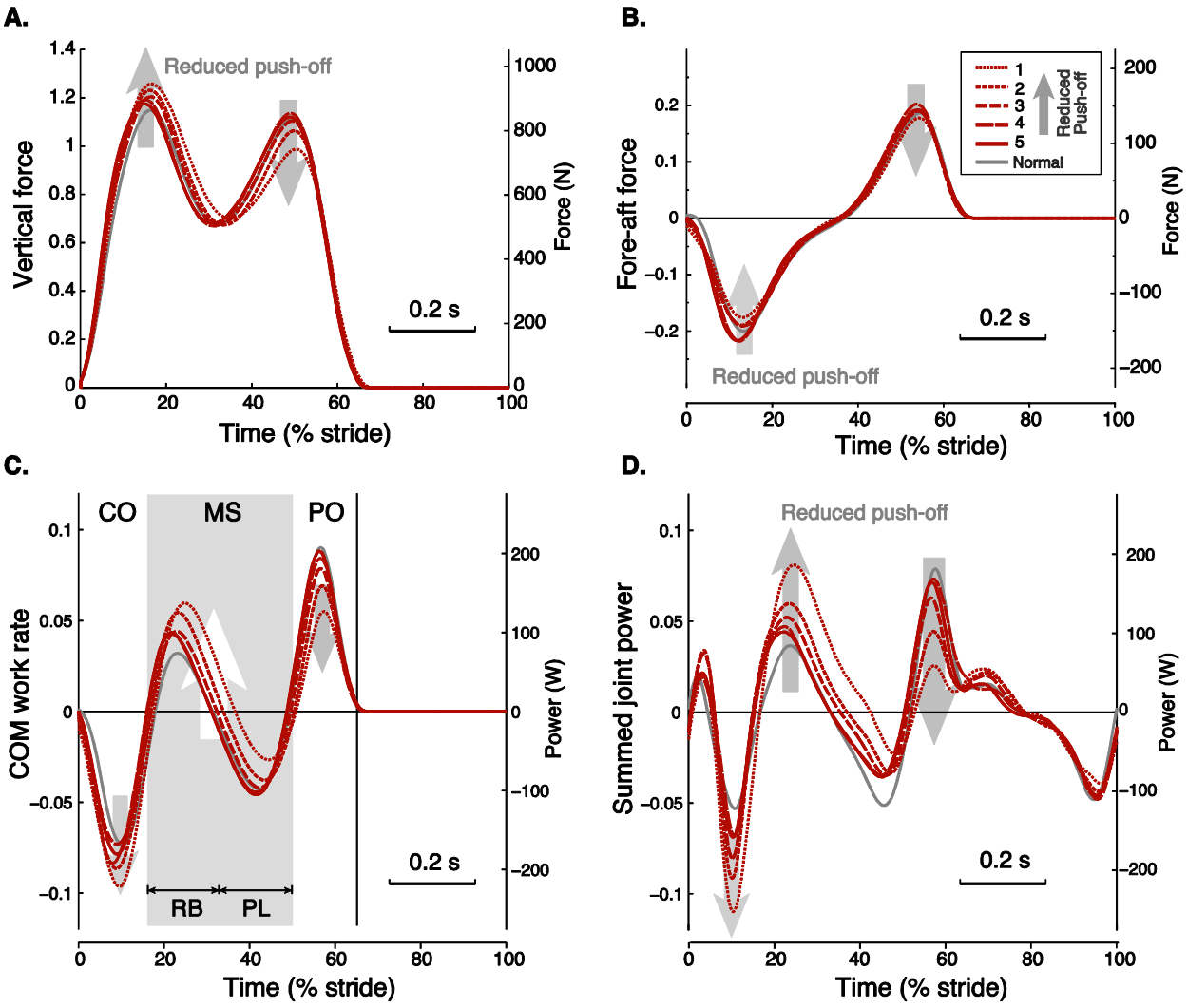

Figure 4.4 Effect of ankle restriction on ground reaction forces and power measures. (A) Vertical ground reaction force and (B) horizontal (fore-aft) ground reaction force versus stride time. (C) Instantaneous center of mass (COM) work rate (dot product of COM velocity with ground reaction force from one leg) versus time. Zero-crossings of COM work rate define collision, middle-stance, and push-off phases of stride (CO, MS, and PO, respectively). Middle-stance is an interval including both positive rebound and negative pre-load work (RB and PL). (D) Summed joint power (sum of ankle, knee and hip powers) versus time. Left-hand vertical axes show dimensionless units, and right-hand vertical axes show equivalent dimensional SI units. Data shown are trajectories averaged across subjects (N = 8).

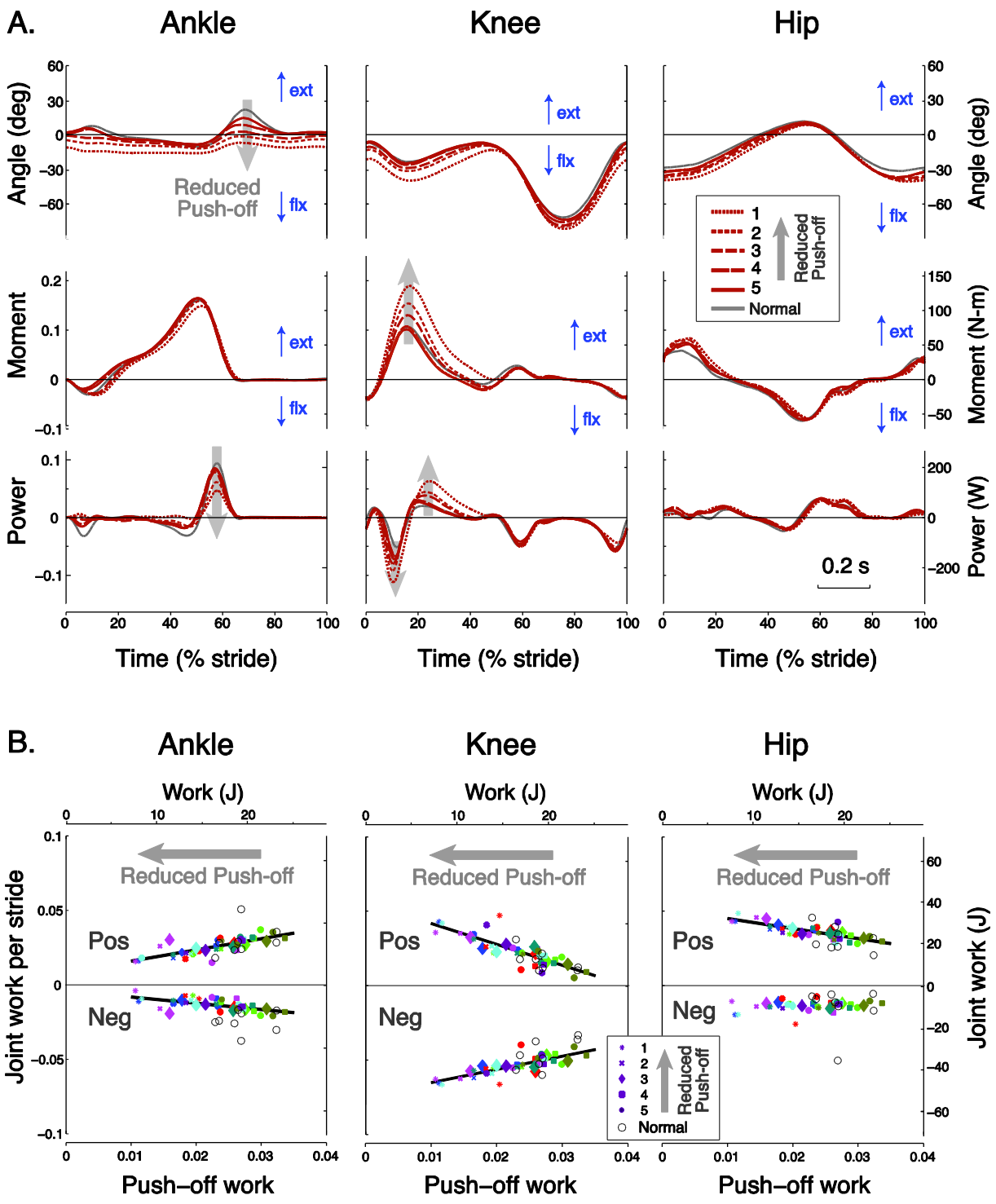

Figure 4.5 Lower extremity joint kinematics and kinetics as function of ankle restrictions. (A) Angle, moment and power trajectories versus time for ankle, knee and hip. Data shown are trajectories averaged across subjects (N= 8). Angles and moments are defined as positive in extension (Ext), and negative in flexion (Flx). (B) Positive and negative joint work per stride for ankle, knee, and hip, as function of push-off work. Data points are shown for each subject and

each condition (denoted by color and symbol, respectively). Vertical axes shown in dimensionless and SI units (left- and right-hand axes, respectively).

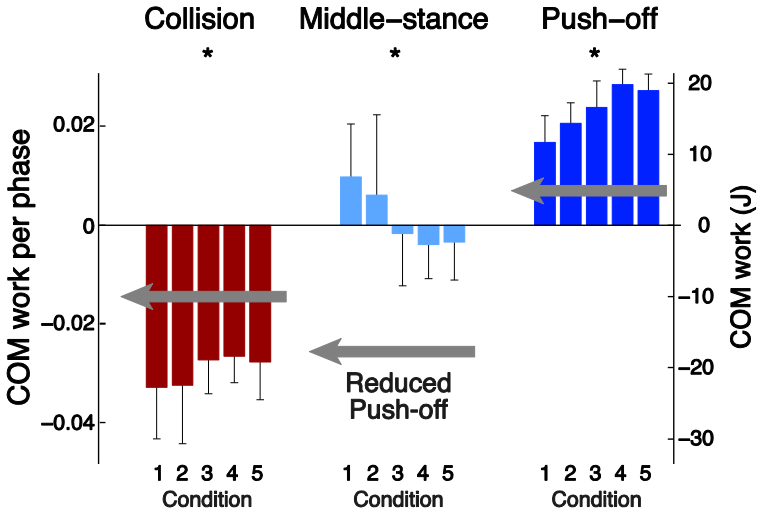

Figure 4.6 Summary of work performed on center of mass (COM work) as function of ankle restriction.
Shown are COM work per step during collision, middle-stance, and push-off phases (W_{CO}, W_{MS}, and W_{PO}, respectively). Error bars denote s.d., asterisk indicates statistically significant differences across conditions ($P < 0.05$, repeated measures ANOVA). Vertical axes are shown with dimensionless and SI units (left- and right-hand sides, respectively).

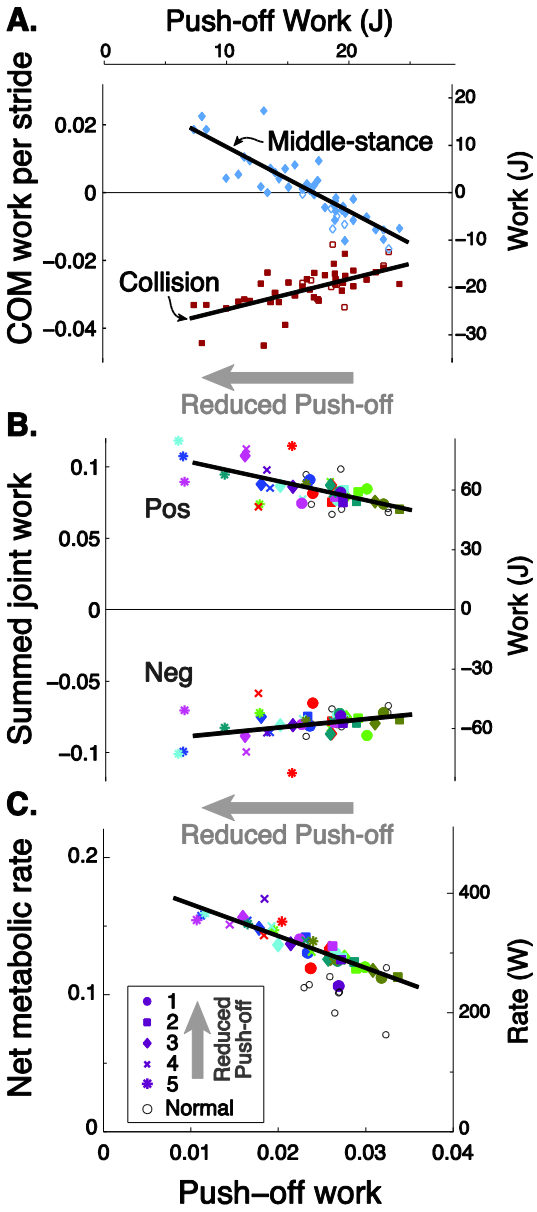

Figure 4.7 Effect of reduced push-off work on overall mechanical work and metabolic energy expenditure.
(A) Collision work and middle stance work per stride ($W_{\mathrm{CO}}$and W_{mid}, respectively) as function of COM Push-off work. (B) Positive and negative summed joint work per step versus push-off work. Summed joint work is defined as integral of positive and negative (Pos and Neg) intervals of summed joint powers (see Figure 4D). (C) Net metabolic rate as function of COM push-off work. Data are shown for each experimental condition (denoted by color and symbol, respectively), along with linear fits (all statistically significant, $P < 0.05$). Vertical axes shown in dimensionless and SI units (left- and right-hand axes, respectively).

Table 4-1: Quantitative results for linear regression against push-off work

Measure	Normal (SI)	Normal (d'less)	Slope ± c.i.	Offset ± s.d.	R^2	S	P
Double support time	0.29 ± 0.02 s	0.27±0.02	-0.83±0.80	0.30±0.01	0.69	*	0.04
Swing time	0.76 ± 0.06 s	0.73 ± 0.02	0.84 ± 0.80	0.70 ± 0.01	0.69	*	0.04
Step length, s	0.73 ± 0.03 m	0.78±0.04	0.10 ±1.55	0.78±0.05	0.89		0.89
Step width	0.14 ± 0.03 m	0.15±0.04	1.80±0.85	0.11±0.02	0.79	*	1e-4
Step frequency, f	1.91 ± 0.11 s^{-1}	0.59±0.02	-0.05±0.99	0.59±0.02	0.75		0.91
Push-off work, W_{PO}	19.75 ± 5.36 J	0.027±0.004	NA	NA	NA		NA
Collision work, W_{CO}	-17.58 ± 4.36 J	-0.025±0.006	0.64±0.36	0.043±0.008	0.74	*	1e-3
Middle-stance work, W_{MS}	-5.24 ± 2.22 J	-0.007±0.006	-1.33±0.41	0.032±0.008	0.82	*	2e-7
Summed joint work, W^{+}_{joint}	55.39 ± 8.62 J	0.0778±0.0122	-1.33±0.52	0.117±0.013	0.86	*	1e-5
Summed joint work, W^{-}_{joint}	-60.61 ± 14.65 J	-0.0859±0.0261	0.60±0.55	-0.094±0.015	0.84	*	0.03
Pos ankle work, W^{+}_{ank}	21.27 ± 6.87 J	0.030±0.010	0.75±0.30	0.009±0.006	0.71	*	2e-5
Neg ankle work, W^{-}_{ank}	-17.81 ± 6.36 J	-0.0245±0.0071	-0.42±0.27	-0.004±0.006	0.72	*	3e-3
Pos knee work, □$^{+}_{\mathrm{kne}}$	11.74 ± 4.64 J	0.0165±0.0071	-1.41±0.47	0.056±0.007	0.72	*	9e-7
Neg knee work, W^{-}_{kne}	-32.70 ± 4.85 J	-0.0464±0.0099	0.89±0.32	-0.074±0.009	0.86	*	4e-6
Pos hip work, W^{+}_{hip}	22.38 ± 5.73 J	0.0315±0.0082	-0.67±0.25	0.053±0.010	0.92	*	8e-6
Neg hip work, W^{-}_{hip}	-10.10 ± 8.91 J	-0.0150±0.0148	0.13±0.26	0.017±0.008	0.87		0.30
Metabolic rate, $\dot{E}$	230.73 ± 40.88 W	0.10 ± 0.02	-2.34±0.59	0.189±0.021	0.89	*	6e-9

List of symbols and abbreviations

COM	center of mass
M	body mass
L	leg length
$\vec{v}_{\mathrm{COM}}$	center of mass velocity
P_{COM}	instantaneous center of mass work rate
$\vec{F}$	ground reaction force
$W^{+}_{\mathrm{joint}}, W^{-}_{\mathrm{joint}}$	sum of joint work per stride
$W^{+}_{\mathrm{ank}}, W^{-}_{\mathrm{ank}},$	ankle joint work per stride
$W^{+}_{\mathrm{kne}}, W^{-}_{\mathrm{kne}}$	knee joint work per stride
$W^{+}_{\mathrm{hip}}, W^{-}_{\mathrm{hip}}$	hip joint work per stride
W_{PO}	center of mass work during push-off
W_{CO}	center of mass work during collision
W_{MS}	center of mass work during middle-stance
g	gravitational acceleration
$\dot{}$	net metabolic rate

Discussion

This study was intended to test the mechanism by which reduced push-off leads to increased energetic cost of walking. A simple model predicts that reduced push-off work from the trailing leg should lead to greater collision losses at the leading leg, which must be offset with more positive work elsewhere in the gait cycle to maintain the same walking speed. We experimentally applied a kinematic restriction to the ankle, and found it to successfully reduce push-off work produced by healthy subjects. This was accompanied by more dissipative collision work, more positive work by the joints over the entire stride, and greater metabolic energy expenditure overall. These results are consistent with the proposed mechanistic link between ankle push-off and overall energy expenditure. The results also yield insight regarding compensation for reduced push-off, with possible implications for patient groups with similar deficits.

Reduced push-off resulted in more work performed elsewhere in the gait cycle, and greater dissipation during the opposite leg's collision. For each 1 J of reduced push-off work, subjects performed an additional 0.64 J of dissipative collision work (from slope of linear fits in Fig. 4.7), as well as about 1.33 J more work during middle-stance. The dissipation was less than one-to-one with respect to push-off, suggesting that subjects were able to adjust their gait to avoid increased collision to some degree. They nevertheless paid a 33% penalty in positive work for performing it elsewhere than at push-off. No such penalty would be expected if walking were solely a matter of performing a constant amount of positive, propulsive work. Our results agree with the model prediction, that a properly timed push-off can reduce the energy dissipated by collision, which then reduces the amount of positive work needed over a stride.

There were several ways that subjects compensated for reduced push-off. The COM work rate during middle-stance shifted positively, in terms of both greater positive rebound work and less negative pre-load work. Here, COM measures are limited in their resolution, and closer examination of joint kinetics reveals that the knee bears the brunt of the compensations for reduced ankle push-off. When ankle push-off was restricted the knee experienced greater flexion while producing considerably greater extension moment during much of the stance phase. The net effect was to contribute substantially more work during most of middle-stance, and particularly during rebound. The knee power also remained positive for part of the (net negative)

preload phase. Thus, there is simultaneous positive and negative work within the limb that is not captured well by COM work.

There were also subtler compensations at the other joints. For example, the ankle appeared to contribute less negative work, particularly during pre-load. This is largely consistent with the expectation that reduced plantarflexion should result in decreases in amount of both negative and positive work at the ankle. A separate model of walking, including series elasticity at the ankle, suggests that elastic pre-load can enhance push-off work through passive dynamics (Zelik et al., 2013). Thus, we would not consider reduced ankle pre-load to be energetically advantageous, even though it contributed to the positive shift in middle-stance work. Separate from that effect, the ankle also appeared to perform slightly less negative work immediately following heelstrike, and the hip performed slightly more positive work over a stride. Our subjects therefore redistributed work across joints and throughout the gait cycle, and performed more of it overall, to compensate for reduced push-off.

A primary consequence of these changes in work was greater metabolic energy expenditure. We observed about an extra 2 W of metabolic power for each 1 W reduction in push-off work. For reference, a 50% reduction in push-off resulted in an energetic penalty comparable to carrying an extra load of about 10 kg (Huang and Kuo, 2014). As discussed above, no increase would be expected if walking were merely a matter of supplying sufficient work. Closer examination of the knee's positive work reveals a distinct possibility that some of it could be powered elastically as a consequence of the immediately preceding collision (Shamaei et al., 2013). Accordingly, the term rebound refers not only to the knee's rapid flexion and extension, but also to the possibility that some of the work could be elastic. We also consider it likely that subjects sought other compensations to substitute for push-off and avoid the penalties incurred by our model, which lacks the degrees of freedom to compensate efficiently. Although it is difficult to predict how humans might adapt to artificially induced deficits, it appears reasonable for them to seek relatively efficient compensations with the many degrees of freedom available to them. However, despite this compensation, it nevertheless appears quite costly to walk with reduced push-off.

While these results demonstrate a clear link between push-off and efficient gait, there are opposing opinions regarding ankle push-off. Others have proposed that push-off aids initiation of the swing phase (Bajd et al., 1997; Meinders et al., 1998), more so than redirection of the COM

(Lipfert et al., 2014). Reduced push-off might then be expected to adversely affect swing initiation. This would be expected to result in either a slower swing phase, or the avoidance of slow swing through compensations such as greater moments and powers at hip and knee. In fact, swing phase appeared slightly faster, not slower, with reduced push-off (as indicated by a positive correlation between swing time and push-off work; Table 1). We did not observe significant change at hip and knee moments and powers. Our data therefore do not suggest a strong detriment in swing phase initiation due to reduced push-off.

The findings presented here are subject to a number of limitations. We reduced push-off work with an artificial kinematic constraint. This may have had unintended consequences, such as causing subjects to exaggerate knee flexion (and thus negative work) during collision (Fig. 4.6). A more direct approach might have been to constrain ankle kinetics more explicitly, for example with mechanical damping, or more invasively through a nerve block to the plantarflexor muscles. There may be yet other ways to reduce push-off more effectively, especially if the intent is to model particular pathologies. Depending on the condition, such as ankle fusion, ankle-foot-orthosis, or prosthesis, the actual effect on push-off in patients, and associated co-morbidities, could potentially be quite different from the constraint applied here. We had sought here to control against such effects by studying able-bodied individuals, but future studies might benefit from experimental models more similar to actual pathologies affecting push-off.

Another challenge we encountered was in the quantification of mechanical work. Our model only predicts broad trends in work without ability to predict how it might be redistributed between the joints. The measurements were similarly broad, with COM and summed joint work both characterizing the overall work performed on the body in roughly similar ways (Fig. 4.4). But positive COM work over a stride appears not to capture the increased work demands resulting from reduced push-off (Doets et al., 2009), which appear to be met by the knee and hip (Fig. 4.5). Increased positive joint work may cancel negative work at other joints, for example the ankle during pre-load, and therefore appear as less negative work on the COM rather than more positive work. We thus find it more suitable to examine the work performed over the middle-stance phase (including both rebound and pre-load phases), which did yield more work with greater ankle restriction, as expected. Middle-stance work is actually more relevant to the simple model, which does not predict the separate effects on rebound and preload phases.

We also caution that all of the work measures are incomplete. Although we find COM work to be a helpful measure for testing some hypotheses (e.g., Adamczyk et al., 2006; Donelan et al., 2001a; Donelan et al., 2002b; Zelik and Kuo, 2010), it does not quantify work performed peripheral to the COM (Zelik and Kuo, 2012b). Summed joint work appears more suitable for that purpose. It also remains helpful to examine the individual joint powers to determine compensations for reduced push-off. But joint powers, like all other non-invasive measures practical for human locomotion, are also only indirect indicators of the work actually performed by muscle fascicles.

Despite these limitations, our findings may have implications for patient groups with reduced push-off. Both the amount and timing of push-off appear important for energy economy, as also suggested by studies of ankle exoskeletons (Malcolm et al., 2013; Sawicki and Ferris, 2008), ankle orthoses (Bregman et al., 2011a), and lower limb prosthetics (Collins and Kuo, 2010; Zelik et al., 2011). If push-off cannot be restored, an alternative is to reduce the collision loss, for example with arc-shaped foot bottoms (Adamczyk and Kuo, 2013; Adamczyk et al., 2006; van Engelen et al., 2010; Vanderpool et al., 2008). Such interventions might help to mitigate the disadvantages of impaired ankle strength or power.

Supplementary Material

We briefly summarize details of the dynamic walking model, which comprises pendulum-like legs and concentrated mass at the pelvis (Kuo, 2002b). During stance phase, the COM moves in an inverted pendulum arc atop the stance leg. The COM moves down-and-forward with a velocity v^- just before heelstrike, and must be redirected to up-and-forward for the next leg's inverted pendulum arc (denoting that velocity v^+). The COM velocity is redirected by a preemptive push-off impulse and a heelstrike collision impulse. Because all the mass is concentrated at the COM, the push-off and collision impulses can only point to the COM, and perpendicular to v^- and v^+ respectively. The COM velocity after push-off and before collision is denoted v_{mid}. The push-off work W_{PO} can be derived as

$$W_{\mathrm{PO}} = \frac{(\hat{F}_{\mathrm{PO}})^2}{2M} \tag{A1}$$

where M is total mass and $\hat{F}_{\mathrm{PO}}$ is the push-off impulse. Similarly the dissipative work by the collision impulse $\hat{F}_{\mathrm{CO}}$ is:

$$W_{\mathrm{CO}} = -\frac{(\hat{F}_{\mathrm{CO}})^2}{2M}. \tag{A2}$$

The relationship between the collision impulse and v_{mid} is

$$\hat{F}_{\mathrm{CO}} = M v_{\mathrm{mid}} \sin(2\alpha - \beta) \tag{A3}$$

where α is the angle between each leg and vertical during the step-to-step transition, and β is the angle between v_{mid} and v^-. Using geometry, we have

$$v_{\mathrm{mid}} = \sqrt{(v^-)^2 + \left(\hat{F}_{\mathrm{PO}}\right)^2/M^2} \tag{A4}$$

$$\beta = \tan^{-1}(\hat{F}_{\mathrm{PO}}/Mv^-) \tag{A5}$$

This yields collision impulse

$$\hat{F}_{\mathrm{CO}} = M\sqrt{(v^-)^2 + \left(\hat{F}_{\mathrm{PO}}\right)^2/M^2}\ \sin^2(2\alpha - \tan^{-1}(\hat{F}_{\mathrm{PO}}/Mv^-)) \tag{A6}$$

Substituting Eqns 4 - 6 into Eqn 2

$$W_{\mathrm{CO}} = -\frac{M}{2}\left((v^-)^2 + \frac{2W_{\mathrm{PO}}}{M}\right)\sin^2\left(2\alpha - \tan^{-1}\left(\frac{\sqrt{2W_{\mathrm{PO}}}}{Mv}\right)\right) \tag{7}$$

Assuming small angle approximations and that v^- is close to the average walking speed v,

$$2\alpha \approx \frac{s}{L} \tag{A8}$$

$$\tan\left(\frac{\sqrt{2W_{PO}}}{Mv}\right) \approx \frac{\sqrt{2W_{\mathrm{PO}}}}{Mv} \tag{A9}$$

Where *s* is step length and *L* leg length. Then we have our final formula for dissipative collision work:

$$W_{\mathrm{CO}} \approx -\frac{M}{2}\left(v^2 + \frac{2W_{\mathrm{PO}}}{M}\right)\left(\frac{s}{L} - \frac{\sqrt{2W_{\mathrm{PO}}}}{Mv}\right)^2 \tag{A10}$$

$$\approx -\frac{Ms^2v^2}{2L^2} + W_{\mathrm{PO}}^{\frac{1}{2}}\left(\frac{2sv}{L}\right) - W_{\mathrm{PO}}^{1}\left(\frac{1}{M} + \frac{s^2}{L^2}\right) + W_{\mathrm{PO}}^{\frac{3}{2}}\left(\frac{2\sqrt{2}s}{MLv}\right) - W_{\mathrm{PO}}^{2}\left(\frac{2}{M^2v^2}\right).$$

For typical human walking speeds, W_{PO} is quite small, and so W_{CO} will generally be dominated by the two terms of lowest order, yielding Eqn. 1.

Chapter 5 Parametric Study on Energetics and Mechanics of Human walking with Compliant Artificial Feet

Abstract

Ankle performs a burst of positive work at late stance phase, which has been shown to reduce the negative work of heel-strike collision and improve human walking economy. For healthy individuals, most of the ankle positive work is contributed by elasticity of the Achilles tendon, which stores and returns energy. The elasticity could reduce the active work demanded of muscles and could be beneficial to walking economy. But this does not explain what spring stiffness would be the most appropriate since any spring could return energy. The particular value of stiffness for the Achilles tendon, and the related parameter of foot length, might be critical to walking economy. Indeed, a dynamic walking model with an compliant ankle predicts an optimal combination of the two, as well as consequences for non-optimal combinations. Too stiff an ankle and too short a foot is predicted to cause early and weak push-off, whereas too long a foot and too compliant an ankle is predicted to cause late push-off. The trade-offs have not, however, been tested experimentally. We therefore tested healthy adults (N = 10) wearing compliant artificial feet walking at constant speed with different ankle stiffnesses and foot lengths. We found later and more elastic push-off for more compliant ankle and short foot. The more elastic push-off was beneficial to the energetic cost, but late push-off diminished the benefit. The trade-off between earlier push-off, for stiffer ankle and shorter foot, and more elastic push-off, for more compliant ankle and longer foot, explained the minimum energetic cost we found for intermediate ankle stiffness and foot length.

Introduction

Human ankle performs a burst of positive work, termed push-off, late in the stance phase, which appears to benefit walking economy(Adamczyk and Kuo, 2009; Huang and Kuo, 2014; Zelik et al., 2013). Much of this ankle push-off is contributed by the elastic Achilles tendon, which stores energy earlier in stance as ankle dorsiflexes, and return during late stance phase, as the ankle plantarflexes (Ishikawa et al., 2005). Patients with gait pathology or lower extremity amputation usually perform much less push-off, which leads to greater energetic cost for walking(Waters and Mulroy, 1999). Several ankle-foot orthoses and prosthetic feet are designed to regenerate the ankle push-off work using passive elastic elements. The elastic push-off seems to be able to improve patients walking economy, but what the main factors determine the amount of elastic push-off, and what the best elastic push-off is are still unknown. Two important parameters affecting the elastic push-off are the compliant ankle stiffness and foot length. Intuitively, too stiff ankle or too compliant ankle cannot perform any elastic push-off, so the energetic cost of walking with too stiff or too compliant ankle should be greater than intermediate stiffness. The too stiff ankle can be considered as a rigid ankle, and too compliant ankle can be considered as a free joint. Either way there is no elastic push-off. On the other hand, too long or too short foot should also have greater energetic cost intuitively. The too long foot may causes problem to maintain the ground clearance and too short foot can also be considered as a free joint, which performed zero elastic push-off. However, it had not been tested systematically and experimentally how the compliant ankle stiffness and the foot length of a compliant ankle affect the energetic cost of human walking. Here we performed a parametric study on the ankle stiffness and length of compliant artificial foot. We sought to determine how ankle stiffness and foot length affect the elastic push-off, as well as the energetic cost of walking.

A number of commercially available prosthetic feet with compliant keel, such as Flex-foot and Seattle foot, are considered preferable to non-compliant designs (Hafner et al., 2002). The elastic properties of these feet can store energy during mid-stance and return it in late stance. Some quantitative improvements have been observed including faster self-selected walking speed(Snyder et al., 1995a), longer stride lengths (Perry and Shanfield, 1993), less peak vertical ground reaction force (Lehmann et al., 1993; Perry and Shanfield, 1993; Powers et al., 1994; Snyder et al., 1995b) and apparently resuced energetic cost of walking (Nielsen et al., 1988). Therefore, it appears that the energy-store-and-return property can improve patients' walking,

although the mechanisms not yet understood. Also, how to design a compliant ankle prosthetic foot providing the best performance for minimal energetic cost of amputee walking is still unclear.

Several dynamic walking models have shown there is an optimal stiffness of compliant ankle for minimal mechanical work (Bregman et al., 2011b; Zelik et al., 2014). In fact, walking can theoretically have zero cost in a model with appropriate ankle stiffness and foot length (Zelik et al., 2014). A compliant ankle dynamic walking model (Fig. 5.1 A) predicts that the heel-strike collision can be modulated by the energy return from the elastic ankle (Zelik et al., 2014). The amount of elastic push-off and the timing of it are the main factors determining the heel-strike collision. The collision can be reduced by the elastic push-off preemptive to heel-strike which redirects COM. The ankle stiffness and foot length are two important factors determining the amount and timing of the elastic push-off. Karl Zelik found that the more compliant ankle and longer foot leads to more and later elastic push-off. The energetic cost is therefore a function of ankle stiffness and foot length (Fig. 5.1 B & C). However, these predictions from the compliant ankle model have not been tested experimentally.

In this study, we tested healthy adults (N = 10) walking wearing compliant artificial feet with different ankle stiffnesses and foot lengths. We expected more and later elastic push-off (Fig 5.1 B & C) for more compliant ankle and longer foot according to the compliant ankle model. Also, we expected optimal ankle stiffness and foot length yielding minimum energetic cost, based on the compliant ankle walking model.

Method

We performed a parametric study on human walking with compliant artificial feet with different ankle stiffnesses and foot lengths (Fig. 5.1 D). We examined these parameters in two separate experiments to measure mechanical work and metabolic cost. First we test how the **ankle stiffness** of artificial ankle affects the energetic cost and mechanics of human walking. Second we test how the **length** of compliant feet affects the energetic cost and mechanics. The compliant artificial feet have rigid base and elastic foot plates made by fiberglass (Garolite). The stiffness of ankle is simulated by the leaf spring construction. The stiffness and foot length can be adjusted by replacing different thickness and length of foot plates. The compliant artificial foot is 0.13 m height and 3 inch wide.

In the stiffness experiment, ten healthy adults (N = 10, 6 male and 4 female) were recruited to walk with four different thicknesses (0.1250, 0.1875, 0.2500 and 0.375 inches) of foot plates with the same length of 9 inch (Fig. 5.1 E). Subjects ranged 18-26 years of age and had average body mass M of 73.16 ±12.92 kg (mean ± s.d.), and leg length L 0.95 ± 0.05 m. We measured the ankle stiffness by the slope of force-displacement curve using material test machine. The corresponding linear stiffnesses are 6.60, 18.68, 38.66, 58.29 $kN \cdot m^{-1}$. In foot length experiment, 8 healthy adult participates(N = 8, 6 male and 2 female) walked with five different lengths (5, 9, 11, 13, 15 inches) of compliant foot with same thickness of 0.25 inches (Fig. 5.1 F). Subjects ranged 18-26 year of age and had average body mass M of 71.79 ± 12.43 and leg length L 0.97 ± 0.06 m. Each subject had two 15 minutes training session before data collection. Subjects were asked to walk on the instrumental treadmill with constant walking speed 1.25 ms^{-1} for at least 8 minutes for each trial to ensure steady state walking. Rates of oxygen consumption and carbon dioxide production were measured (Carefusion, Vernon Hills, IL, USA) to estimate the metabolic rate, expressed in unit of power (W) using standard conversion factor(Brockway, 1987b). The ground reaction force of each leg was measured using an instrumented force treadmill (Bertec, Columbus, OH, USA). Lower extremity kinematic data were collected using marker-based motion capture system (VICON, Los Angeles, CA, USA).

Data analysis

We calculated the instantaneous COM power P_{COM} as inner product of ground reaction force $\vec{F}$ of each leg and the COM velocity $\vec{v}_{COM}$(Donelan et al., 2002d).

$$P_{\mathrm{COM}} = \vec{F} \cdot \vec{v}_{\mathrm{COM}} \qquad (5\text{-}1)$$

The stance phase of each leg can be divided into Collision, Rebound, Preload and Push-off according to the sign of instantaneous COM work rate (Fig 5.4A). The Rebound and Pus-off phases are also called Middle-stance phase. We calculated the average COM work rate $\dot{W}_{\mathrm{COM}}$ as COM work per stride W_{COM} times step frequency f, where COM work per step was calculated by integrating the instantaneous COM work rate P_{COM} over a step.

$$\dot{W}_{COM} = \int P_{\mathrm{COM}}\, dt \times f \qquad (5\text{-}2)$$

We also calculated COM Collision, Rebound, Preload and Push-off work rate defined as the integral of COM power over each period times the stride frequency.

Joint angles, moments and powers of knee and hip were calculated using inverse dynamic technique with commercial software (Visaul3D, C-motion, Germantown, MS, USA). Artificial ankle power P_{ankle} was calculated as sum of translational power performed on the distal end of shank, defined as inner product of the ground reaction force $\vec{F}$ and translational velocity at the fulcrum of the leaf spring $\vec{v}_{\text{ankle}}$, and rotational power performed on the distal end of shank, defined as the inner product of artificial ankle moment about the fulcrum of leaf spring $\vec{T}_{\text{ankle}}$ and angular velocity of the shank $\vec{\omega}_{\text{shank}}$ (Caldwell and Forrester, 1992; Gordon et al., 1980; Prince et al., 1994).

$$P_{\text{ankle}} = \vec{F} \cdot \vec{v}_{\text{ankle}} + \vec{T}_{\text{ankle}} \cdot \vec{\omega}_{\text{shank}} \quad (5\text{-}3)$$

To quantify the timing of elastic push-off, we defined mid push-off time as the time (% stride) when half of elastic energy is returned.

We also calculated the individual joint work rate, defined as the integral of positive/negative portion of joint power over a stride, times stride frequency, similar to the COM work rate.

To quantify the effects of ankle stiffness and foot length on the measurements, we first tested for a second-order fit using least square regression method among each measurement as function of ankle stiffness and foot length.

Second-order fit :

$$a_k k_{\text{ank}}^2 + b_k k_{\text{ank}} + c_k \quad (5\text{-}4)$$

$$a_l l^2 + b_l l + c_l \quad (5\text{-}5)$$

Use the completing the square technique, we can rearrange Eqn. 5-4 and 5-5:

$$a_k \left(k_{\text{ank}} - k_{\text{opt}}\right)^2 + e_k \quad (5\text{-}6)$$

$$a_{\text{l}} \left(l - l_{\text{opt}}\right)^2 + e_l \quad (5\text{-}7)$$

Where e_{k} and $e_{\mathrm{l}}$are the extreme value of the measurements within the range of ankle stiffness and foot length, and k_{opt} and l_{opt} are the corresponding ankle stiffness and foot length.

A second-order fit was considered significant if the confident interval of the quadratic coefficient (a_k & a_l) does not include zero. If the significant second-order fit is not found, we then test for first-order (linear) fit.

First-order fit:

$$b_k k_{\mathrm{ank}} + c_k \quad (5\text{-}8)$$

$$b_l l + c_l \quad (5\text{-}9)$$

To compare subjects with different size, we normalized all measurement by body mass M, leg length l, and gravity acceleration g (9.81 ms^{-1}). Work and moment were normalized by mgl (776.39 ± 151.78 J). Power was normalized by $mg^{15}l^{0.5}$ (2337.5 ± 432.2 W). Stiffness was normalized by mgl^{-1} (664.87 ± 112.38 Nm^{-1}).

Results

Both ankle stiffness and foot length of the compliant artificial foot had significant effects on the mechanics and energetic cost of walking. We found that intermediate values of stiffness and foot length yielded the minimum metabolic rate. Low stiffnesses resulted in late elastic energy return and greater heel-strike collision loses. High stiffnesses resulted in less elastic energy store and return. Short feet resulted in less elastic energy store and return and greater heel-strike collision loses. Longer feet resulted in late and greater elastic energy return, but more negative knee work. All these observation above could be disadvantageous for energetic economy. The trend of work performed by the active biological joints (knee + hip) matched the trend of metabolic rate.

Ankle stiffness

There are several qualitative observations to be made regarding ground reaction force and power trajectories. As ankle stiffness increased, the first peak of vertical ground reaction force decreased, indicating less impact at heel-strike. The second peak of vertical ground reaction increased with stiffer ankle (Fig 5.2 A). The COM power trajectories also changed with different

ankle stiffness (Fig. 5.3). Larger peaks were observed during Collision and Rebound for more compliant ankle. On the other hand, stiffer ankle had greater amplitude of COM power during Preload and Push-off. The active biological power trajectories (summed of knee and hip) had smaller amplitude in positive period (15-50 % stride) and negative period (50 – 62 % stride) for stiffer ankle. The compliant ankle power had less amplitude in both positive and negative periods for stiffer ankle. Knee power and hip power trajectories also changed with different ankle stiffnesses and foot lengths, but trends were more complicated and no monotonic trend was observed.

Besides joint power trajectories, we also made some qualitative observation on joint angles and moment. For stiffer ankle, there was less dorsiflexion at compliant ankle in stance phase but greater plantarflexion moment. Knee had less flexion during the stride for stiffer ankle, and less extension moment during Rebound and greater flexing moment during Preload. No obvious change was observed at hip angle, but hip extension moment was less during Collision for stiffer ankle (Fig. 5.4).

The metabolic rates $\dot{E}$ exhibited a U-shape trend as a function of the ankle stiffness (Fig. 5.6 A). The optimal ankle stiffness was about 63.3 (dimensionless), which yielded a minimal metabolic rate of 0.18 (412.39 W).

We found significant second-order fits for ankle stiffness results in positive/negative COM work rates ($\dot{W}^{+}_{\mathrm{COM}}$ & $\dot{W}^{-}_{\mathrm{COM}}$), active biological work rates ($\dot{W}^{+}_{\mathrm{bio}}$ & $\dot{W}^{-}_{\mathrm{bio}}$), COM Collision, Middle stance and Push-off work rates ($\dot{W}_{\mathrm{CO}}, \dot{W}_{\mathrm{mid}}$ & $\dot{W}_{\mathrm{PO}}$), knee negative work rate ($\dot{W}^{-}_{\mathrm{kne}}$) and stride frequency ($f$). We also found significant first order fits in ankle, knee and hip positive work rates ($\dot{W}^{+}_{\mathrm{ank}}, \dot{W}^{+}_{\mathrm{kne}}$ & $\dot{W}^{+}_{\mathrm{hip}}$) and mid push-off time with negative slopes indicating reduction for stiffer ankle. No significant fit was found ankle and hip negative work rates ($\dot{W}^{-}_{\mathrm{ank}}$ & $\dot{W}^{-}_{\mathrm{hip}}$). More details about the fitting can be found in Table 5.1, Fig. 5.6 and 5.7.

Foot length

There are several qualitative observations to be made regarding ground reaction force and power trajectories. As foot length increased, the first peak of vertical ground reaction force decreased, while the second peak maintained similar (Fig. 5.2 B). For different foot length, the positive

period (15-50% stride) of biology power changed with no monotonic trend. The amplitude of biology power in negative period (50-62 % stride) increased with longer foot. The compliant ankle power (Fig. 5.3) had less amplitude in both positive and negative periods for stiffer ankle, and greater amplitude for longer foot. Knee power and hip power trajectories also changed with different foot lengths, but trends were more complicated and no monotonic trend was observed (Fig. 5.3).

Besides joint power trajectories, we also made some qualitative observation regarding joint angles and moment for different foot lengths. For longer foot, compliant ankle had more dorsiflexion angle and moment during stance phase. Knee had more flexion during swing phase and greater flexion moment during Preload for longer foot. No obvious change was observed at hip angle and moment (Fig. 5.5).

The metabolic rates exhibited a U-shape trend as a function of foot length (Fig. 5.6 A). The optimal foot length was about 0.23 (dimensionless) yielding the minimal metabolic rate of 0.18 (423.32 W).

We found significant second-order fits for foot length results in positive/negative COM work rates ($\dot{W}^{+}_{\mathrm{COM}}$ & $\dot{W}^{-}_{\mathrm{COM}}$), active biological work rates ($\dot{W}^{+}_{\mathrm{bio}}$ & $\dot{W}^{-}_{\mathrm{bio}}$), COM Collision work rates ($\dot{W}_{\mathrm{CO}}$), knee positive/negative work rate ($\dot{W}^{+}_{\mathrm{kne}}$ & $\dot{W}^{-}_{\mathrm{kne}}$), hip positive work rate ($\dot{W}^{+}_{\mathrm{hip}}$) and stride frequency ($f$). W e also found significant first order fits in COM Push-off work rate ($\dot{W}_{\mathrm{PO}}$), ankle positive/negative work rates ($\dot{W}^{+}_{\mathrm{ank}}$ & $\dot{W}^{-}_{\mathrm{ank}}$), hip negative work rate ($\dot{W}^{-}_{\mathrm{hip}}$) and mid push-off time, which all increased with longer foot length. More details about the fitting can be found in Table 5.2, Fig. 5.6 and 5.7.

Table 5-1: Qualitative results for walking with different ankle stiffnesses.

	a_k± c.i	b_k± c.i	c_k± s.d.	R^2	p	k_{opt}	e_{k}	SI unit
COM work rate, $\dot{W}^{+}_{\text{COM}}$	7.3±7.2E-7	-1.3±0.8E-4	2.3±0.2E-2	0.78	0.05	91.9	0.017	38.82
COM work rate, $\dot{W}^{-}_{\text{COM}}$	-1.1±0.7E-6	1.5±0.8E-4	-2.3±0.2E-2	0.78	4E-3	67.7	-0.017	-40.71
Bio work rate, $\dot{W}^{+}_{\text{bio}}$	3.3±3.2E-6	-4.3±3.3E-4	5.9±0.6E-2	0.62	0.04	65.2	0.045	105.23
Bio work rate, $\dot{W}^{-}_{\text{bio}}$	-1.8±1.6E-6	2.8±1.6E-4	-3.3±0.4E-2	0.76	0.03	79.4	-0.020	-47.49
Collision work rate, $\dot{W}_{\text{CO}}$	-1.8±0.8E-6	2.6±0.9E-4	-1.9±0.3E-2	0.89	2E-4	74.1	-0.009	-20.66
Mid stance work rate, $\dot{W}_{\text{mid}}$	2.5±0.8E-6	2.5±0.8E-6	1.1±0.5E-2	0.93	3E-6	79.3	-0.003	-7.53
Push-off work rate, $\dot{W}_{\text{PO}}$	-1.2±0.4E-6	1.6±0.4E-5	6.1±1.5E-3	0.89	1E-5	68.2	0.011	26.65
Ankle work rate, $\dot{W}^{+}_{\text{ank}}$	N/A	-4.5±3.0E-5	1.5±0.4E-2	0.79	6E-3	N/A	N/A	NaN
Ankle work rate, $\dot{W}^{-}_{\text{ank}}$	N/A	5.0±7.8E-5	-3.4±1.2E-2	0.82	0.20	N/A	N/A	NaN
Knee work rate, $\dot{W}^{+}_{\text{kne}}$	N/A	-2.9±3.0E-5	9.2±2.0E-3	0.52	0.06	N/A	N/A	NaN
Knee work rate, $\dot{W}^{-}_{\text{kne}}$	-1.6±1.4E-6	2.7±1.5E-4	-3.0±0.4E-2	0.82	0.03	81.4	-0.019	-44.70
Hip work rate, $\dot{W}^{+}_{\text{hip}}$	N/A	-7.0±7.6e-5	4.5±0.7E-2	0.60	0.07	N/A	N/A	NaN
Hip work rate, $\dot{W}^{-}_{\text{hip}}$	N/A	3.0±8.0E-6	-1.4±1.0e-3	0.75	0.45	N/A	N/A	NaN
Metabolic rate, $\dot{E}$	6.4±3.4E-6	-8.3±3.6E-4	2.0±0.02e-1	0.52	5E-4	63.3	0.18	412.39
Stride frequency, f	3.8±2.8eE-6	-5.2±3.0E-4	3.1±0.14e-01	0.90	0.01	69.3	0.29	0.88
Mid push-off time	N/A	-2.2±0.8E-2	59±1	0.88	7E-6	N/A	N/A	NaN

Table 5-2: Qualitative results for walking with different foot lengths

	a_l± c.i	b_l± c.i	c_l± s.d.	R^2	p	l_{opt}	e_l	SI unit
COM work rate, $\dot{W}^{+}_{\text{COM}}$	4.6±1.3E-1	-1.9±0.6E-1	4.0±0.4E-2	0.87	6E-8	0.21	0.017	46.48
COM work rate, $\dot{W}^{-}_{\text{COM}}$	-3.6±1.2E-1	1.5±0.6E-1	-3.2±0.6E-2	0.92	7E-7	0.207	-0.017	-40.35
Bio work rate, $\dot{W}^{+}_{\text{bio}}$	1.4±0.5	-6.8±2.6E-1	1.3±0.1E-1	0.75	9E-6	0.24	0.045	115.37
Bio work rate, $\dot{W}^{-}_{\text{bio}}$	-7.0±3.1E-1	2.7±1.4E-1	-5.0±0.8E-2	0.80	6E-5	0.19	-0.023	-55.30
Collision work rate, $\dot{W}_{\text{CO}}$	-3.2±1.3E-1	1.9±0.6E-1	-3.3±0.4E-2	0.88	1E-5	0.30	-0.006	-14.92
Mid stance work rate, $\dot{W}_{\text{mid}}$	4.8±2.6E-1	-2.9±1.2E-1	3.8±0.2e-2	0.73	8E-4	0.30	-0.006	-13.342
Push-off work rate, $\dot{W}_{\text{PO}}$	N/A	2.9±0.9E-02	6.2±2.3E-3	0.76	7E-8	N/A	N/A	NaN
Ankle work rate, $\dot{W}^{+}_{\text{ank}}$	N/A	1.4±0.2E-1	-7.1±6.5E-3	0.85	1E-12	N/A	N/A	NaN
Ankle work rate, $\dot{W}^{-}_{\text{ank}}$	N/A	-1.2±0.5E-1	-2.1±1.5E-2	0.75	4E-6	N/A	N/A	NaN
Knee work rate, $\dot{W}^{+}_{\text{kne}}$	4.1±1.6E-1	-1.8±0.7E-01	2.9±0.4E-2	0.77	9E-6	0.22	0.010	23.42
Knee work rate, $\dot{W}^{-}_{\text{kne}}$	-5.8±2.9E-1	2.3±1.4E-1	-4.4±0.8E-2	0.80	3E-4	0.20	-0.020	-48.27
Hip work rate, $\dot{W}^{+}_{\text{hip}}$	1.0±0.4	-5.1±2.0E-1	1.0 ±0.1E-1	0.79	2E-5	0.25	0.039	91.36
Hip work rate, $\dot{W}^{-}_{\text{hip}}$	N/A	-1.62±0.7E-3	-5.7±33E-4	0.82	1E-4	N/A	N/A	NaN
Metabolic rate, $\dot{E}$	3.0±0.8	-1.40±0.4	3.4±0.2E-1	0.82	1E-8	0.23	0.18	423.32
Stride frequency, f	9.1±5.2E-1	-6.5±2.4E-1	4.1±0.1E-1	0.87	1E-3	0.36	0.29	0.87
Mid push-off time	N/A	36±4	48±0.5	0.90	9E-17	N/A	N/A	NaN

Discussion

The goal of this study was to examine how ankle stiffness and foot length affect the mechanics and energetic cost of human walking. We observed a U-shape metabolic (Fig. 5.6) rate as a function of ankle stiffness and foot length implying the trade-off between compliant and stiff ankle, and the trade-off between short and long foot of the compliant artificial feet in human walking. The too compliant ankle and too short foot caused greater COM collision (Fig. 5.7 A) due to less COM push-off than stiffer ankle and longer foot, requiring more bio work rate (Fig. 5.6 B) than intermediate ankle stiffness and foot length to compensate. The too stiff ankle had more COM push-off work than softer ankle, but had more knee work contributed to the COM push-off work, ending up more active joint work (hip + knee work) than intermediate ankle stiffness. The too long foot had greater elastic push-off, but the push-off work was dissipated by knee due to the late timing, ending up more active joint work (hip + knee work) than intermediate foot length. The active joint work therefore exhibited similar U-shape as a function of ankle stiffness and foot length comparing to the metabolic rate.

The energetic cost of normal human walking has been shown to be depending on the positive mechanical work performed by lower extremity (Donelan et al., 2002d; Huang and Kuo, 2014), including the COM push-off work and rebound work. Ideally, the active mechanical work requirement can be zero if all the mechanical work, both positive and negative work, is performed by elastic mechanism. If there is energy dissipation somewhere besides the elastic material due to heel-strike collision or active negative joint work, it will require active mechanical work to compensate no matter how we design the elastic mechanism. Therefore, reducing the energy dissipation due to heel-strike collision and negative joint work is the key point to reduce energetic cost of walking.

The simplest dynamic walking model predicts that the push-off can reduce the heel-strike collision (Kuo et al., 2005b). In our experiment, we observed this relationship between COM push-off and collision, which more COM push-off led to less collision. For overly compliant ankle and short foot, we there was less COM push-off work and greater collision. Therefore there is more active positive joint work causing greater energetic cost of walking.

In normal human walking, COM push-off is mostly contributed by ankle push-off, and more COM push-off accompanies with more ankle push-off. In the stiffness experiment, however, we observed a reversed trend between COM push-off work and elastic ankle push-off work. For stiffer ankle, there was more COM push-off but less elastic ankle push-off. Instead, knee joint contributed more positive work during push-off for the stiffer ankle than more compliant ankle. Therefore, although too stiff ankle had more COM push-off and less collision, there was more active summed joint work which requires more metabolic energy.

Another important factor of the elastic push-off is the timing of it. The simplest dynamic walking model predicts that it would be the best if the push-off happens right before heel-strike. The compliant ankle model also found the optimal gait when the elastic push-off happens slightly before the heel-strike. Both too early and too late elastic push-off is not as effective in terms of reducing collision. In our experiments, the timing of push-off was after heel-strike for most of the trials except the extremely short foot, and was later for more compliant ankles and longer feet (Fig. 5.8). To perform earlier push-off, it requires enough ankle moment to lift the heel. The amount of ankle moment needed to lift heel depends on the foot length and the total body weight. For more compliant ankle, there was less ankle elastic moment than stiffer ankle and therefore later elastic push-off. For longer foot, although there was more elastic ankle moment, the required moment to lift heel was even larger due to the longer foot length. Therefore, although there was more energy stored in the compliant ankle for longer feet, it required the support from the leading leg and knee flexion to release energy. The elastic push-off for longer foot ends up dissipated by knee flexion.

Another possible factor for the metabolic rate besides the active biological work for longer foot is knee hyperextension. Close examinations of the positive biological work rate and gross metabolic rate (Fig. 5.6 A) reveals that metabolic rate increased faster than the positive biological work rate, implying other factors could also cause the metabolic rate increase. When the foot was longer, the center of pressure (COP) moved more forward in front of knee during stance phase and inducing an external knee hyperextension moment. The human knee performed larger flexion moment (Fig. 5.5, 40 % stride) to counter this effect. Although the knee power did not change much, this knee flexion moment could be costly due to greater muscle forces provided to avoid discomfort. We also observed similar but less severe increases in knee flexion

moment with stiffer ankle (Fig. 5.4, 40% stride), which could be also due to the COP moving too far forward of the knee. The primary concern is therefore with regards to foot length, rather than ankle stiffness.

In this study, we used mechanical work performed by knee and hip to explain the metabolic rate. There are still other factors, such as muscle force and co-contraction etc., which also contribute to the metabolic rate. Here we found the mechanical work alone can well explain the metabolic rate, which implies that other factors may not have significant change when walking with different ankle stiffness and foot length, or the effects of them were coupled to the mechanical work.

There are several limitations of this study. First, we tested healthy adults walking with compliant ankle using simulator boots, which increased the leg length by 13 cm. This increase could potentially affect the energetics and mechanics of walking. Secondly, we did not discuss the energetic cost due to other factors when explaining the metabolic rate. For example, the energetic cost due to the discomfort of knee hyperextension was not quantified in this study.

The results of this study indicate the importance of choosing proper ankle stiffness and foot length of human walking with compliant artificial ankle. Although we tested healthy subjects, the results can be implicated into design of prosthetic feet and ankle foot orthoses to improve patient walking economy. Also, this study can also potentially benefit the design of bipedal robots, which usually only have rigid or compliant ankle due to the difficulty to transfer power to the end of leg.

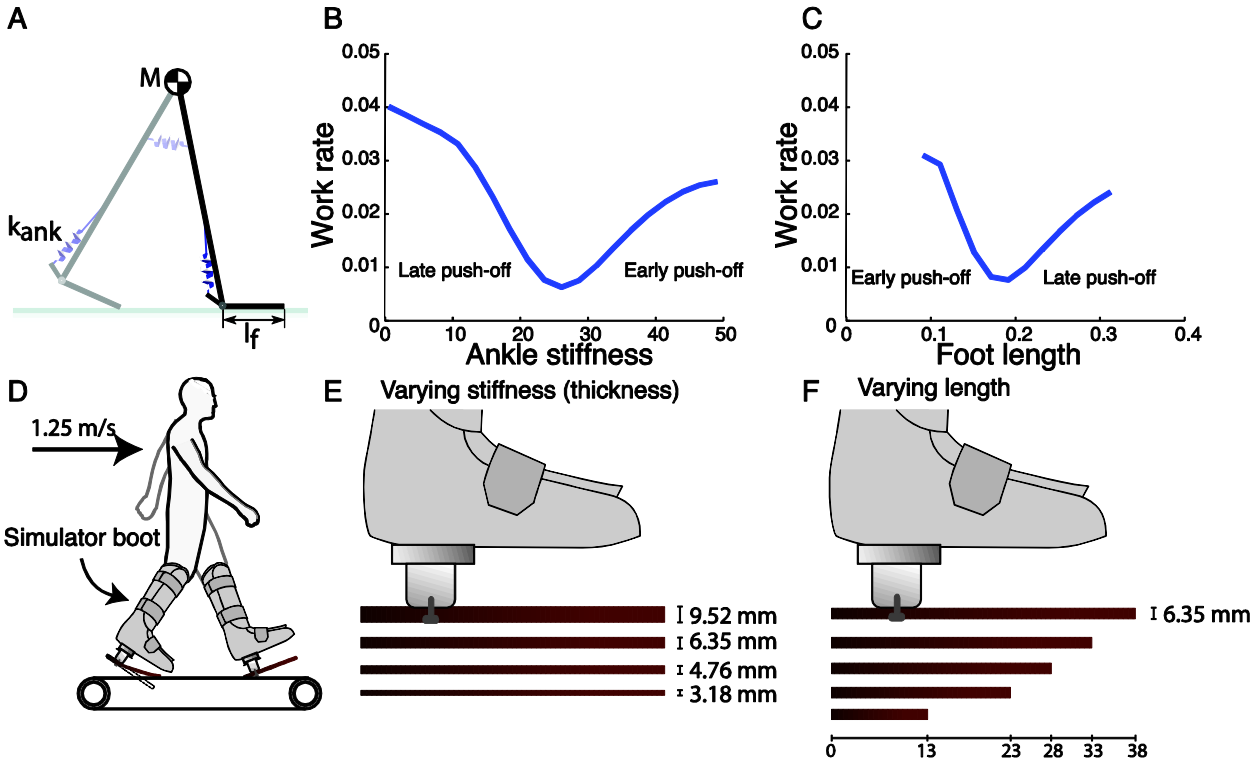

Figure 5.1 The energetic cost of springy ankle dynamic walking model (Zelik et al., 2013) and experiment set up.
(A)Springy ankle dynamic walking model has torsional spring at ankle and hip. The hip spring is used to modulate step frequency. (B) The energetic cost of springy ankle dynamic walking model as a function of ankle stiffness. The elastic push-off happened earlier for stiffer ankle. (C) The energetic cost of springy ankle dynamic walking model as a function of foot length. The elastic push-off happened earlier for shorter foot. (D) Subjects walking on an instrumental treadmill with constant speed wearing the simulator boots with compliant artificial foot attached at the bottom. The simulator boots fixated the ankle of the subjects. (E)The stiffness of the artificial ankle depends on the thickness of the fore-plate. Four thicknesses were tested in stiffness experiment, and (F) five lengths of foot plates for foot length experiment.

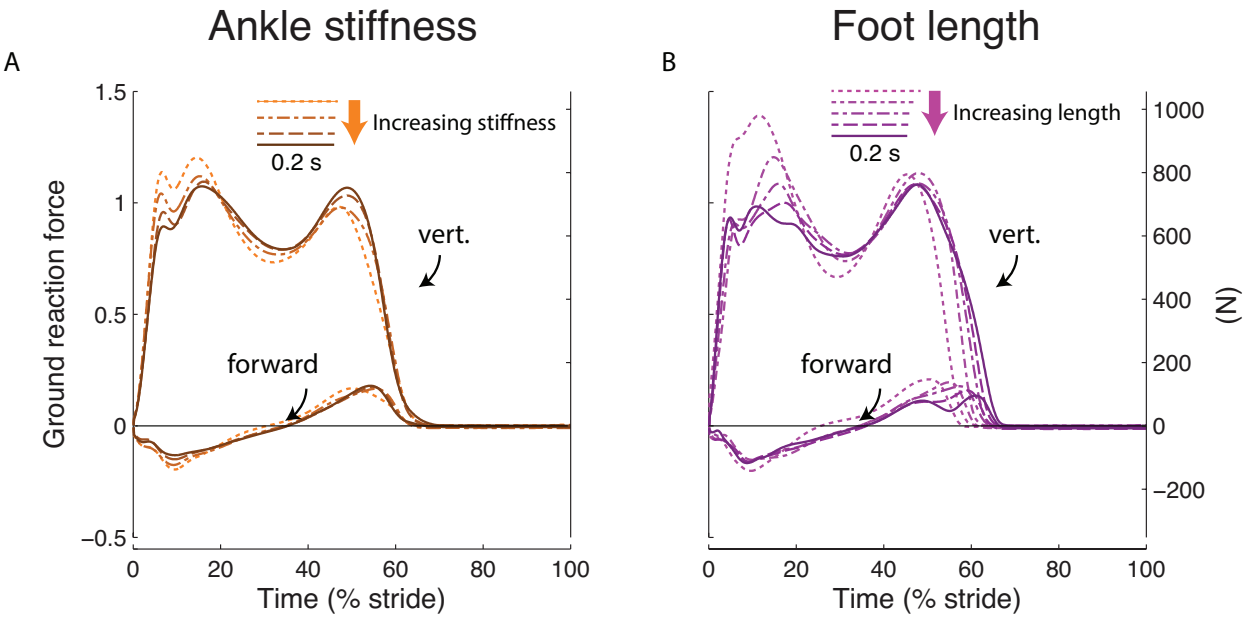

Figure 5.2 Ground reaction forces.
Vertical and horizontal (fore-aft) ground reaction force vs. stride time for different (A) ankle stiffnesses and (B) foot lengths. The hodograph, vertical COM velocity vs. horizontal (fore-aft) COM velocity, for different (C) ankle stiffnesses and (D) foot lengths Left-hand vertical axes show dimensionless quantities, right-hand axes show dimensional SI units. Data shown are trajectories averaged across subjects ($N = 8$).

.

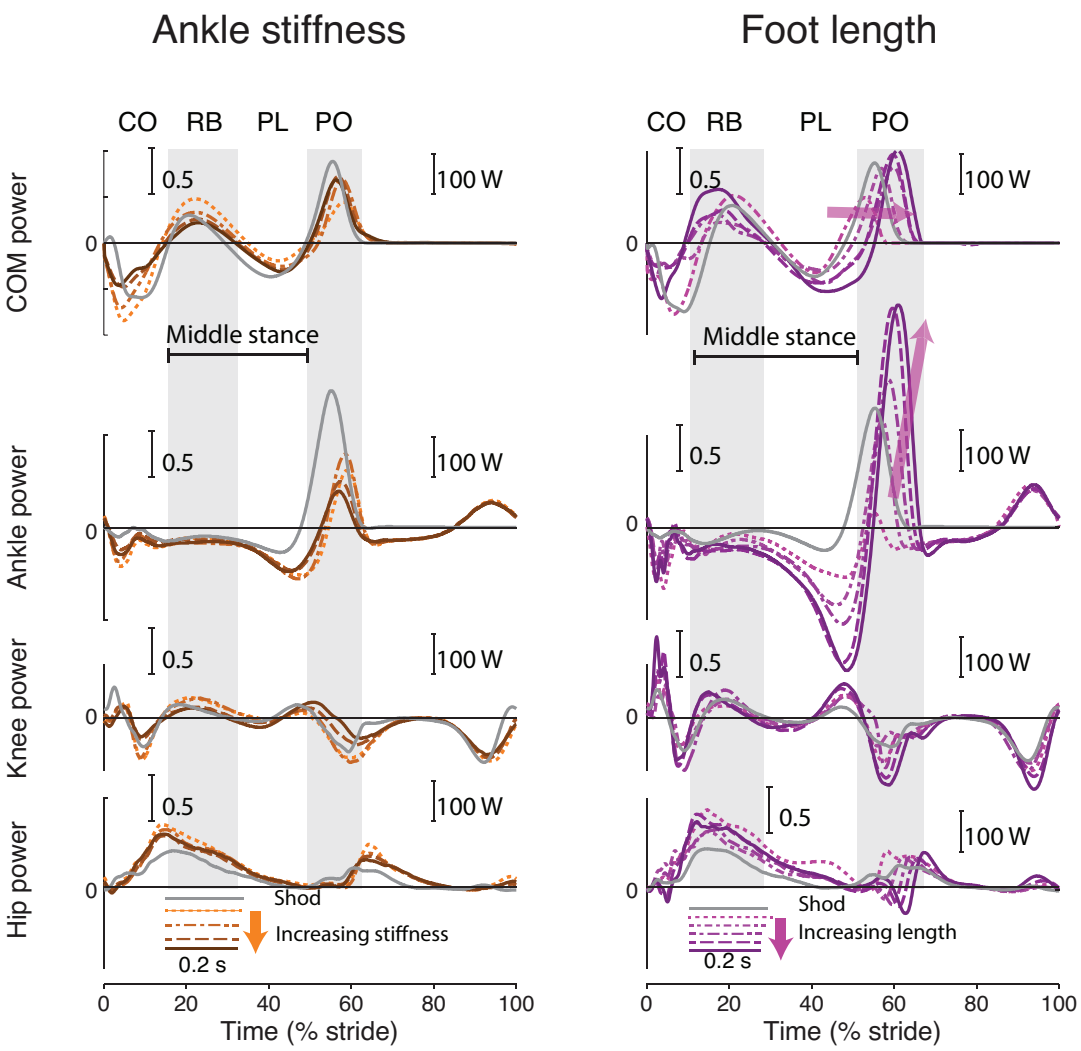

Figure 5.3Mechanial power measures vs stride time, for different ankle stiffnesses (first column) and foot lengths (second column).
Left-hand vertical axes show dimensionless quantities, right-hand vertical axes show dimensional SI units. Data shown are trajectories averaged across subjects ($N = 8$).

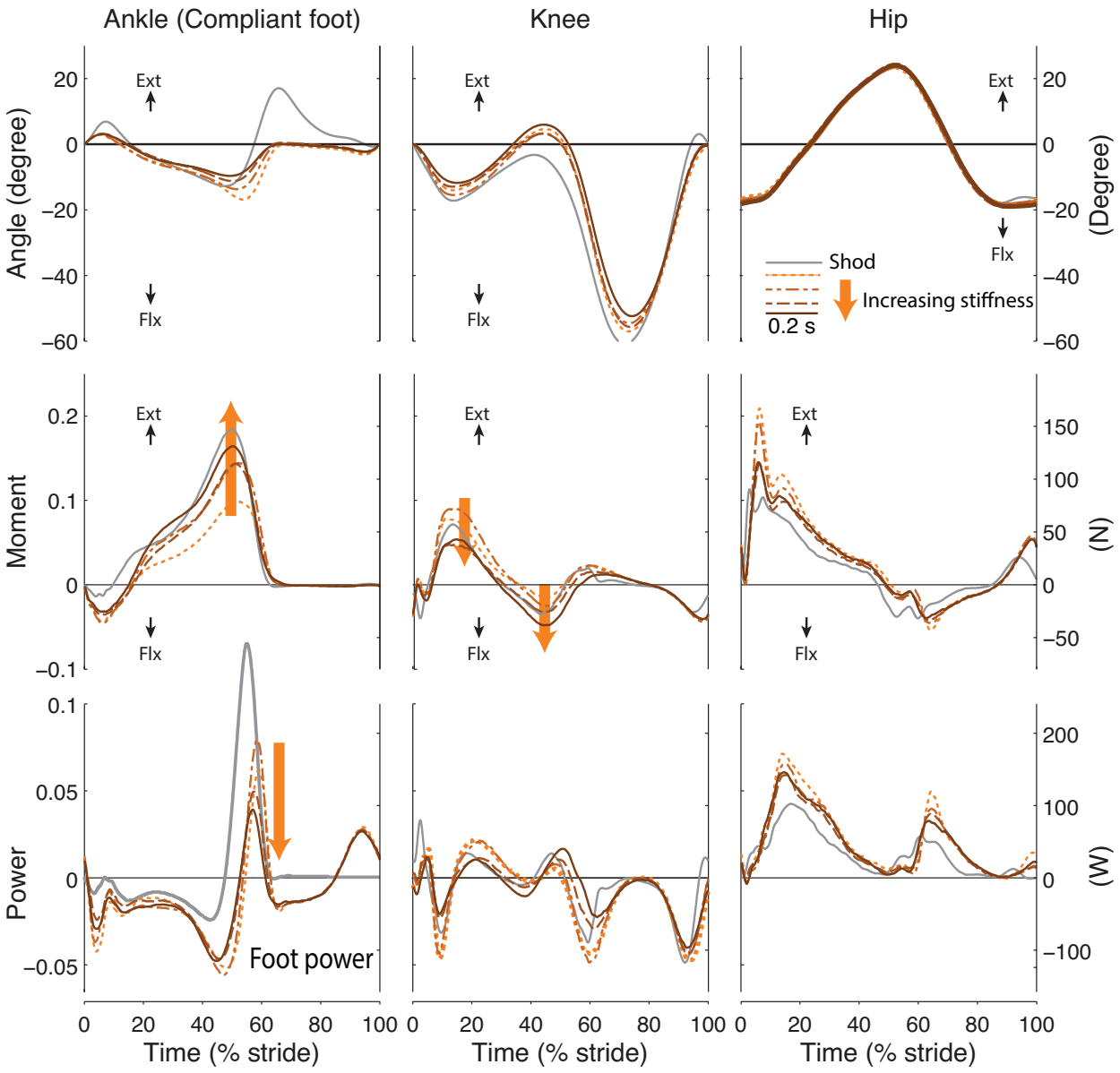

Figure 5.4 Joint kinematics and kinetics vs. stride time with different ankle stiffnesses. Angle, moment and power trajectories are shown for ankle (artificial), knee and hip. Data shown are trajectories averaged across subjects (N = 8). Positive angle and moments are defined in extension (Ext) as opposed to flexion (Flx). Left-hand vertical axes show dimensionless quantities, right-hand axes show dimensional SI units. Data shown are trajectories averaged across subjects ($N = 8$).

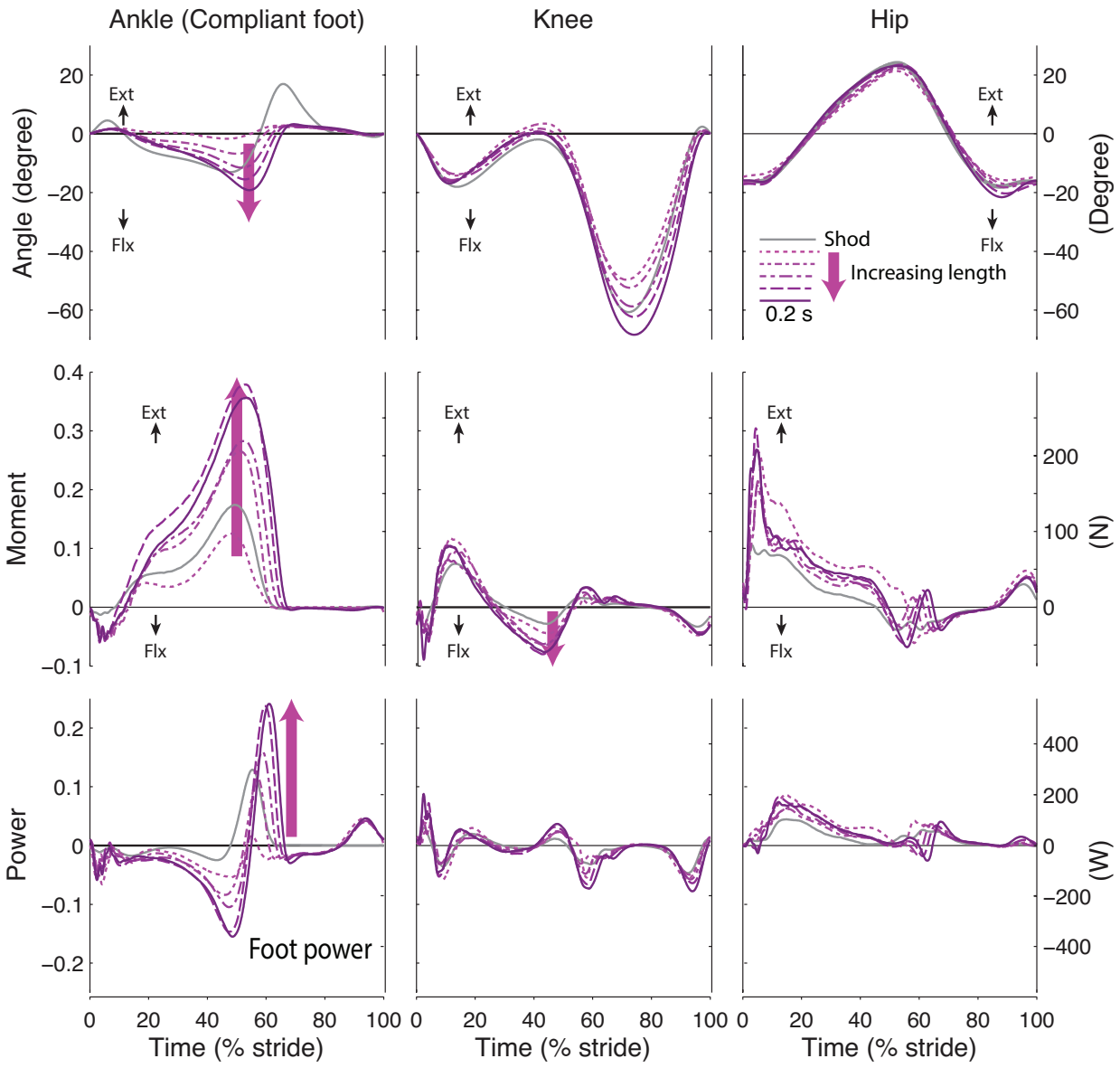

Figure 5.5 Joint kinematics and kinetics vs. percent stride time with different foot lengths. Angle, moment and power trajectories are shown for ankle (artificial), knee and hip. Data shown are trajectories averaged across subjects (N = 8). Positive angle and moments are defined in extension (Ext) as opposed to flexion (Flx). Left-hand vertical axes show dimensionless quantities, right-hand axes show dimensional SI units. Data shown are trajectories averaged across subjects ($N = 8$).

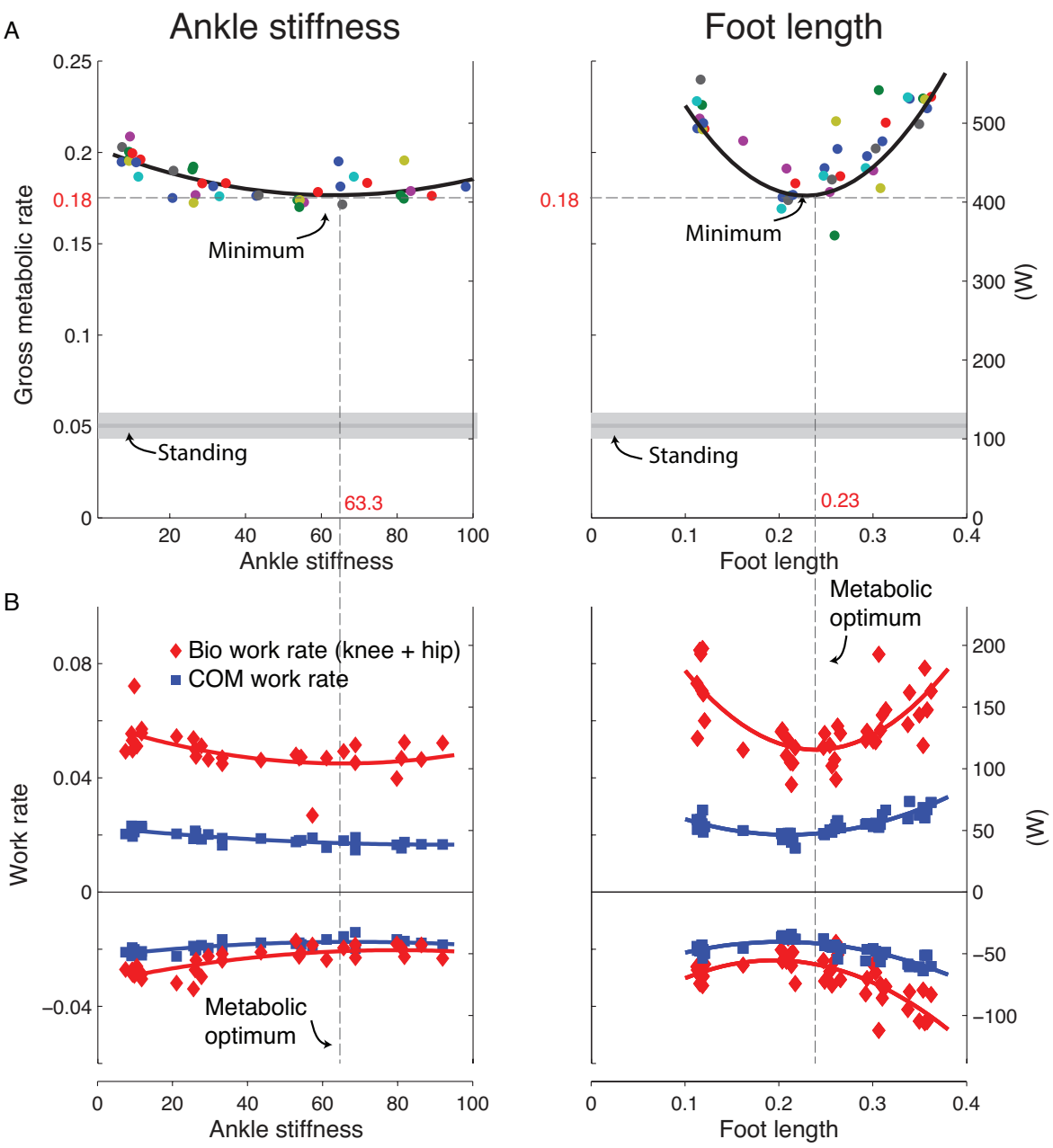

Figure 5.6 Gross metabolic rate and mechanical work rates vs. ankle stiffness (left column) and foot length (right column).
(A) Gross metabolic rate. Each color represents one subject. The gray bars represent normal walking and standing metabolic rate from previous study (Huang and Kuo, 2014). (B) Average COM work rate (red diamond) and bio work rate (blue square). The bio work rate represents the active biological work rate, defined as sum of knee and hip work rate. Left-hand vertical axes show dimensionless quantities, right-hand axes show dimensional SI units.

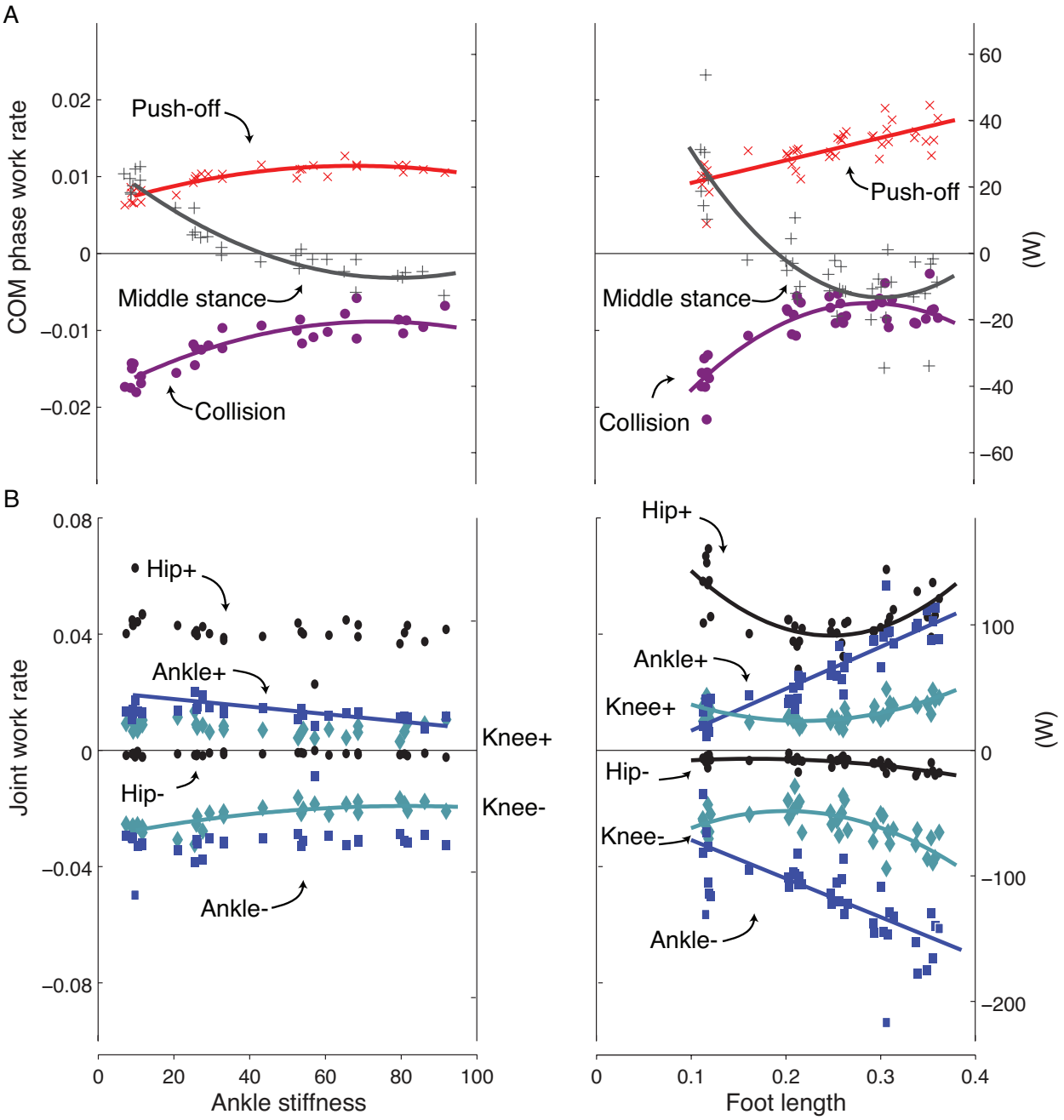

Figure 5.7 COM Collision, Middle stance and Push-off work rates (A) and individual joint work rates (B) vs. ankle stiffness (Left column) and foot length (right column).

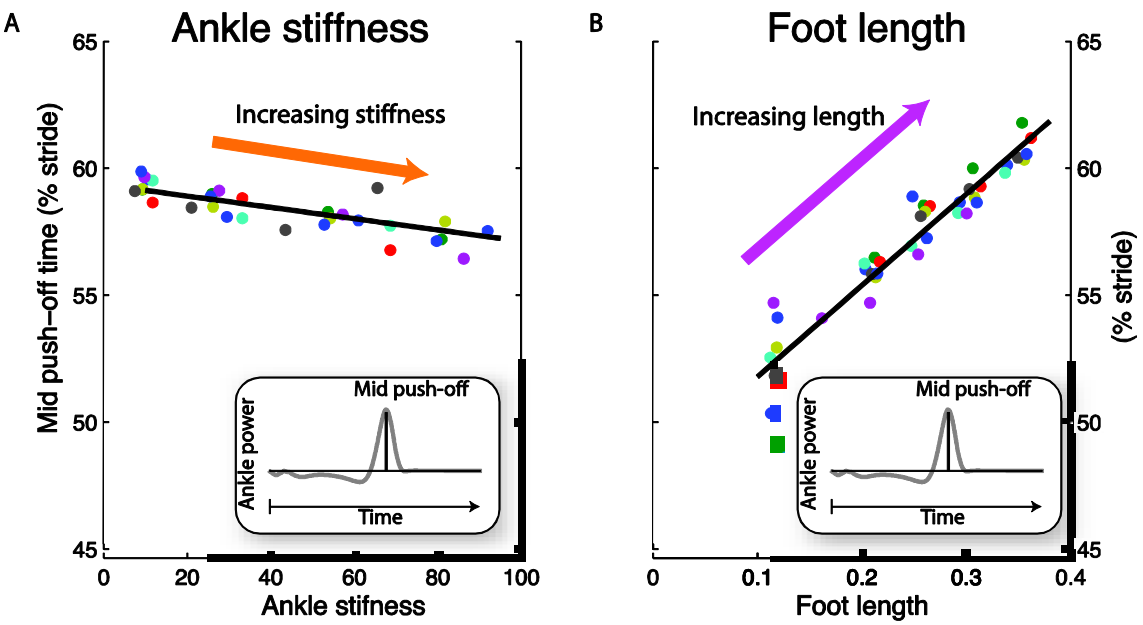

Figure 5.8 Mid push-off time vs. (A)ankle stiffness and (B) foot length

Chapter 6 Conclusions

I used the dynamic walking models to predict the energetic cost of human walking at different walking speeds with carried load, with constrained and with elasticity at ankle. I also tested these predictions experimentally by testing healthy subjects walking in constrained conditions. The energetic cost of human walking highly depends on the amount of positive mechanical work performed by the lower extremity muscles. One of the important reasons for the positive mechanical work is to compensate the energy dissipated during walking, especially the dissipation due to heel-strike collision. One way to perform positive mechanical work is to perform a push-off, a burst of positive work at late stance. A push-off, often contributed by ankle for healthy individuals, can not only compensate the heel-strike collision but also reduce amount of heel-strike collision according to simplest dynamic walking models.

The main questions I want to answer in my study are that whether the dynamic walking models can explain the energetic cost of human walking with challenging conditions. The dynamic walking models consist simplified lower extremity model and passive dynamics. The energetic cost of the models is due to the rigid impact at the heel-strike, which dissipates kinetic energy, requiring positive mechanical work to maintain walking speed. Performing positive mechanical work should cost energy according basic thermodynamic principles. I therefore hypothesized that the positive mechanical work can explain the energetic cost of human walking with challenging conditions, and the dynamic walking models can predict the amount of positive mechanical work required for human walking. I then designed human experiments to test the model predictions, and discuss about the limitations of the models.

We found that the inverted pendulum model extends well to predict for load carriage. The model predicts the proportionality between the positive mechanical work performed by each leg on COM and the total mass of body. I therefore tested healthy subjects walking with carried load and estimate the metabolic rate and mechanical work performed by lower extremity. We found

the work performed on COM is proportionate to the carried load. The metabolic rate is proportionate to the positive COM work rate with a constant delta efficiency.

Besides carrying load, the energetic cost of human walking also increases substantively to faster walking speed. The simplest dynamic walking model with rigid legs also predict that the energetic cost of human walking at different speeds to be proportionate to the total body mass times the walking speed raised to the power of 3.42. Hypothesizing the proportionality between the energetic cost and positive mechanical work, I expected the energetic cost should be proportionate to the total body mass times the walking speed raised to the power of 3.42. I tested these predictions by testing healthy subjects walking at different speeds with carried load. We found the COM work rate of walking at different speeds with carried load agrees to the prediction and the proportionality between net metabolic rate and positive COM work rate.

The rigid-leg model has the limitations that it cannot predict the double support duration and the pattern of ground reaction forces. I then used a compliant-leg model to predict the double support duration and the pattern of ground reaction forces. Assuming that the natural frequency of the compliant leg corresponds to the stride frequency, the compliant leg model can predict the double support duration and the pattern of ground reaction forces. Therefore, I concluded the rigid-leg model can predict the COM work and the energetic cost, and the compliant-leg model can complementarily predict the double support duration and the pattern of ground reaction forces of human walking at different speed with carried load.

The simplest waking model is based on the push-off –collision relationship, which also predicts that the reduced push-off should lead to greater heel-strike collision, and requires more positive work to compensate. The reduced push-off should therefore be energetic costly. This hypothesis has not been tested experimentally before. I thus studied how the push-off affects the energetics and mechanics of human walking. We tested healthy subjects walking with ankle restriction, which reduced push-off. We found the more collision dissipation and more total joint work for reduced push-off, agreeing with the model prediction. The metabolic rate therefore increased for less push-off.

The simplest walking model has shown the benefit of push-off in terms of reduce the energetic cost by reducing collision. Most of the push-off is contributed by the elastic Achilles tendon for

healthy individuals. How the elasticity at ankle could benefit human walking is unclear. A springy ankle dynamic walking model shows how ankle stiffness and foot length affect the energetic cost, but have not been tested experimentally. I therefore tested the energetics and mechanics of human walking with compliant artificial feet with different stiffnesses and foot lengths. I found the trade-off between stiff and complaint ankle, and the trade-off between long and short feet. Both ankle stiffness and foot lengths affect the amount and the timing of elastic push-off. Stiff ankle and short foot have less and earlier push-off. Compliant ankle and long foot have more and postponed push-off. Less and postponed elastic push-off requires more joint work for walking and cost more energy. Therefore, we found minimal metabolic rate for intermediate ankle stiffness and foot length.

The timing and amount of push-off are critical to the walking economy. Reduced push-off leads to greater heel-strike collisions requiring additional mechanical work to compensate. The energetic cost therefore becomes higher with reduced push-off. The elasticity at ankle can contribute to push-off by storing and returning energy, but specific stiffness and foot length is required to achieve proper timing and amount of push-off for maximizing the benefit of elasticity. The optimal ankle stiffness and foot vary for different body weight, leg lengths and perhaps walking speeds. An AFO or a prosthetic foot with automated mechanism, which can adjust the ankle stiffness or foot length for different conditions, could be potentially more beneficial to patients' walking economy.

The inverted pendulum walking model can well predict the energetic cost of normal walking and walking with challenging conditions, but has a limitation to predict some gait parameters, such as double support duration, and COM fluctuations. A more complex model, such as compliant-leg model, would be able to explain more complex phenomena in human walking. However, a complex model usually requires more assumptions or systematic parameter tuning to obtain reasonable results. Therefore, the complex model could have less predictive value than the simple model.

The mechanical work performed by each leg is able to explain the metabolic rate of these tasks. There are still other factors, such as muscle forces or muscle co-activation, which could contribute to the metabolic rate of walking. These factors are either maintain unchanged in these tasks or coupled with the mechanical work. In this thesis, we did not try to isolate these factors

from mechanical work. In the future, it would be interesting to design an experiment to de-couple these factors from the mechanical work and explore the contribution of these factors on the energetic cost.

References

Adamczyk, P. G. and Kuo, A. D. (2009). Redirection of center-of-mass velocity during the step-to-step transition of human walking. *J. Exp. Biol.* **212**, 2668–2678.

Adamczyk, P. G. and Kuo, A. D. (2013). Mechanical and energetic consequences of rolling foot shape in human walking. *J. Exp. Biol.* **216**, 2722–2731.

Adamczyk, P. G., Collins, S. H. and Kuo, A. D. (2006). The advantages of a rolling foot in human walking. *J. Exp. Biol.* **209**, 3953–3963.

Alexander, R. M. (1991). Energy-saving mechanisms in walking and running. *J. Exp. Biol.* **160**, 55 –69.

Attwells, R. L., Birrell, S. a, Hooper, R. H. and Mansfield, N. J. (2006). Influence of carrying heavy loads on soldiers' posture, movements and gait. *Ergonomics* **49**, 1527–37.

Bajd, T., Stefancic, M., Matjacić, Z., Kralj, A., Savrin, R., Benko, H., Karcnik, T. and Obreza, P. (1997). Improvement in step clearance via calf muscle stimulation. *Med. Biol. Eng. Comput.* **35**, 113–116.

Birrell, S. A. and Haslam, R. A. (2009). The effect of military load carriage on 3-D lower limb kinematics and spatiotemporal parameters. *Ergonomics* **52**, 1298–1304.

Bregman, D. J. J., van der Krogt, M. M., de Groot, V., Harlaar, J., Wisse, M. and Collins, S. H. (2011b). The effect of ankle foot orthosis stiffness on the energy cost of walking: a simulation study. *Clin. Biomech. Bristol Avon* **26**, 955–961.

Bregman, D. J. J., Harlaar, J., Meskers, C. G. M. and de Groot, V. (2011a). Spring-like Ankle Foot Orthoses reduce the energy cost of walking by taking over ankle work. *Gait Posture*.

Bregman, D. J. J., Harlaar, J., Meskers, C. G. M. and de Groot, V. (2012). Spring-like Ankle Foot Orthoses reduce the energy cost of walking by taking over ankle work. *Gait Posture* **35**, 148–153.

Brockway, J. M. (1987a). Derivation of formulae used to calculate energy expenditure in man. *Hum. Nutr. Clin. Nutr.* **41**, 463–471.

Brockway, J. M. (1987b). Derivation of formulae used to calculate energy expenditure in man. *Hum. Nutr. Clin. Nutr.* **41**, 463–471.

Caldwell, G. and Forrester, L. (1992). Estimates of mechanical work and energy transfers: demonstration of a rigid body power model of the recovery leg in gait. *Med. Sci. Sports Exerc.* **24**, 1396–1412.

Cavagna, G. A. and Kaneko, M. (1977). Mechanical work and efficiency in level walking and running. *J Physiol* **268**, 467–81.

Chow, D. H. K., Kwok, M. L. Y., Au-Yang, A. C. K., Holmes, A. D., Cheng, J. C. Y., Yao, F. Y. D. and Wong, M. S. (2005). The effect of backpack load on the gait of normal adolescent girls. *Ergonomics* **48**, 642–56.

Collins, S. H. and Kuo, A. D. (2010). Recycling energy to restore impaired ankle function during human walking. *PLoS One* **5**, e9307.

Collins, S. H., Adamczyk, P. G., Ferris, D. P. and Kuo, A. D. (2009). A simple method for calibrating force plates and force treadmills using an instrumented pole. *Gait Posture* **29**, 59–64.

Dean, J. C. and Kuo, A. D. (2011). Energetic costs of producing muscle work and force in a cyclical human bouncing task. *J. Appl. Physiol.* **110**, 873 –880.

DeVita, P., Helseth, J. and Hortobagyi, T. (2007). Muscles do more positive than negative work in human locomotion. *J. Exp. Biol.* **210**, 3361–73.

Doets, H. C., Vergouw, D., Veeger, H. E. J. (Dirkjan) and Houdijk, H. (2009). Metabolic cost and mechanical work for the step-to-step transition in walking after successful total ankle arthroplasty. *Hum. Mov. Sci.* **28**, 786–797.

Doke, J. and Kuo, A. D. (2007). Energetic cost of producing cyclic muscle force, rather than work, to swing the human leg. *J. Exp. Biol.* **210**, 2390–2398.

Doke, J., Donelan, J. M. and Kuo, A. D. (2005). Mechanics and energetics of swinging the human leg. *J. Exp. Biol.* **208**, 439–445.

Donelan, J. M., Kram, R. and Kuo, A. D. (2001a). Mechanical and metabolic determinants of the preferred step width in human walking. *Proc. R. Soc. Lond. B Biol Sci* **268**, 1985–92.

Donelan, J. M., Kram, R. and Kuo, A. D. (2001b). Mechanical and metabolic determinants of the preferred step width in human walking. *Proc R Soc Lond B* **268**, 1985–1992.

Donelan, J. M., Kram, R. and Kuo, A. D. (2002a). Mechanical work for step-to-step transitions is a major determinant of the metabolic cost of human walking. *J. Exp. Biol.* **205**, 3717–3727.

Donelan, J. M., Kram, R. and Kuo, A. D. (2002b). Mechanical work for step-to-step transitions is a major determinant of the metabolic cost of human walking. *J. Exp. Biol.* **205**, 3717–27.

Donelan, J. M., Kram, R. and Kuo, A. D. (2002c). Simultaneous positive and negative external mechanical work in human walking. *J. Biomech.* **35**, 117–24.

Donelan, J. M., Kram, R. and Kuo, A. D. (2002d). Mechanical work for step-to-step transitions is a major determinant of the metabolic cost of human walking. *J. Exp. Biol.* **205**, 3717–3727.

Fukunaga, T., Kubo, K., Kawakami, Y., Fukashiro, S., Kanehisa, H. and Maganaris, C. N. (2001). In vivo behaviour of human muscle tendon during walking. *Proc. Biol. Sci.* **268**, 229–233.

Gaesser, G. A. and Brooks, G. A. (1975). Muscular efficiency during steady-rate exercise: effects of speed and work rate. *J. Appl. Physiol.* **38**, 1132–1139.

Geyer, H., Seyfarth, A. and Blickhan, R. (2006). Compliant leg behaviour explains basic dynamics of walking and running. *Proc. R. Soc. B-Biol. Sci.* **273**, 2861–2867.

Ghori, G. M. U. and Luckwill, R. G. (1985). Responses of the lower limb to load carrying in walking man. *Eur. J. Appl. Physiol.* **54**, 145–150.

Goldman, R. F. and Iampietro, P. F. (1962). Energy cost of load carriage. *J. Appl. Physiol.* **17**, 675 –676.

Gordon, D., Robertson, E. and Winter, D. A. (1980). Mechanical energy generation, absorption and transfer amongst segments during walking. *J. Biomech.* **13**, 845–854.

Grenier, J. G., Peyrot, N., Castells, J., Oullion, R., Messonnier, L. and Morin, J.-B. (2012). Energy cost and mechanical work of walking during load carriage in soldiers. *Med. Sci. Sports Exerc.* **44**, 1131–1140.

Grieve, D. W. (1968). Gait patterns and the speed of walking. *Biomed. Eng.* **3**, 119–122.

Griffin, T. M., Roberts, T. J. and Kram, R. (2003). Metabolic cost of generating muscular force in human walking: insights from load-carrying and speed experiments. *J. Appl. Physiol.* **95**, 172–183.

Hafner, B. J., Sanders, J. E., Czerniecki, J. and Fergason, J. (2002). Energy storage and return prostheses: does patient perception correlate with biomechanical analysis? *Clin. Biomech. Bristol Avon* **17**, 325–344.

Hanavan Jr., E. P. (1964). *A Mathematical Model of the Human Body*. Wright-Patterson AFB, OH: Air Force Aerospace Medical Research Lab.

Harman, E., Hoon, K., Frykman, P. and Pandorf, C. (2000). *The effects of backpack weight on the biomechanics of load carriage*. Natick, MA: Army Research Inst. of Environmental Medicine.

Holt, K. G., Wagenaar, R. C., LaFiandra, M. E., Kubo, M. and Obusek, J. P. (2003). Increased musculoskeletal stiffness during load carriage at increasing walking speeds maintains constant vertical excursion of the body center of mass. *J. Biomech.* **36**, 465–471.

Huang, T. P. and Kuo, A. D. (2014). Mechanics and energetics of load carriage during human walking. *J. Exp. Biol.* **217**, 605–613.

Ishikawa, M., Komi, P. V., Grey, M. J., Lepola, V. and Bruggemann, G.-P. (2005). Muscle-tendon interaction and elastic energy usage in human walking. *J. Appl. Physiol.* **99**, 603 – 608.

Kim, S. and Park, S. (2011). Leg stiffness increases with speed to modulate gait frequency and propulsion energy. *J. Biomech.* **44**, 1253–1258.

Knapik, J., Harman, E. and Reynolds, K. (1996). Load carriage using packs: A review of physiological, biomechanical and medical aspects. *Appl. Ergon.* **27**, 207–216.

Kuo, A. D. (2001). A simple model of bipedal walking predicts the preferred speed-step length relationship. *J. Biomech. Eng.* **123**, 264–269.

Kuo, A. D. (2002a). Energetics of actively powered locomotion using the simplest walking model. *J. Biomech. Eng.* **124**, 113–120.

Kuo, A. D. (2002b). Energetics of actively powered locomotion using the simplest walking model. *J. Biomech. Eng.* **124**, 113–120.

Kuo, A. D., Donelan, J. M. and Ruina, A. (2005a). Energetic consequences of walking like an inverted pendulum: step-to-step transitions. *Exerc. Sport Sci. Rev.* **33**, 88–97.

Kuo, A. D., Donelan, J. M. and Ruina, A. (2005b). Energetic consequences of walking like an inverted pendulum: step-to-step transitions. *Exerc. Sport Sci. Rev.* **33**, 88–97.

Lehmann, J. F., Price, R., Boswell-Bessette, S., Dralle, A. and Questad, K. (1993). Comprehensive analysis of dynamic elastic response feet: Seattle Ankle/Lite Foot versus SACH foot. *Arch. Phys. Med. Rehabil.* **74**, 853–861.

Lipfert, S. W., Günther, M., Renjewski, D. and Seyfarth, A. (2014). Impulsive ankle push-off powers leg swing in human walking. *J. Exp. Biol.* **217**, 1218–1228.

Malcolm, P., Derave, W., Galle, S. and De Clercq, D. (2013). A simple exoskeleton that assists plantarflexion can reduce the metabolic cost of human walking. *PloS One* **8**, e56137.

Margaria, R. (1968). Positive and negative work performances and their efficiencies in human locomotion. *Int. Z. Für Angew. Physiol. Einschließlich Arbeitsphysiologie* **25**, 339–351.

Margaria, R. (1976). *Biomechanics and energetics of muscular exercise*. London: Oxford.

Martin, P. E. and Nelson, R. C. (1986). The effect of carried loads on the walking patterns of men and women. *Ergonomics* **29**, 1191–1202.

Meinders, M., Gitter, A. and Czerniecki, J. M. (1998). The role of ankle plantar flexor muscle work during walking. *Scand. J. Rehabil. Med.* **30**, 39–46.

Nielsen, D. H., Shurr, D. G., Golden, J. C. and Meier, K. (1988). Comparison of energy cost and gait efficiency during ambulation in below-knee amputees using different prosthetic feet-a preliminary report. *JPO J. Prosthet. Orthot.* **1**, 24–31.

O'Connor, S. M., Xu, H. Z. and Kuo, A. D. (2012). Energetic cost of walking with increased step variability. *Gait Posture* **36**, 102–107.

Perry, J. and Shanfield, S. (1993). Efficiency of dynamic elastic response prosthetic feet. *J. Rehabil. Res. Dev.* **30**, 137–143.

Pierrynowski, M. R., Norman, R. W. and Winter, D. A. (1981). Mechanical energy analyses of the human during local carriage on a treadmill. *Ergonomics* **24**, 1–14.

Powers, C. M., Torburn, L., Perry, J. and Ayyappa, E. (1994). Influence of prosthetic foot design on sound limb loading in adults with unilateral below-knee amputations. *Arch. Phys. Med. Rehabil.* **75**, 825–829.

Prince, F., Winter, D. A., Sjonnesen, G. and Wheeldon, R. K. (1994). A new technique for the calculation of the energy stored, dissipated, and recovered in different ankle-foot prostheses. *Rehabil. Eng. IEEE Trans. On* **2**, 247–255.

Quesada, P. M., Mengelkoch, L. J., Hale, R. C. and Simon, S. R. (2000). Biomechanical and metabolic effects of varying backpack loading on simulated marching. *Ergonomics* **43**, 293–309.

Sawicki, G. S. and Ferris, D. P. (2008). Mechanics and energetics of level walking with powered ankle exoskeletons. *J. Exp. Biol.* **211**, 1402 –1413.

Shamaei, K., Sawicki, G. S. and Dollar, A. M. (2013). Estimation of quasi-stiffness of the human knee in the stance phase of walking. *PloS One* **8**, e59993.

Singer, S., Klejman, S., Pinsker, E., Houck, J. and Daniels, T. (2013). Ankle arthroplasty and ankle arthrodesis: gait analysis compared with normal controls. *J. Bone Joint Surg. Am.* **95**, e191(1–10).

Snyder, R. D., Powers, C. M., Fountain, C. and Perry, J. (1995a). The effect of five prosthetic feet on the gait and loading of the sound limb in dysvascular below-knee amputees. *J. Rehabil. Res. Dev.* **32**, 309–315.

Snyder, R. D., Powers, C. M., Fountain, C. and Perry, J. (1995b). The effect of five prosthetic feet on the gait and loading of the sound limb in dysvascular below-knee amputees. *J. Rehabil. Res. Dev.* **32**, 309–315.

Soule, R. G., Pandolf, K. B. and Goldman, R. F. (1978). Energy expenditure of heavy load carriage. *Ergonomics* **21**, 373–381.

Stuempfle, K. J., Drury, D. G. and Wilson, A. L. (2004). Effect of load position on physiological and perceptual responses during load carriage with an internal frame backpack. *Ergonomics* **47**, 784–789.

Taylor, C. R., Heglund, N. C., McMahon, T. A. and Looney, T. R. (1980). Energetic cost of generating muscular force during running: A comparison of large and small animals. *J. Exp. Biol.* **86**, 9–18.

Tilbury-Davis, D. C. and Hooper, R. H. (1999). The kinetic and kinematic effects of increasing load carriage upon the lower limb. *Hum. Mov. Sci.* **18**, 693–700.

Torburn, L., Powers, C. M., Guiterrez, R. and Perry, J. (1995). Energy expenditure during ambulation in dysvascular and traumatic below-knee amputees: a comparison of five prosthetic feet. *J. Rehabil. Res. Dev.* **32**, 111–119.

Unnithan, V. B., Dowling, J. J., Frost, G. and Bar-Or, O. (1996). Role of cocontraction in the O2 cost of walking in children with cerebral palsy. *Med. Sci. Sports Exerc.* **28**, 1498–1504.

Van Engelen, S. J. P. M., Wajer, Q. E., van der Plaat, L. W., Doets, H. C., van Dijk, C. N. and Houdijk, H. (2010). Metabolic cost and mechanical work during walking after tibiotalar arthrodesis and the influence of footwear. *Clin. Biomech. Bristol Avon* **25**, 809–815.

Vanderpool, M. T., Collins, S. H. and Kuo, A. D. (2008). Ankle fixation need not increase the energetic cost of human walking. *Gait Posture* **28**, 427–433.

Waters, R. L. and Mulroy, S. (1999). The energy expenditure of normal and pathologic gait. *Gait Posture* **9**, 207–31.

Whittington, B. R. and Thelen, D. G. (2008). A Simple Mass-Spring Model With Roller Feet Can Induce the Ground Reactions Observed in Human Walking. *J. Biomech. Eng.* **131**, 011013–011013.

Winter, D. A. (2005). *Biomechanics and motor control of human movement*. Hoboken, NJ: J. Wiley and Sons, Inc.

Zelik, K. E. and Kuo, A. D. (2010). Human walking isn't all hard work: Evidence of soft tissue contributions to energy dissipation and return. *J. Exp. Biol.* **213**, 4257–4264.

Zelik, K. E. and Kuo, A. D. (2012a). Mechanical work as an indirect measure of subjective costs influencing human movement. *PloS One* **7**, e31143.

Zelik, K. E. and Kuo, A. D. (2012b). Mechanical work as an indirect measure of subjective costs influencing human movement. *PloS One* **7**, e31143.

Zelik, K. E., Collins, S. H., Adamczyk, P. G., Segal, A. D., Klute, G. K., Morgenroth, D. C., Hahn, M. E., Orendurff, M. S., Czerniecki, J. M. and Kuo, A. D. (2011). Systematic

Variation of Prosthetic Foot Spring Affects Center-of-Mass Mechanics and Metabolic Cost During Walking. *Ieee Trans. Neural Syst. Rehabil. Eng.* **19**, 411–419.

Zelik, K. E., Huang, T.-W. P., Adamczyk, P. G. and Kuo, A. D. (2013). The role of series ankle elasticity in bipedal walking. *J. Theor. Biol.* **346C**, 75–85.

Zelik, K. E., Huang, T.-W. P., Adamczyk, P. G. and Kuo, A. D. (2014). The role of series ankle elasticity in bipedal walking. *J. Theor. Biol.* **346**, 75–85.